Effects of Additives in Solution Crystallization

Dissertation

zur Erlangung des akademischen Grades

Doktor–Ingenieur (Dr.–Ing.)

genehmigt durch die

Mathematisch–Naturwissenschaftlich–Technische Fakultät
(Ingenieurwissenschafticher Bereich)
der Martin–Luther–Universität Halle–Wittenberg

von Herrn M.Sc. Eng. Sattar Al–Jibbouri
geboren am 29.12.1972 in Kadisia/Irak

Dekan der Fakultät: Prof. Dr. Dr. rer. nat. habil. H. Pöllmann

Gutachter:
1. *Prof. Dr. J. Ulrich*
2. *Prof. Dr. M. Pietzsch*
3. *Prof. Dr. A. König*

Merseburg, 19.12.2002

urn:nbn:de:gbv:3-000004666
[http://nbn-resolving.de/urn/resolver.pl?urn=nbn%3Ade%3Agbv%3A3-000004666]

Dedication

To my wife.

Sattar Al-Jibbouri

Acknowledgment

My grateful appreciation to my supervisor, Prof. Dr-Ing. habil. Joachim Ulrich, for his helpful, guidance and a continued encouragement throughout this work.

Also deep thanks are to examining committee Prof. Dr. Roggendorf, Prof. Dr. König, Prof. Dr. Pietzsch, Prof. Dr. Lempe, Prof. Dr. Kressler, Prof. Dr. Leps and PD Dr. Brendler.

My deep thanks are extended to the Martin-Luther-Universität Halle-Wittenberg for their support of this project which led to this work.

My deep thanks for all my colleagues, (Dr. Mohring, Dr. Wanko, Tero, Junjun, Christine, Stefan, Torsten, Bernd, Kim, Dannail, Aiman, Mirko, Mandy, Peter, Andrea and Uta), and especially (Mrs. Dr. Heike Glade, Mrs. Cornelia Lorentz and Mrs. Ing. Frauke Mätsch) for their help during my studying.

Sattar Al-Jibbouri

Table of Contents

Abstract

In this study a fluidized bed crystallizer is employed to investigate the growth and dissolution rate of $MgSO_4 \bullet 7H_2O$ and $NaCl$ crystals. In the experiments the supersaturation, impurity concentration and pH-values in the solution were varied. The electrophoretic mobility measurements by Laser-Doppler electrophoresis (ζ–potential measurements) are reported for $MgSO_4 \bullet 7H_2O$ crystals. These measurements for inorganic salt have been made for the first time and allow the surface charge to be predicted for $MgSO_4 \bullet 7H_2O$ crystals in their saturated solution. Therefore, knowing the surface potential by measuring ζ–potential can help to explain the crystallization phenomena which are not clear up to now. In general, the results show that the $MgSO_4 \bullet 7H_2O$ crystals have a positive *ζ–potential* charge. At low pH the surface will acquire more positive charge and at high pH a build up of negative charge will take place, hence, the crystal growth is suppressed. In this study it was proven that the growth rates of $MgSO_4 \bullet 7H_2O$ crystals are suppressed by traces of Fe^{+2}/Ni^{+2} ions.

***Keywords**: Inorganic salt, growth rate, impurity, kinetic effects, thermodynamic effects, surface potential, surface charge, zeta–potential.*

In dieser Studie wird ein Flüssigbettkristallisator eingesetzt, um die Wachstum- und Auflösungrate $MgSO_4 \bullet 7H_2O$ und $NaCl$ der Kristalle nachzuforschen. In den Experimenten wurden die Übersättigung, die Störstellenkonzentation und die pH-werte in der Lösung verändert. Die elektrophoretischen Mobilität Maße durch Laser-Doppler Elektrophorese (Zeta Potential Maße) für $MgSO_4 \bullet 7H_2O$ Kristalle berichtet. Diese Maße für anorganisches Salz sind zum ersten Mal gebildet worden und erlauben, daß die Oberflächenaufladung für $MgSO_4 \bullet 7H_2O$ Kristalle in ihrer gesättigten Lösung vorausgesagt wird. Folglich kann das Kennen des Oberflächenpotentials, indem es Zeta Potential mißt, helfen, die Kristallisation Phänomene zu erklären, die nicht zu jetzt aufräumen sollen. Im allgemeinen zeigen die Resultate, daß die $MgSO_4 \bullet 7H_2O$ Kristalle eine positive Zeta Potential Aufladung haben. Bei niedrigem pH erwirbt die Oberfläche positivere Aufladung und bei hohem pH findet ein Aufbau der negativen Aufladung statt, folglich wird das Kristallwachstum unterdrückt. In dieser Studie wurde es nachgewiesen, daß die Wachstumsraten der $MgSO_4 \bullet 7H_2O$ Kristalle durch Spuren der Ionen Fe^{+2}/Ni^{+2} unterdrückt werden.

***Keywords**: Anorganisches Salz, Wachstumsrate, Störstellen, Kinetische Effekte, Thermodynamische Effekte, Oberflächenpotentials, Oberflächenaufladung, Zeta–Potential.*

1. Introduction

Crystallization is a separation and purification process used in the production of a wide range of materials from bulk commodity chemicals to speciality chemicals and pharmaceuticals in terms of purity and crystal size distribution (CSD).

In order to design a crystallization process it needs kinetic data especially those of crystal growth. The techniques used to measure crystal growth rates can be divided into two main groups. The first group is comprised of methods that rely on the growth of a single crystals to obtain the needed data. The second set of methods involves the growth of a suspension of crystals in solution. The aim is to allow the crystals to grow at a known growth rate without any nucleation occurring. This implies, therefore, that the supersaturations used in these experiments must be controlled.

It has been known, that the shape and purity of the crystals are influenced by impurities, which alter the kinetic parameters as the rates of nucleation, growth and dissolution and even the shape of the crystals. The effect of impurities on the crystallization kinetics, most probably, is due to the impurity adsorption on the crystal surface. *Therefore, an understanding of impurity effects is a great interest.*

The present investigations are concentrated to discuss all issues concerning the influence of impurities on the crystal growth processes only for inorganic salts in aqueous solutions. To show that the impurity’s action can be changed by process conditions like supersaturation and temperature level. Therefore, this thesis should be an attempted to discuss the thermodynamic and kinetic effects, caused by the impurity’s effect, on the crystal growth processes. Furthermore, new explanations for the effect of impurities by measuring crystal surface potential should be introduced.

The growth of crystals in a supersaturation solution is a very complex process that has not been completely understood up to now. The main reason of this complexity is the number of mass transfer steps and the heat transfer involved in the process [1-3]. In a supersaturated solution, the first step is a new surface by nucleation then a diffusion of solute to the surface, following the adsorption of solute on the surface and integration of solute into the crystal lattice. The further steps, which were almost always ignored, are heat related effects from the liberation of the crystallization heat when the crystal grow, and from the heat transfer connected with the mass transfer from and to the phase boundary (liquid/solid). Different physical laws govern all these steps and the present state of science is not able to explain all the phenomena in crystallization.

Growth rate dispersion (GRD) is one of those phenomena which are difficult to explain. Crystallization is a surface phenomenon, but in fact, surface properties were often omitted. Especially, in dissolution no other step than diffusion was considered. As it is already shown by Fabain [4] and Fabain and Ulrich [5] that the dissolution rate of K_2SO_4 shows a dissolution rate dispersion (DRD), which is not possible to explain by the present knowledge that accepts only dissolution as a diffusion-controlled phenomenon. Therefore, other surface phenomena should be taken into account to overcome these explanation difficulties.

Consequently, the presence of small amounts of transition metal ions in aqueous solutions (as impurities) may effect whole crystallization process. The structure of the solution is only effected by the presence of hydronium ions in the solution. The interaction between the present species and the solvent depends on the structure properties in the solution due to the present ions. The smaller the ion is the stronger is the interaction (higher hydration energy) between the ion and water molecules in the coordination sphere. Up to todate, most studies do not consider a hydration of univalent, divalent and trivalent positive ions (cations) in aqueous solution to generate hydronium ions and may be changed the pH value of the solution and hence the potential and the charge of the diffusion layer will be effected.

It has been shown a long time ago that most particles in aqueous solutions are charged for various reasons, such as ionization of surface groups, specific adsorption or desorption of ions. This causes to the formation of the electrical double layer. Any ion, which will be incorporated into the crystal lattice, should pass this electrical double layer which gives extra resistance to the crystal growth. If the formation of the electrical double layer is accepted, external effects on this layer and on the crystallization kinetics can be explained more easily. Unfortunately, there is no detailed experimental research on the surface charge (potential) determination of highly soluble salts in the literature. This can be made e.g. by zeta Potential determination, but the high conductivity of saturated solutions causes some measurement problems. Therefore, the importance of surface potential in the crystal growth kinetics should be investigated by measuring ζ–potential in order to emphasize that the hydration of lattice ions does have a significant influence on the surface charge. I.e. the external effects on the electrical double layer and hence on the crystallization kinetics can be explained more easily by measuring of ζ–potential.

2. State of the art

Any substances other than the crystallizing compound is considered an impurity. Thus, a solvent used for growth and any other compound deliberately added to the growth medium or inherently present in it is an impurity. Different terms, such as additive, admixture, inhibitor or poison, are used in the literature for foreign substances other than the solvent. Irrespective of its concentration, a deliberately added impurity is called *additive*. By the term of *admixture* is mean an impurity added in relatively large amounts (up to several percent) [6]. An impurity can accelerate or slow down the crystal growth process. The impurity that slows down growth is called a *poison* or an *inhibitor*, while the one that accelerates growth is said to be a growth *promotor*.

The literature on the effect of impurities on crystal growth is quite multifarious, and has been reviewed several times [7-11]. The effect of impurity on the growth mechanism can be divided into kinetic effects (crystal side), based on the concept of adsorption of impurity at kinks, steps, and terraces of a growing surface, and thermodynamic effects (solution side), based on the thermodynamic properties of the saturated solution (in the case of aqueous solutions and inorganic compounds).

2.1. Kinetic effects *(crystal side)*

After the publication of the classic monograph by Buckley [12], studies on the effect of impurities were diverted to understand the mechanisms involved in changing the growth habit on the microscopic level [13, 14]. The first phase of important experimental works in this direction was published during the late fifties and sixties [15-17]. The experimental data on impurities deal with different topics as explained in ***Table 2.1.***.

Many models describing the effect of impurities on the crystal growth process are based on the concept of adsorption impurities species (ions, atoms or molecules) at kink, steps and terraces of a growing surface. Cabrera and Vermilyea [14] considered theoretically the adsorption of impurity molecules on surface terraces in the motion of ledges across the surface. Bliznakov [15] introduced the model of reduction of growth sites on face, and reported experimental results in support of the model for a number of water-soluble compounds. Sears [47] and Dunning and Albon [34] proposed the model of adsorption of impurities molecules at ledges of face, and tested the validity of their model against the background of the dependence of rates of motion of growth layer on impurity concentration. Apart from the above kinetics models involving adsorption at surface terrace (Cabrera–Vermilyea model), steps (Sears model), and kink (Bliznakov model), on the basis of their experimental results on growth forms of alkali halides as a function of supersaturation and impurity concentration. The second phase of investigations on impurity effects start from the work of Davey [48] and Davey and Mullin [35, 33], who studied layer displacement rates as a function of impurity concentration, and confronted the experimental data with kinetic models of impurity adsorption.

Recently, Kubota and Mullin [49] advanced a new kinetic model of growth in the presence of impurities. The model describes the adsorption of an impurity along steps and introduced an effectiveness parameter, α, for the impurity adsorption. In contrast to the value of $\alpha = 1$ in the Bliznakov model, $0 \leq \alpha \leq \infty$ in the Kubota–Mullin model. Consequently, as shown by these authors for different crystals, when adsorption accours at active sites along steps, their model explains the kinetic data better. However, as in the Cabrera–Vermilyea model, Kubota and Mullin [49] used Langmuir adsorption isotherm connecting fractional coverage, θ, of the two-dimensional surface by impurity molecules with bulk impurity concentration, c_{imp}, and adsorption constant, K, but defined it as the coverage of one-dimensional step. These authors did not give any justification for the use of linear coverage conjunction with the Langmuir isotherm.

Table 2.1.: *Different topics for the effect of impurities on crystallization process.*

	Topic	Ref.
1.	Habit modification and morphology	18-21
2.	Kinetic data on face growth rates	15, 16, 22-33
3.	Layer displacement rates	34-38
4.	Observation of the presence of dead zones at low impurities concentration	25-28, 39-42
5.	Nucleation and precipitation kinetics	41, 42
6.	Chemical constitution of impurity species and chemistry of adsorption in solution growth	29, 36, 37, 43-46

2.2. Thermodynamic effects *(solution side)*

For many multicomponent systems the solubility data available are scarce and frequently unreliable, thus becoming of little use for most engineering purposes. Because entire phase diagrams cannot be obtained through experiment in a reasonable length of time, several thermodynamic models have been proposed to predict the solubility of salts in aqueous brines. Some of the most successful models make use of the Pitzer equation to describe the thermodynamic properties of aqueous electrolytes, over large ranges of ionic strength [50-52]. The Pitzer model also allows to extend these calculations to elevated temperatures, if some empirical functions of temperature obtained from binary and ternary data were included. Therefore, the solubility of electrolyte solutions can be calculated from the thermodynamic considerations provided that equilibrium constants and the activity coefficients can be obtained. The solubility of the main salt may be changed by adding either another salt as impurities or a high concentrations of acid or base (changing pH-value of the solution).

Consequently, the pH of the solution may affect not only the growth and dissolution rate [53, 54], but also the different physical properties of the saturated solution like osmotic pressure, the density, the surface tension and the metastable region [55]. Only a limited number of studies deals with the effect of pH level on the crystallization kinetics. Some studies considered the effect of the pH of a solution (water as solvent) on the crystallization kinetics in the system, in which hydrogen ion is incorporated in the equilibrium constant of the main salt that should be crystallized. Examples in this category are the phosphate salts [56-58] and calcium carbonate [59, 60]. Other studies (Seifert [61], Langer [62]) investigated the effect of controlling the pH of the solution, by the addition of an acid or base to the required solution, on the crystallization kinetic. Seifert [61] investigated the influence of the pH on the growth rate of KCl. He reported that no effect in the acidic medium on the replacement velocity of the (100) face of single crystals, but an increase in the growth rate was found in the alkaline medium. This increase in growth rate is dramatically pronounced by pH vales of ≥ 12. The different pH levels in the solution are achieved by addition of HCl and KOH. Langer [62] studied the effect of pH on the growth rate of $NaCl$. His results show a maximum crystal growth in the neutral solution, with lower crystal growth rates in both acidic and alkaline solutions.

There are several more or less satisfactory explanations of the effect of pH on crystallization. A plausible explanation tells that the presence of free acids or bases modifies the nature and the concentration of ions in solution [12]. Mohameed and Ulrich [54] explain the effect of pH on crystal growth in terms of a structure in a solution, namely of a hydration of ions. Most cations and OH^- ions are hydrated, the largest hydration enthalpy has the H^+ ion so that its presence in solution has a stronger tendency of interaction with water molecules than, e.g., the K^+ ion so that a competition of ions to acquire water molecules takes place. The K^+ ions have smaller chances to be fully hydrated and therefore they tend to drift towards the crystal surface rather than to remain in the solution. On the another hand, the OH^- ions as a structure former has a stabilizing effect on the solution so that K^+ ions try to remain in the solution; nevertheless, at high OH^- concentrations, the tendency of hydration of the OH^- ions prevails and the K^+ ions are pushed off from the solution again. Kuznetsov and Hodorowicz [63] presented a hypothesis that thermal vibrations of ions in the solution excite electromagnetic waves with the frequency of which depends, among others, on the concentration of the hydroxonium ions. A correlation of the frequency with the vibrations of particles in the crystal lattice can affect the crystallization rate.

Recently there has been more attention paid to the effect of the pH value on crystallization kinetics, especially in combination with other additives e.g. Kubota et al. [64] studied the effect of four chromium (III) salts as impurities on the growth and dissolution rates of K_2SO_4 over a wide range of pH. In this study, it was reported that the adsorption of H^+ ions at the crystal surface is not possible and if that would be the case, the dissolution rate would be lower. Baes and Mesmer [65] proved that in the case of presence of some chrome complexes in aqueous solutions, the degree of change of the pH level is the key factor by which impurity affects the crystallization process. The experimental results reported by Mullin et al. [57] show that the pH level of the solution in the presence of Cr^{+3}, Fe^{+3}, Al^{+3} affects the habit of *ADP* and *KDP* single crystals. Takaski et al. [60] studied the effect of the presence of ferrous ions as hydroxide on the growth rate of calcium carbonate. It was found that in the range of pH between 7 and 8 there is no effect on the growth rate.

The effect of hydronium ions on the potential of the diffusion layer was not considered in the previous studies. The dissociation of a proton from water molecules may effect the structure of the solution and the potential of the crystal/solution interface.

If it is assumed that the protons will be adsorbed at the surface of the crystal, the crystals will be changed and this leads to the development of the so called electrical double layer (see Ch. 3) between the counterions in the solution near the surface and the charge on the surface.

2.3. The aim of the present work

The growth of a single seed crystal differs from the environment in an industrial crystallizer where many crystals are growing in a suspension. The most common method to obtain crystal growth kinetics involving suspension involves the use of a stirred tank crystallizer (MSMPR) or a fluidized bed crystallizer. Therefore, the aim of the present work is:

- To evaluate the relative magnitude of the two resistances in series, *diffusion* and *surface integration* by curve fitting of the growth data.
- To show that *the kinetic models* for crystal growth in the presence of impurities adsorbing at kinks and surface terraces on the F faces of single crystals *are also valid for suspension growth condition* as in industrial crystallizers.
- To propose a physical explanation for the influence of univalent or divalent positive ions (cations) on the structure of the solution based on the thermodynamic properties of the saturated solution. *(i.e. the effect of impurities can be explained by a mechanism in which the hydrolysis product (hydro-complex) is adsorbed on the growth layer of crystal surface and retard growth).*

The major objective of the present investigation is to propose a new explanation for the effect of impurities or changing the pH value of the solution on the crystallization kinetics, based on the hypothesis, that the crystal growth rate of salts is dominated by the surface potential distribution. Specific cation/anion adsorption is the main reason for the occurrence of changing on the surface charge and this adsorption is a function of the surface quality. The adsorption of cation/anion ions on the crystal surface has a very strong effect on the electrical double layer. Consequently, they should have a specific effect on crystal growth, depending on how the surface charge is it will affect in same way (increasing /decreasing or reversing) the sign of the charge. This means that any electrical potential on the crystal surface may lead to an increase or decrease in the crystal growth rate, or have no effect on it, depending on the dominant effect.

3. Theory

Crystallization is a separation and purification technique employed to produce a wide variety of materials. Crystallization may be defined as a phase change in which a crystalline product is obtained from a solution. A *solution* is a mixture of two or more species that form a homogenous single phase. Solutions are normally thought of in terms of liquids, however, solutions may include solids suspension. Typically, the term *solution* has come to mean a liquid solution consisting a solvent, which is a liquid, and a solute, which is a solid, at the conditions of interest. The solution to be ready for crystallization must be *supersaturated*. A solution in which the solute concentration exceeds the equilibrium (saturated) solute concentration at a given temperature is known as a supersaturated solution [66]. There are four main methods to generate supersaturation that are the following:

- *Temperature change (mainly cooling),*
- *Evaporation of solvent,*
- *Chemical reaction, and*
- *Changing the solvent composition (e.g. salting out).*

The Ostwald-Miers diagram shown in ***Fig. 3.1.*** illustrates the basis of all methods of solution growth. The solid line represents a section of the curve for the solute / solvent system. The upper dashed line is referred to as the super-solubility line and denotes the temperatures and concentration where spontaneous nucleation occurs [67]. The diagram can be evaluated on the basis of three zones:

- *The stable (unsaturated) zone where crystallization is impossible,*
- *The metastable (supersaturated) zone where spontaneous nucleation is improbable but a crystal located in this zone will grow and*
- *The unstable or labile (supersaturated) zone where spontaneous nucleation is probable and so the growth.*

Crystallization from solution can be thought of as a two step process. The first step is the phase separation, (or birth), of a new crystals. The second is the growth of these crystals to larger size. These two processes are known as *nucleation* and *crystal growth*, respectively. Analysis of industrial crystallization processes requires knowledge of both nucleation and crystal growth.

The birth of a new crystals, which is called nucleation, refers to the beginning of the phase separation process. The solute molecules have formed the smallest sized particles possible under the conditions present. The next stage of the crystallization process is for these nuclei to grow larger by the addition of solute molecules from the supersaturated solution. This part of the crystallization process is known as crystal growth. Crystal growth, along with nucleation, controls the final particle size distribution obtained in the system. In addition, the conditions and rate of crystal growth have a significant impact on the product purity and the crystal habit. An understanding of the crystal growth theory and experimental techniques for examining crystal growth from solution are important and very useful in the development of industrial crystallization processes. The many proposed mechanisms of crystal growth may broadly be discussed under a few general headings [67-70]:

- *Surface energy theories*
- *Adsorption layer theories*
- *Kinematic theories*
- *Diffusion - reaction theories*
- *Birth and spread models*

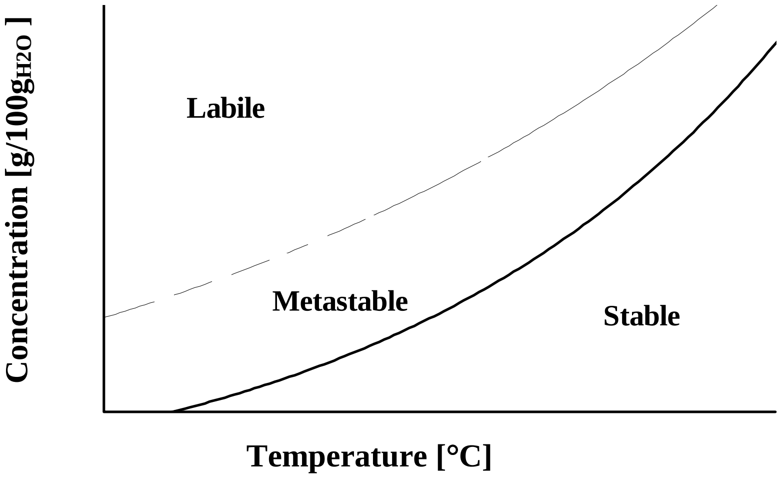

Figure 3.1.*: Ostwald-Miers diagram for a solute/solvent system [67].*

3.1. The Three-Step-model

Modelling of crystal growth in solution crystallization is often done by the Two-Step-Model. The Two-Step-model describes the crystal growth as a superposition of two resistances: bulk diffusion through the mass transfer boundary layer, i.e. diffusion step, and incorporation of growth unites into the crystal lattice, i.e. integration step [67, 68]. The overall growth rate is expressed as:

$$R_G = k_d\,(C_b - C_i) \qquad \text{(diffusion step),} \tag{3.1}$$

$$R_G = k_r\,(C_i - C^*)^r \qquad \text{(integration step),} \tag{3.2}$$

$$R_G = k_G\,(\mathrm{C_b} - \mathrm{C}^*)^{\mathrm{g}} \qquad \text{(overall growth),} \tag{3.3}$$

where $(C_b - C^*)$ is the supersaturation.

The Two-Step-Model is totally ignoring the effect of heat transfer on the crystal growth kinetics. In the literature there is little evidence for the effects of heat transfer on the crystal growth kinetics in the case of crystallization from solution. Matsuoka and Garside [3] give an approach describing the combined heat and mass transfer in crystal growth processes. The so called Three-Step-model of combined mass and heat transfer takes the above mentioned effects into account [1-3]. A mass transfer coefficient is defined which includes a dimensionless temperature increment at the phase boundary constituted by the temperature effect of the liberated crystallization heat and the convective heat transfer. For simplicity the transport processes occurring during growth will be described in terms of the simple film theory. This has the advantage that the resulting equations can be easily solved and the predictions do not differ significantly from those derived using the boundary layer theory [71, 72]. Conditions in the fluid adjacent to the growing crystal surface are illustrated in ***Fig. 3.1.1.***. The mass transfer step can be presented by the equation:

$$\begin{aligned} R_G &= k_d\,(C_b - C_i) = k_d\,[(C_b - C^*_b) - (C_i - C^*_i) - (C^*_i - C^*_b)] \\ &= k_d\,[\Delta C_b - \Delta C_i - (T_i - T_b)\,\frac{dC^*}{dT}] \end{aligned} \tag{3.4}$$

where C^*_i and C^*_b are the saturation concentrations evaluated at the interface and bulk temperatures, respectively. The effect of bulk flow, important at high mass fluxes, is neglected in Eq. 3.4. It is also assumed that the temperature difference $(T_i - T_b)$ is sufficiently small for the solubility curve to be assumed linear over this temperature range. A heat balance relating heat evolution to convective transfer gives:

$$R_G = \frac{h(T_i - T_b)}{-\Delta H} \qquad \text{(heat transfer)}, \tag{3.5}$$

Combination of Eqs. 3.4 and 3.5 gives

$$R_G = \frac{k_d}{1 + \frac{-\Delta H \times k_d}{h} \cdot \frac{dC^*}{dT}} (\Delta C_b - \Delta C_i) = \frac{k_d}{1 + \beta_d} [\Delta C_b - \Delta C_i) = k_d{'}(\Delta C_b - \Delta C_b) \tag{3.6}$$

$$\beta_d = \frac{-\Delta H \times k_d}{h} \cdot \frac{dC^*}{dT} \tag{3.7}$$

Where β_d is defined by Matsuoka and Garside [3] as a dimensionless number for the temperature increase at the crystal surface and therefore as measure of the heat effect on growth kinetics.

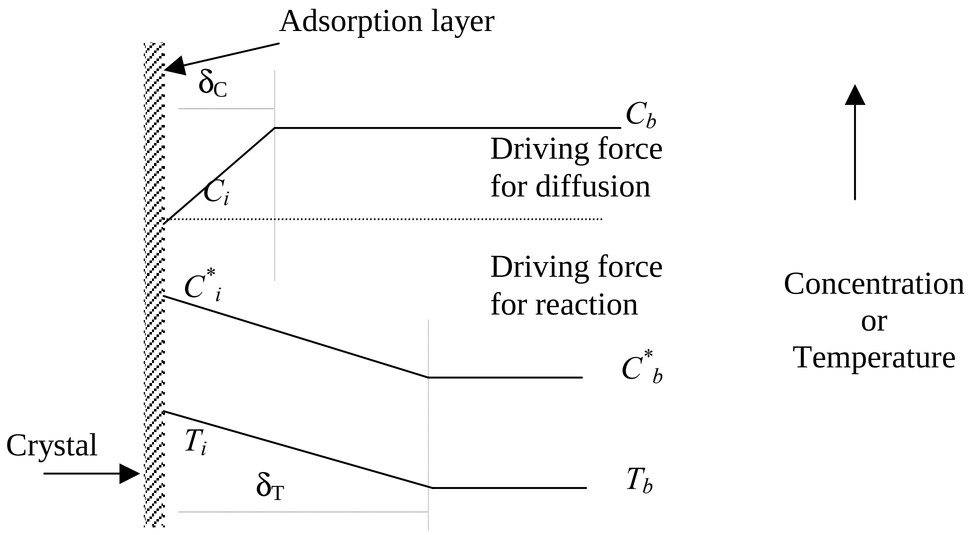

Figure 3.1.1.: *Concentration and temperature profiles to the crystal surface as assumed in the simple film theory [1].*

The analogy between mass transfer and heat transfer is given by [73]:

$$\frac{h}{k_d} = \rho_c \, cp \left(\frac{Sc}{Pr} \right)^{2/3} \equiv \rho_c \, cp \, Le^{2/3} \tag{3.8}$$

substitution Eq. 3.8 into Eq. 3.7 gives the following equation:

$$\beta_d = \frac{-\Delta H}{\rho_c \, cp \, Le^{2/3}} \cdot \frac{dC^*}{dT} \tag{3.9}$$

The general expression for the overall growth rate can be obtained by combining Eqs. 3.1, 3.2 and 3.6:

$$R_G = k_r \left[(C_b - C^*) - R_G \frac{1+\beta_d}{k_d}) \right]^r \tag{3.10}$$

Matsuoka and Garside [3] give a limit β_d must be > 10^{-2}, for values below which the influence of the heat transfer on the crystal growth kinetics can be neglected.

The dissolution process is, on the contrary, quite frequently described only by use of the diffusion step. What is not true since there is definitely a surface disintegration step [4, 5]. In other words dissolution is the 100 % opposite of crystal growth. However, a justification for the model assumption that dissolution can be seen as just diffusion controlled is due to experimental results which show a linear dependence on the concentration difference (undersaturation). Furthermore, the dissolution process is happening according to literature much faster (4 to 6 times) than the crystal growth process so that a possible surface reaction resistance is here difficult to observe [4, 5]. The assumption that the dissolution of crystals involves the sole diffusion step is therefore, in many case valid:

$$R_D = k_d\, (C^* - C_b) \tag{3.11}$$

Two methods, the differential and integration method, are mainly used for the measurements of the growth rates in fluidized bed experiments [74]. In this study the differential method was used. In the differential method, the crystallization is seeded by adding a few grams of crystals with a known sieve aperture into a supersaturated solution. The seed crystals grow in the supersaturated solution. Since the amount of crystals is small, it is assumed that the concentration of the solution does not change during the growth. The other assumptions are as follows:

- The number of seed crystals put into the crystallizer is equal to the number of crystals taken out from the crystallizer.
- There is no crystal loss, an assumption which is always valid for an experienced experiment.
- The shape factor of the growing crystals are considered to be the same. This assumption is not always true especially in the case of surface nucleation. In this case, growth values are thought of as average values.

If the amount of the crystals put into the crystallizer is M_1 and the amount of the crystals taken out from the crystallizer is M_2, they can be related to the size of the crystals L as shown in the following equations [75]:

$$M_1 = \alpha\rho L_1^3, \tag{3.12}$$

$$M_2 = \alpha\rho L_2^3, \tag{3.13}$$

where L_1 and L_2 are the characteristic size of the crystals input and the output, respectively. The overall linear growth rate G (m/s) is defined as the rate of change of characteristic size:

$$G = \frac{\Delta L}{t} \tag{3.14}$$

The expression for the growth rate in terms of size of the seed crystals and the weight of the crystals can be given by:

$$G = \frac{L_1}{t}\left[\left(\frac{M_2}{M_1}\right)^{1/3} - 1\right] \tag{3.15}$$

G and R_G are related to each other as follows:

$$R_G = \frac{3\alpha_1}{\beta_1}\rho_c G \tag{3.16}$$

where β_1 and α_1 are surface and volume shape factors, respectively. M_1 and M_2 are experimentally obtained. The growth rate, R_G, and the dissolution rate, R_D, are calculated from Eq. 3.16 by knowing L_1 and t.

3.2. The concept of effectiveness factors

When crystals grow the rate at which solute is deposited in the crystal lattice is controlled by two resistances in series, those offered by diffusion through the boundary layer and by reaction at the crystal surface. If the rate equations for these two steps are known, the overall crystal growth rate can be easily calculated. It is much more difficult to deduce the kinetics of the individual resistances from measured overall growth rates. Therefore, a quantitative measure of the degree of diffusion or surface integration control may be made through the concept of effectiveness factors. A crystal growth rate effectiveness factors, η, is defined by Garside [76] as the ratio of the overall growth rate to the growth rate that would be obtained if diffusion offered negligible resistance is given by:

$$\eta_r = (1 - \eta_r D_a)^r \tag{3.17}$$

where η_r is the integration effectiveness factor and D_a is the Damköhler number for crystal growth which represents the ratio of the pseudo first order rate coefficient at the bulk conditions to the mass transfer coefficient, defined by:

$$D_a = \frac{k_r}{k_d} (C_b - C^*)^{r-1} \tag{3.18}$$

It will also be convenient to define a diffusion effectiveness factor, η_d as:

$$\eta_d = D_a (1 - \eta_d)^r \tag{3.19}$$

The heat of crystallization produced at the crystal surface will change the solution temperature at this point and hence alter the rates of the kinetics processes. Consequently the effectiveness factor will change from that evaluated under bulk conditions. The non-isothermal effectiveness factor, η', is defined as the ratio of actual growth rate to the rate that would be obtained if the bulk liquid conditions assumed to exist at the crystal surface:

$$\eta' = \frac{growth\ rate\ at\ \Delta C_i\ and\ T_i\ (i.e.\ interface\ conditions)}{growth\ rate\ at\ \Delta C_b\ and\ T_b\ (i.e.\ bulk\ conditions)} \tag{3.20}$$

an analysis similar to that of Carberry and Kulkrani [72] for chemical reaction can be applied to the crystal growth case to yeild

$$\eta' = Da\ (1-\eta')^r \exp\left[-\varepsilon_0\left(\frac{1}{1+\eta' D_a \beta (1+\beta_d)^{-1}} - 1\right)\right] \tag{3.21}$$

where the Damköhler number crystal growth, Da, is defined by

$$D_a = \frac{k_{r,b}}{k_d'} (\Delta C_b)^{r-1} \tag{3.22}$$

and represent the ratio of the pseudo-first order rate coefficient at the bulk conditions to the mass transfer coefficient. The Arrhenius number is defined by:

$$\varepsilon_0 = E/RT_b \tag{3.23}$$

and

$$\beta = \frac{-\varDelta H}{\rho_c \, cp \, Le^{2/3}} \cdot \frac{\varDelta C_b}{T_b} \tag{3.24}$$

is the ratio of the interface adiabatic temperature rise to the bulk temperature. When β_d<<1, Eq. 3.21 becomes identical to that given by Carberry and Kulkrani [72], i.e.:

$$\eta' = Da\ (1-\eta')^{r}\ exp\left[-\varepsilon_0\left(\frac{1}{1+\eta' D_a \beta}-1\right)\right] \tag{3.25}$$

3.3. Model for crystal growth in the presence of impurities

It is well known that the influence of impurities on the crystal form and the growth rate is based on the adsorption of the foreign molecules on the surface. The change of crystal form is based on a difference in adsorption energies on different crystal faces. Foreign molecules will be adsorbed preferentially on surfaces where the free adsorption energy has its maximum. Surface adsorbed impurities can reduce the growth rate of crystals by reducing or hindering the movement of growth steps. Depending on the amount and strength of adsorption, the effect on crystal growth can be very strong or hardly noticeable.

The step advancement velocity is assumed [49] to be hindered by impurity species adsorbing on the step lines at kink sites by a modified mechanism, the original version of which was proposed by Cabrera and Vermileya [14]. Step displacement is pinned (or stopped) by impurities at the points of their adsorption and the step is forced to curve as shown schematically in ***Fig. 3.3.1.***.

The advancement velocity of a curved step, v_r, decreases as the radius of curvature, ρ, is reduced and it becomes zero just at a critical size, $r = r_c$. It is given simply by the following equation [78], if the relative supersaturation is small (σ << 1):

$$\frac{v_r}{v_0} = 1 - \frac{r_c}{r}, \tag{3.26}$$

where v_0 is the velocity of linear step and r_c is the critical radius of a two-dimensional nucleus. At $r \le r_c$ the step cannot move. The instantaneous step advancement velocity changes with time during the step squeezes out between the adjacent adsorbed impurities because the curvature changes with time. The maximum velocity is v_0 (of a linear step) and the minimum instantaneous step velocity v_{min} is given at a curvature of $r = l/2$ (l is average spacing between the adjacent adsorbed impurities) by:

$$\frac{v_{min}}{v_0} = 1 - \frac{r_c}{(l/2)}. \tag{3.27}$$

Time-averaged advancement velocity v of a step is approximated by the arithmetic mean of v_0 and v_{min} [77] as:

$$v = (v_0 + v_{min})/2\ . \tag{3.28}$$

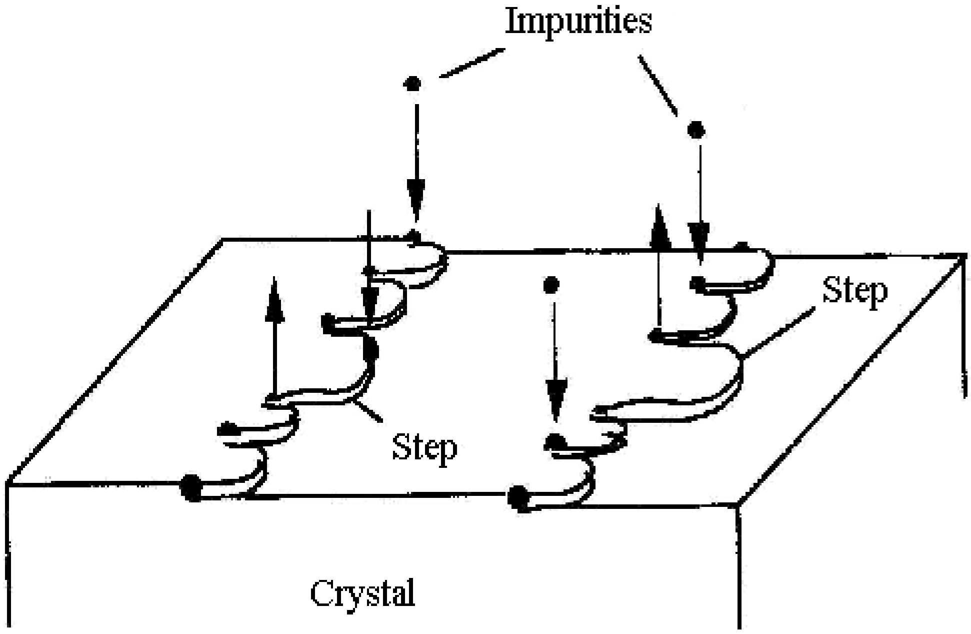

Figure 3.3.1.: *Model of impurity adsorption. Impurity species are assumed to be adsorbed on the step lines at kink sites and to retard the advancement of the steps [77].*

Combining Eqs. 3.27 and 3.28 one obtains the following equation for the average step advancement velocity as a function of the average spacing between the impurities, l:

$$\frac{v}{v_0} = 1 - \frac{r_c}{l}. \tag{3.29}$$

while $v = 0$ for $l \le r_c$.

This simple equation was thus obtained by assuming the linear array of sites on the step lines and by using the arithmetic mean of the maximum and minimum step velocities as an average step velocity.

The coverage of active sites by impurities θ can be related to the average distance between the active sites λ, from a simple geometric consideration, under the assumption of linear adsorption on the step lines (linear array) as:

$$\theta = \lambda/l \tag{3.30}$$

on the other hand, the critical radius of a two-dimensional nucleus is given by Burton et al. [78] as:

$$r_c = \left(\frac{\gamma a}{k_B T\sigma}\right) \qquad \text{(for } \sigma << 1\text{)} \tag{3.31}$$

Insertion of Eqs. 3.30 and 3.31 into Eq. 3.29 gives the following equation:

$$\frac{v}{v_0} = 1 - \left(\frac{\gamma a}{k_B T\sigma\lambda}\right)\theta, \tag{3.32}$$

where γ is the linear edge free energy of the step, a is the size of the growth unit (area per growth unit appearing on the crysatl surface), k_B is the Boltzmann constant, T is the temperature in Kelvin.

As soon as kinks and steps are occupied by foreign molecules, the coverage of crystal faces causes a reduction in growth rate [48]. If all active centres for growth are blocked, growth rates can be reduced to zero. Kubota et al. [77], introduce the impurity effectiveness factor, α. The effectiveness factor α is a parameter accounting for the effectiveness of an impurity under a given growth condition (temperature and supersaturation). Thus, the step advancement velocity can be written as a function of temperature and supersaturation:

$$\alpha = \left(\frac{\gamma a}{k_B T\sigma\lambda}\right) \tag{3.33}$$

Eq. 3.32 can be changed to

$$\frac{v}{v_0} = 1 - \alpha\theta, \qquad \text{(for } \alpha\theta < 1\text{)} \tag{3.34}$$

where $v = 0$ for $\alpha\theta \geq 1$.

This impurity effectiveness factor can be less than or equal or greater than one. α decreases with increasing supersaturation and is independent of K. In ***Fig. 3.3.2.***, the relative step velocities, calculated from Eq. 3.34, are shown for different effectiveness factors, α, as a function of the dimensionless impurity concentration Kc_{imp}.

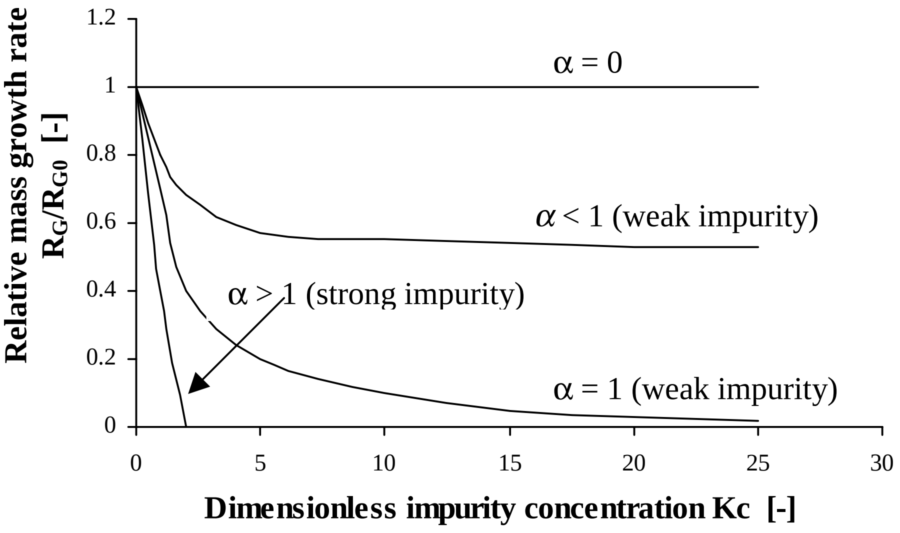

Figure 3.3.2.: *Theoretical relationship between the relative mass growth rate, R_G/R_{Go}, and the dimensionless impurity concentration, Kc, for different value of α. (diagram based on the work of [77]).*

It is clear from ***Fig. 3.3.2.*** that, when $\alpha > 1$, the relative velocity decreases very steeply with increasing impurity concentration and reaches zero at a small value of Kc_{imp}. For $\alpha = 1$, a full coverage of the crystal surface leads to step velocity equal to zero. For $\alpha < 1$, however, the step velocity never approaches zero but approaches a non-zero value as Kc_{imp} is increased. This value is increasing with smaller α and is one at a value of $\alpha = 0$.

If an equilibrium adsorption is assumed for an impurity [49, 77], the surface coverage θ in Eq. 3.36 is replaced by an equilibrium value θ_{eq}:

$$\frac{v}{v_0} = 1 - \alpha\theta_{eq} \tag{3.35}$$

and the step advancement velocity may be related to the concentration of the impurity c_{imp} if an appropriate isotherm is employed. Although any adsorption isotherm can be used for this purpose. Therefore, the coverage, θ_{eq}, of adsorption sites may be described by the usual adsorption isotherms [35, 79, 80]:

$$\theta_{eq} = \frac{Kc_{imp}}{1 + Kc_{imp}} \qquad \text{(Langmuir isotherm)} \qquad (3.36)$$

In this equation K is constant. The constant K of Eq. 3.36 is given by [79, 80]:

$$K = exp(Q_{diff} / R\ T) \qquad (3.37)$$

where Q_{diff} is the differential heat of adsorption corresponding to θ_{eq}.

In the case of a spiral growth mechanism, the relationship between the step velocity at a crystal face, v, and the fraction coverage, θ_{eq}, of the surface may be given by [81, 82]:

$$(v - v/vo)^{\ n} = \alpha^n \theta_{eq} \qquad (3.38)$$

The exponent n=1 and 2 represents the case at which impurity adsorption occurs at kinks in step edges and on the surface terrace, respectively.

The relative step velocity in Eq. 3.38, can be replaced by the relative growth rate R_G/R_{Go} if the growth rate is assumed to be proportional to the step velocity:

$$(R_{Go} - R_G / R_{Go})^{\ n} = \alpha^n \theta_{\mathrm{eq}} \qquad (3.39)$$

The previous model of impurity adsorption considering kinks and the surface terraces deal with the kinetic aspect of adsorption of impurities of F faces, neglecting the thermodynamic effects. Therefore, for all the above equations it is true that growth rates are reduced, when impurities are present in the solution. Generally, experiments carried out in a fluidized bed crystallizers [83-86] showed that the addition of small amounts of impurities lead to a decrease in growth rates. This is in good agreement with theoretical predictions published in the literature [84, 87].

3.4. Electrical double layer

The charge that develops at the interface between a particle surface and its liquid medium may arise by any of several mechanisms. Among these are the dissociation of inorganic groups in the particle surface and the differential adsorption of solution ions in to the surface region. The net charge at the particle surface affects the ion distribution in the nearby region, increasing the concentration of counter-ions close to the surface. Thus, an *electrical double layer* is formed in the region of the particle-liquid interface [88-90]. The *electric double layer* plays a major role in diverse area such as adhesion, self-assembly, filtration, wetting, electrokinetics, and it is perhaps the major determinant the colloidal interactions and colloid stability.

If a liquid moves tangential to a charged surface, then so called *electrickinetic* phenomena. *Electrickinetic* phenomena can be divided into four categories [88-90]:

- *Electrophoresis*: the movement of charged particles suspended in a liquid under the influence of an applied electric field.
- *Electroosmosis*: the movement of liquid in contact with a stationary charged solid, again in response to an applied electric field.
- *Streaming Potential*: is generated when a liquid is forced under pressure to move in contact with a stationary charged solid.
- *Sedimentation Potential*: may be regarded as the converse of *electrophoresis*. It arises when charged particles move through a stationary liquid under the influence of gravity.

In all these phenomena the z*eta (ζ) potential* plays a crucial role.

What is *zeta (ζ) potential* ?

Most particles in a polar medium such as water posses a *surface charge*. A charged particle will attract ions of the opposite charge in the dispersant, forming a strongly bound layer close to the surface of the particle. These ions further away from the core particle make up a *diffuse layer*, more loosely bound to the particle. Within this *diffuse layer* is a notional boundary, inside which the particle and its associated ions act as a single entity, diffusing through the dispersion together. The plane at this boundary is known as the *surface of shear*, or the slipping plane [88].

Surface of shear is an imaginary surface which considered to lye to the solid surface and within which the fluid is stationary. In the case of a particle undergoing *electrophoresis*, the surface forms a sheath which envelopes the particle. All of the material inside that sheath forms the kinetic unit. So that the particle moves along with a certain quantity of the surrounding liquid and its contained charge. Measurement of *electrophoretic mobility* (i.e. the velocity per unit electric field) therefore gives a measure of the net charge on the solid particle. The analysis of the forces on the solid or the liquid can be carried out in terms of either charge or electrostatic potential. In the later case one calculates the average potential in the *surface of shear*; this is called the *ζ-potential* [88].

Why not use the *surface charge*?

The interaction of particles in a polar liquid is not governed by the electrical potential at the surface of the particle, but by the potential that exists at the slipping plane (*surface of shear*). The *ζ-potential* and *surface charge* can be entirely unrelated, so measurement of *surface charge* is not an useful indication of particle interaction. Therefore, to utilize electrostatic control, it is the *ζ-potential* of a particle that is needed to know rather than its *surface charge*.

3.4.1. Origins of surface charge

Most particles acquire a surface electric charge when brought into contact with a polar (e.g. aqueous) medium. The more important mechanisms which caused to acquire the particle a charge are [88]:

- Ion dissolution, and
- Ionization of surface groups.

As a result:

- Ions of opposite charge (*counter–ions*) are attracted towards the surface.
- Ions of the same charge (*co–ions*) are repelled away from the surface.

The above mentioned leads to the formation of an *electric double layer* made up of the charged surface and a neutralising excess of counter-ions over co-ions distribution in a diffuse manner in the aqueous solution.

3.4.1.1. Ion dissolution

This is defined as acquiring a surface charge by unequal dissolution of the oppositely charged ions of which they are composed. For the *AgI*/water system, for instance, the charge separation at the interface between the crystal and an aqueous electrolyte solution can be thought of as being due to either the differential of adsorption of ions from an electrolyte solution on to a solid surface, or the differential solution of one type of ion over the other from a crystal lattice. The surface of the crystal may be treated as a separate phase and, at equilibrium, the electrochemical potential of both Ag^+ and I^- ions must be the same in this phase as they are in the bulk aqueous solution:

$$\mu^0{}_l\,(Ag^+) + k_BT\,ln\,[a_l\,(Ag^+)] + zq\Phi_l = \mu^0{}_s\,(Ag^+) + k_BT\,ln[a_s\,(Ag^+)] + zq\Phi_s \qquad (3.40)$$

$\mu^0{}_s\,(Ag^+)$ and $\mu^0{}_l\,(Ag^+)$ are the chemical standard potential at the crystal surface and in solution, respectively. Φ_s and Φ_l are the Galvani potential in the crystal and in the solution. In particular, the equation is valid at the *point of zero charge* (the concentration of the *potential-determined ion* at which the colloid has no net charge is called the *point of zero charge, pzc*) [88, 92]:

$$\mu^0{}_l\,(Ag^+) + k_BT\,ln\,[a_l^{pzc}\,(Ag^+)] = \mu^0{}_s\,(Ag^+) + k_BT\,ln[a_s^{pzc}\,(Ag^+)] + zq\,\Delta\chi^{pzc} \qquad (3.41)$$

$\Delta\chi^{pzc}$ is the difference of the Galvani potentials, which is caused solely by dipoles in the interface, not by free charges. The subtract Eqs. 3.40 and 3.41 lead to:

$$k_BT\,ln\,\frac{a_l(Ag^+)}{a_l^{pzc}(Ag^+)} = zq\,(\Phi_s - \Phi_l - \Delta\chi^{pzc}) \qquad (3.42)$$

It is assumed that $a_s\,(Ag^+) = a_s^{pzc}\,(Ag^+)$. The expression in brackets is called *surface potential*, ψ_0. Thus one obtains the Nernst equation:

$$\Psi_0 = \frac{k_BT}{zq}\,ln\,\frac{a_l(Ag^+)}{a_l^{pzc}(Ag^+)} \qquad (3.43)$$

The concentration of Ag^+ (and thus that of I^-) determines the *surface potential*. During the derivation it is assumed that $a_s\,(Ag^+) = a_s^{pzc}\,(Ag^+)$. That means that during the charging of the AgI surface the activity of the Ag^+ ions on the surface do not change. This assumption is justified to a large extent, because the number of Ag^+ ions on the surface changes only slightly. The relative number of ions, i.e. the number of the additinally adsorbed ions upon a variation of the potential, is very small.

3.4.1.2. Ionization of surface groups

The ionization of surface groups, i.e. charge development, is commonly observed with carboxylic acid, amine and oxide surface faces. In these systems the charge development (and its sign) depends on the pH of the solution. The potential determining ions are OH^- and H_3O^+. Oxide surfaces, for example, are considered to posses a large number of amphoteric hydroxyl groups which can undergo reaction with either H_3O^+ or OH^- depending on the pH [88, 90-94]:

$$\left.\begin{array}{l} -MOH + H_3O^+ \leftrightarrow MOH^+{}_2 + H_2O \\ \\ -MOH + OH^- \leftrightarrow MO^- + H_2O \end{array}\right\} \tag{3.44}$$

This shows the amphoteric nature of the surface. At high pH the surface is negatively charged, and low pH it is positively charged. The surface potential, Ψ_0, is given by the Nernst equation as a function of H_3O^+/OH^- ions:

$$\Psi_0 = -2.303\ \frac{k_B T}{q}\ (pH - pH_{pzc}) \tag{3.45}$$

is no longer satisfactory for describing the surface potential because the assumption that $a_s\ (H_3O^+) = a_s^{pzc}\ (H_3O^+)$ is clearly untenable. In these systems there are very few H_3O^+ ions present on the surface at the pzc and it is certainly not true that the number of additional H_3O^+ ions required to establish the charge is insignificant by comparison. A modified Nernst equation was derived by Smith [97]. Essentially Eq. 3.45 must be replaced by:

$$\Psi_0 = -2.303\ \frac{k_B T}{q}\left[pH - pH_{pzc} + \log\frac{a_s(H^+)}{a_s^{pzc}(H^+)}\right] \tag{3.46}$$

The additional term has the effect of lowering the expected double layer potential which is in keeping with the experimental observation.

3.4.2. Electrophoresis

Electrophoresis is defined as the migration of ions under the influnce of an electric field. The force ($F = qE$) imparted by the electrical field is proportional to its effective charge, q, and the electric field strength, E. The translation movement of the ion is opposed by a retarding frictional force ($F_f = fv$), which is proportional to the velocity of the ion, v, and the friction coefficient, f. the ion almost instantly reaches a steady state velocity where the acceleration force equals the frictional force.

$$qE = f\,v \qquad \Rightarrow \qquad v = (q/f)\,E = u\,E \tag{3.47}$$

Here u is the electrophoretic mobility of the ion, which is a constant of proportionality between the velocity of the ion and the electric field strength. The electrophoretic mobility is proportional to the charge of the ion and inversely proportional to the friction coefficient. The friction coefficient of the moving ion is related to the hydrodynamic radius, a_1, of the ion and the viscocity, μ, of the surrounding medium, $f = 6\pi\mu a_1$, because $u = q/f$, a larger hydrodynamic radius translates to a lower electrophoretic mobility.

The effective charge arises from both the actual surface charge and also the charge in the double layer. The thickness of the double layer is quantified by a_1 parameter with the dimensions of inverse length k, so that the dimensionless number ka_1 effectively measures the ratio of particle radius to double layer thickness. The figure below illustrates the typical situation.

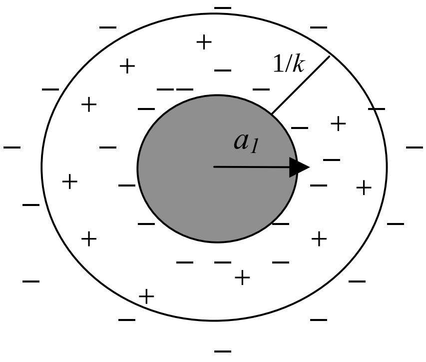

Figure 3.4.1.: *Apparent charge distiribution around a spherical particale at low potential [88].*

It turns out that q can be estimated using some approximations. Providing that the value of charge is *low*, (zeta potential less than 30 mV or so) the Henry equation can be applied [88, 98-100]:

$$u = (2\varepsilon\zeta / 3\mu)\, f(ka_1) \qquad (3.48)$$

Henry‘s function, $f(ka_1)$, vaires smoothly from 1 to 1.5 as ka vaires from 0 to ∞, these corresponding to limiting cases where the particle is much smaller than the double layer thickness, or much larger.

3.4.3. The diffusion double layer (The Gouy–Chapman model)

Surface charge cause an electrical field. This electrical field attracts counter ions. The layer of surface charges and counter ions is called *electrical double layer*. The first theory for the description of *electrical double layers* comes from Helmholtz started with the fact that a layer of counter ions binds to the surface charges [88-96]. The counter ions are directly adsorbed to the surface. The charge of the counter ions exactly compensates the surface charge. The electrical field generated by the surface charge is accordingly limited to the thickness of a *molecular layer*. Helmholtz could interpret measurements of the capacity of double layers; electrokinetic experiments, however, contradicted his theory.

Gouy and Chapman went a step further. They considered a possible thermal motion of the counter ions. This thermal motion leads to the formation of a *diffuse layer*, which is more extended than a *molecular layer* [88]. For the one-dimensional case of a planar, negatively charged plane this is shown in the illustration. Gouy and Chapman applied their theory on the *electrical double layer* of planar surface. Later, Debye and Hückel calculated the behaviour around spherical solids.

Fig. 3.4.2. portrays schematically the discrete regions into which the inner part of the double layer has been divided. First there is the layer of dehydrated ions (i.e. *Inner Helmholtz Plane, I.H.P.*) having potential, Ψ_0, and surface charge, σ_0, and second there is the first layer of hydrated ions (i.e. *Outer Helmholtz Plane, O.H.P.*) having potential, Ψ_d, and charge, σ_d. The *O.H.P.* marks beginnings of the diffuse layer [88, 92].

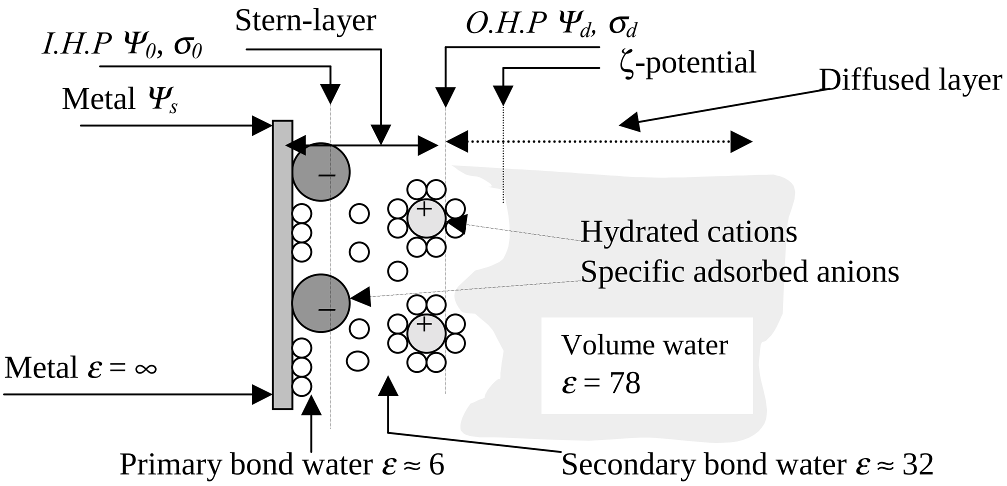

***Figure 3.4.2.**: Schematic representation of the solid-liquid interface [92].*

3.4.3.1. The Poisson-Boltzmann equation

The aim is to calculate the electrical potential, Ψ, near charged interfaces. Therefore, here a plane is considered with a homogenous distributed electrical charge density, ρ, which is in contact with a liquid. Generally charge density and potential are related by the Poisson equation [88-90]:

$$\nabla^2\Psi = \frac{\partial^2\Psi}{\partial x^2} + \frac{\partial^2\Psi}{\partial x^2} + \frac{\partial^2\Psi}{\partial x^2} = -\frac{\rho_e}{\varepsilon\varepsilon_0} \tag{3.49}$$

With the Poisson equation the potential distribution can be calculated once the position of all charges are known. The complication in our case is that the ions in solution are free to move. Since their distributions, and thus the charge distribution in the liquid, is unknown, the potential cannot be found only by applying the Poisson equation. Additional information is required.

This additional formula is the Boltzmann equation. If we have to bring an ion in solution from far away closer to the surface, electric work W_i has to be done. The local ion density would be:

$$n_i = n_i^0 \, e^{-W_i/k_B T} \tag{3.50}$$

n_i^0 is the density of the i^{th} ion sort in the volume phase, given in particles/m^3. The local ion concentration depends on the electrical potential at the respective place. For example, if the potential at a certain place in the solution is positive, then at this place there will be more anions, while the cation concentration is reduced.

Now it is assumed that only electrical work has to be done. It is furthermore neglected for instance that the ion must displace other molecules. In addition, it is assumed that only a 1:1 salt is dissolved in the liquid. The electrical work required to bring a charged cation to a place with potential Ψ is $W^+ = q\Psi$. For an anion it is $W^- = -q\Psi$. The local anion and cation concentration n^- and n^+ are related with the local potential Ψ through the Boltzmann factor:

$$n^- = n_0\, e^{q\Psi/k_BT} \quad , \quad n^+ = n_0\, e^{-q\Psi/k_BT} \tag{3.51}$$

n_0 is the volume concentration of the salt. The local charge density is:

$$\rho_e = q(n^- - n^+) = n_0\, q \left(e^{-\frac{q\Psi}{k_BT}} - e^{\frac{q\Psi}{k_BT}} \right) \tag{3.52}$$

Substituting the charge density into Poisson eduation gives the Poisson–Boltzmann equation:

$$\nabla^2\Psi = \frac{n_0\, q}{\varepsilon\varepsilon_0} \left(e^{\frac{q\Psi(x,y,z)}{k_BT}} - e^{-\frac{q\Psi(x,y,z)}{k_BT}} \right) \tag{3.53}$$

This is a partial differential equation of second order. In most cases, it cannot be solved analytically. Nevertheless, some simple cases can be treated analytically.

One dimensional geometry

A simple case is the one-dimensional situation of a planar, infinitely extended plane. In this case the Poisson-Boltzmann equation only contains the coordinate vertical to the plane:

$$\frac{d^2\Psi}{dx^2} = \frac{n_0\, q}{\varepsilon\varepsilon_0} \left(e^{\frac{q\Psi(x)}{k_BT}} - e^{-\frac{q\Psi(x)}{k_BT}} \right) \tag{3.54}$$

before it is solved this equation for the general case, it is illustrative to treat a special case:

A. Low potential

How does the potential change with distance for small surface potential? “Small” means, strictly speaking $q|\Psi_0| << k_BT$. At room temperature that would be ≈ 25 mV. Often the result is valid even for higher potentials, up to approximately 50-80 mV. With small potentials it can be expanded that the exponential functions into a series and neglect all but the first (i.e. the linear) term:

$$\frac{d^2\Psi}{dx^2} \approx \frac{n_0 q}{\varepsilon\varepsilon_0}\left(1+\frac{q\Psi}{k_BT}-1+\frac{q\Psi}{k_BT}\pm....\right)=\frac{2n_0 q^2}{\varepsilon\varepsilon_0 k_BT}\Psi \tag{3.55}$$

This is some times called the linearized Poisson-Boltzmann equation. The general solution of the linearized Poisson-Boltzmann equation is:

$$\Psi(x) = C_1\, e^{-kx} + C_2\, e^{kx} \tag{3.56}$$

with

$$k=\sqrt{\frac{2n_0 q^2}{\varepsilon\varepsilon_0 k_BT}} \tag{3.57}$$

C_1 and C_2 are constants which are defined by boundary conditions. For a simple double layer the boundary conditions are $\Psi(x \to \infty) = 0$ and $\Psi(x = 0) = \Psi_0$. The first boundary condition guarantees that with very large distances the potential disappears and does not grow infinitely. From this follows $C_2 = 0$. From the second boundary condition follows $C_1 = \Psi_0$. Hence, the potential is given by:

$$\Psi = \Psi_0\, e^{-kx} \tag{3.58}$$

The potential decreases exponentially. The typical decay length is given by $\lambda_D = k^{-1}$. It is called the *Debye length*.

The *Debye length* decreases with increasing salt concentration. That is intuitively clear: The more ions are in the solution, the more effective is the shielding of the surface charge. If one quantifies all the factors for water at room temperature, then for a monovalent salt with concentration c the *Debye length* is $\lambda_D = 3/\sqrt{c}$ Å, with c in mol/l.

B. Arbitrary potential

Now comes the general solution of the one-dimensional Poisson-Boltzmann equation. It is convenient to treat the equation with dimensionless potential $y \equiv q\Psi/kT$. The Poisson-Boltzmann equation becomes thereby:

$$\frac{d^2y}{dx^2} \approx \frac{n_0\, q}{\varepsilon\varepsilon_0\, k_B T}\left(e^{y} - e^{-y}\right) = \frac{2n_0\, q^2}{\varepsilon\varepsilon_0\, k_B T} . \frac{1}{2}\left(e^{y} - e^{-y}\right) = k^2 \, sinhy \tag{3.59}$$

To obtain this it is used:

$$\frac{d^2y}{dx^2} \approx \frac{q}{k_B T}\frac{d^2\Psi}{dx^2} \qquad \text{and} \qquad sinh\, y = 1/2\ \left(e^{y} - e^{-y}\right)$$

The solution of the differential equation 3.59 is:

$$\ln\left(\frac{e^{y/2} - 1}{e^{y/2} + 1}\right) = -kx + C \tag{3.60}$$

The potential must correspond to the surface potential for x = 0, that means $y(x = 0) = y_0$. With the boundary condition one gets the integration constant

$$\ln\left(\frac{e^{y_0/2} - 1}{e^{y_0/2} + 1}\right) = C \tag{3.61}$$

substitution results in

$$\left.\begin{aligned}
&\ln\left(\frac{e^{y/2} - 1}{e^{y/2} + 1}\right) - \ln\left(\frac{e^{y_0/2} - 1}{e^{y_0/2} + 1}\right) = \ln\left(\frac{e^{y/2} - 1 + e^{y_0/2} + 1}{e^{y/2} + 1 + e^{y_0/2} - 1}\right) = -kx \\
&\Rightarrow e^{-kx} = \frac{e^{y/2} - 1 + e^{y_0/2} + 1}{e^{y/2} + 1 + e^{y_0/2} - 1}
\end{aligned}\right\} \tag{3.62}$$

solving the Eq. 3.62 for $e^{y/2}$ leads to the alternative expression:

$$e^{y/2} = \frac{e^{y_0/2} + 1 + (e^{y_0/2} - 1)e^{-kx}}{e^{y_0/2} + 1 - (e^{y_0/2} - 1)e^{-kx}} \tag{3.63}$$

The potential and the ion concentrations are shown as an example in the illustration. A surface potential of 50 mV and a salt concentration (monovalent) of 0.1 M were assumed.

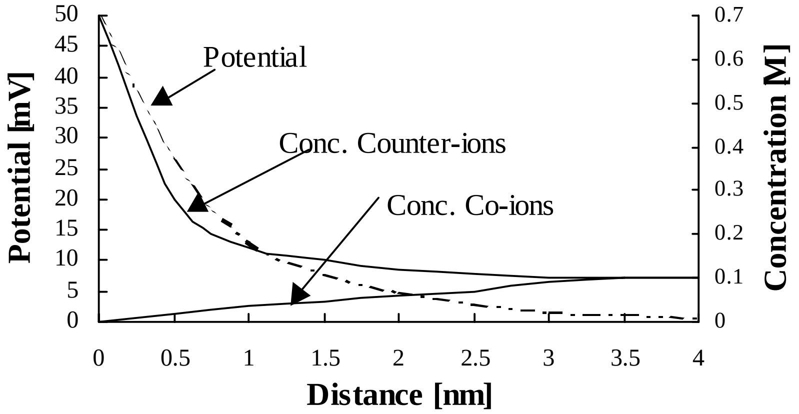

Figure 3.4.3.: *The relation between the surface potential and salt concentrations.*

It is clear that:

- *The potential decreases approximately exponentially with increasing distance.*
- *The salt concentration of the counter ions decreases more rapidly than the potential.*
- *The total ion concentration close to the surface is increased.*

In the following illustration the potential, which is calculated with the linearized form of the Poisson-Boltzmann equation (dashed), is compared with the potential which results from the complete expression. It can be seen that the decrease of the potential becomes steeper with increasing salt concentration. This reflects that the *Debye length* decreases with increasing salt concentration.

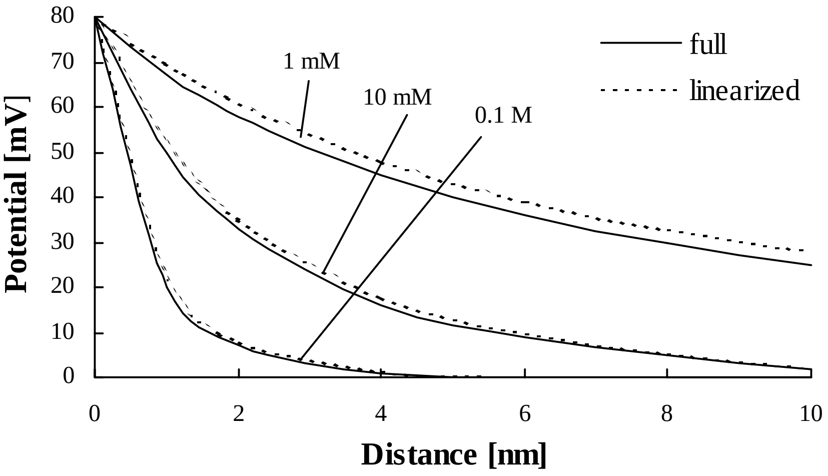

Figure 3.4.4.: *The relation between the surface potential and electrical double layer thickness at different salt concentrations.*

3.4.3.2. The Grahame equation

How are surface charge and surface potential related? This question is important, since the relation can be examined with the help of a capacity measurement. Theoretically this relation is described by the Grahame equation. One can deduce the equation easily from the so called electroneutrality condition. This condition demands that the total charge, i.e. the surface charge plus the charge of the ion in the whole double layer, must be zero. The total charge in the double layer is $\int_0^\infty \rho_e \, dx$ and it is leads to:

$$\sigma = -\int_0^\infty \rho_e \, dx = \varepsilon\varepsilon_0 \int_0^\infty \frac{d^2\Psi}{dx^2} \, dx = -\varepsilon\varepsilon_0 \left.\frac{d\Psi}{dx}\right|_{x=0} \tag{3.64}$$

in the final step we has used $d\Psi/dx\,|_{x=\infty} = 0$. With

$\frac{dy}{dx} = \frac{d(q\Psi/k_BT)}{dx} = \frac{q}{k_BT}\frac{d\Psi}{dx}$ and $\frac{dy}{dx} = -2k \sinh\frac{y}{2}$ follows

$$\sigma = \sqrt{8\, n_0\, \varepsilon\varepsilon_0\, k_BT}\, \sinh\left(\frac{q\Psi_0}{2k_BT}\right) \tag{3.65}$$

For small potential one can expand $sinh$ into a series ($\sinh x = x + x^3/3! + \ldots$) and break off after the first term. That leads to the simple relation:

$$\sigma = \frac{\varepsilon\varepsilon_0\Psi_0}{\lambda_D} \tag{3.66}$$

The following illustration shows the calculated relation between surface tension and surface charge for different concentrations of a monovalent salt.

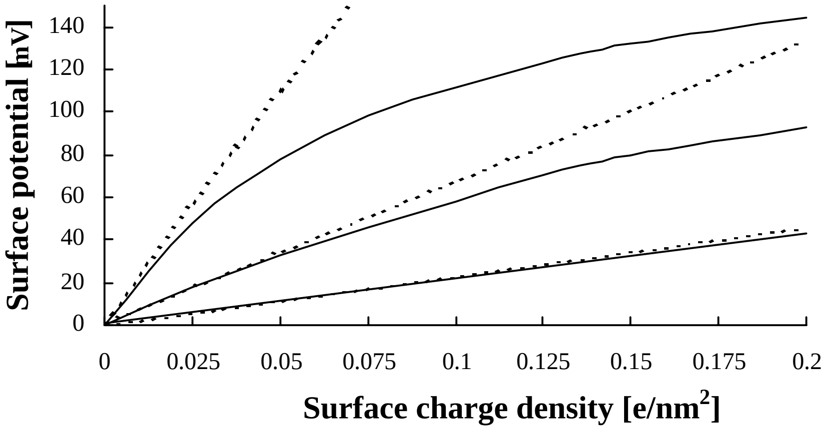

***Figure 3.4.5.**: The relation between the surface potential and surface charge density at different salt concentrations.*

It is clear that:

- *For small potential* σ *is proportional to* Ψ_0.
- *For high potential* σ *rises more steeply then* Ψ_0.
- *The capacity* $d\sigma/d\Psi_0$ *grows with increasing surface potential.*
- *Depending on the salt concentration, the linear approximation (dashed) is valid till* $\Psi_0 \approx 40....80\ mV$.

3.4.3.3. The capacity of the double layer

A plate capacitor has the capacity:

$$C = dQ/dU = \varepsilon\varepsilon_0 A/d \tag{3.67}$$

Q: Charge, U: Applied voltage, A Area, d: Distance. The capacity of the electrical double layer per area is thus

$$C = \frac{d\sigma}{d\Psi_0} = \sqrt{\frac{2q^2 n_0 \varepsilon\varepsilon_0}{k_B T}} cosh\left(\frac{q\Psi_0}{2k_B T}\right) = \frac{\varepsilon\varepsilon_0}{\lambda_D} cosh\left(\frac{q\Psi_0}{2k_B T}\right) \tag{3.68}$$

it can be expanded *cosh* into a series ($cosh\ x = 1 + x^2/2! + x^4/4! + ...$) and for small potential it can be broken off after the second term, then results:

$$C = \frac{\varepsilon\varepsilon_0}{\lambda_D} \tag{3.69}$$

3.4.4. Additional description of the *electrical double layer*

The Gouy-Chapman model is unrealistic for high surface potential Ψ_0 and small distances because then the ion concentration becomes too high. Stern tried to handle this problem by dividing the region close to the surface into two regions:

- The Stern-layer, consisting of a layer of ions, which as assumed by Helmholtz, are directly adsorbed to the surface.

- A diffuse Gouy-Chapman layer.

In reality all models can only describe certain aspects of the *electrical double layer*. The real situation at a metal surface might for instance look like in the following illustration.

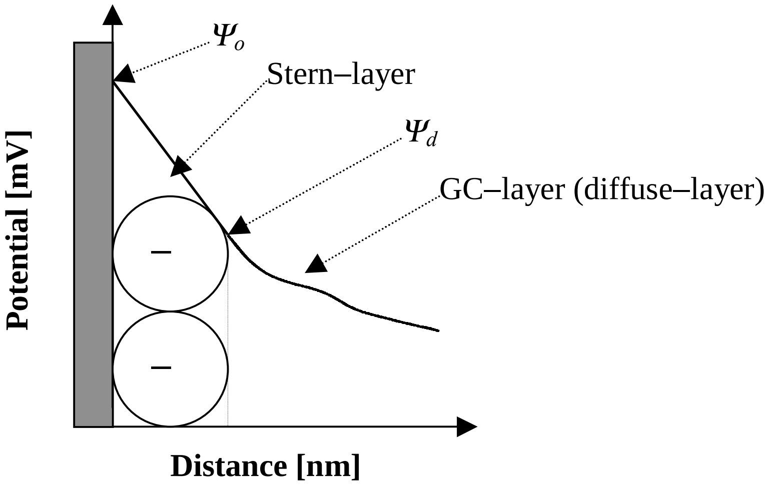

***Figure 3.4.3.**: Schematic represantation of the double layer, Stern layer and diffusion layer (GC layer)*

The surface potential, Ψ_0, is determined by the external potential and by adsorbed ions. These ions are not distinguishable from the metal itself (e.g. Ag^+ or I^- on AgI). Next comes a layer or relatively tightly bound, hydrated ions (e.g. H^+ or OH^- on oxides or proteins). If this layer exists it contributed to Ψ_0. The so called *Inner Helmholtz Plane, I.H.P.,* marks the centre of these ions. The Stern layer consists of adsorbed, hydrated ions. The *Outer Helmholtz Plane, O.H.P.*, goes through the centre of these ions. Finally there is the *diffuse layer*. The potential at the distance where it originates corresponds roughly to the z*eta-potential*.

4. Experimental work

4.1. Fluidized bed experiments

4.1.1. Fluidized bed measurement equipment

The fluidized bed crystallization system, already used and discussed e.g. by [1, 4, 62, 101] is consists of a pump and two heat exchangers in addition to cell. The fluidized bed cell is shown in ***Fig. 4.1.***, and is made of acrylicglass. The crystallization system is assembled in the process of chemical engineering department's laboratory. The pump is a centrifugal pump (Iwaki magnet pump, model MD 30R-220N), the two heat exchangers were connected to two water baths, one (HAAKE N3, typ 001-5722) adjusted to keep the solution undersaturation in the vessel (heating) while the other (HAAKE F3, typ 002-0991) operates as a cooler to create the required supersaturation and undersaturation level in the growth and dissolution zone, each water bath is connected to a centrifugal pump.

4.1.2. Procedure

The experimental setup of the fluidized bed crystallization system is shown in ***Fig. 4.1..*** It consists of a pump and two heat exchangers in addition to a cell. The fluidized bed cell is made of acrylglas. The pump is a centrifugal pump. The two heat exchangers were connected to two water baths. One to keep the solution undersaturation in the vessel (heating). The second heat exchanger operates as a cooler or heater to create the required supersaturation or undersaturation level in the growth and dissolution zone, respectively.

A saturated solution of $NaCl/MgSO_4 \bullet 7H_2O$ is prepared according to the solubility data of Mullin [67]. The solution was prepared by dissolving the required amount of $NaCl/MgSO_4 \bullet 7H_2O$ in 7 liters of distilled water. The saturated solution is transferred to the reservoir of the crystallization system. The solution started circulation through the crystallization system. The temperatures of the two water baths were adjusted to keep the solution undersaturation in the reservoir (heating) and slightly supersaturated or undersaturated in the growth and dissolution zone (cooling/heating). Usually a temperature is decreased less than the saturation temperature to have the solution in the metastable zone for the growth rate measurements. For dissolution rate measurements, a temperature higher than the saturation temperature is enough to create the required undersaturation. In case of growth rate measurements in dependence of an impurity concentration a carefully weighed amount of impurity is added to the solution.

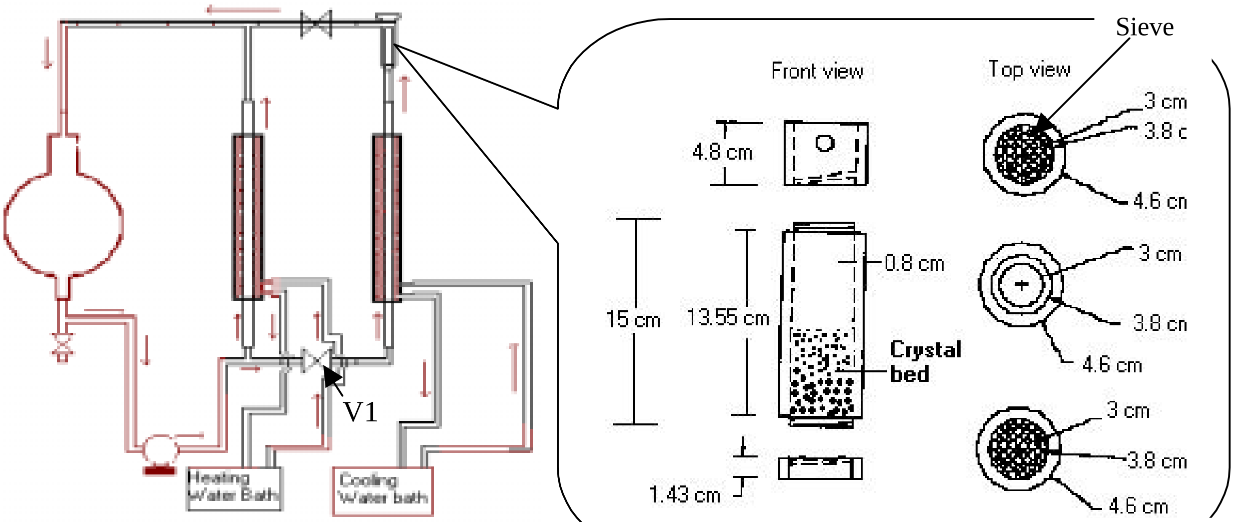

Details of the acrylglas fluidized bed cell

***Figure 4.1.**: Fluidized Bed Experimental Setup.*

With *NaCl* experiments the saturation temperature was 30°C the seed crystals were 315–250 µm and the initial weight for all runs was 5 g. These seeds were put into the cell. When the temperature of the solution reached the required temperature, the cell was fixed in its place. Adjusting the valve V1 in the system controlled the fluidization velocity. A stopwatch was used to evaluate the operating time for each run. At the end of the run, valve V1 was fully opened to keep the solution away from the cell then the cell content was filtered and washed with ethyl alcohol. The filtered crystals were dried at 50°C for 4 hours. After that, the crystals were cooled to ambient temperature and weight. The difference in weight of the crystals before and after the experiment is used in calculating the growth rate or the dissolution rate, respectively.

While, in the case of $MgSO_4 \bullet 7H_2O$ experiments the saturation temperature was 25°C, the seed crystals were obtained from sieve fractions with a mean size 1mm. In all runs the initial weight of seed crystals was 3 g. After 15 of growth minutes the crystals were washed with ethanol, dried at room temperature and weighed.

Changing the pH-value of the solution is done by addition of H_2SO_4 to obtain acidic solutions and *NaOH* to obtain alkaline solutions. In case of growth rate measurements in dependence of impurity concentrations a carefully weighed amount of impurity is added to the solution.

Table 4.1.: *The operation conditions of NaCl solution in a fluidized bed crystallizer at a saturated temperature = 30°C.*

Condition	*Values*
Super/undersaturated temperature °C	1–7°C / 1–6°C, respectively
Impurity species (ppm)	
$CuSO_4 \bullet 5H_2O$	5, 10, 25
$K_4Fe(CN)_6 \bullet 3H_2O$	1, 10
$MgCl_2$	50, 100, 250
$PbCl_2$	0.5, 1, 10

Table 4.2.: *The operation conditions of $MgSO_4 \bullet 7H_2O$ solution in a fluidized bed crystallizer at a saturated temperature = 25°C.*

Condition	*Values*
Super/undersaturated temperature °C	0.2–1°C
pH value of the solution	2.5, 3.8, 7.7, 8.6
Impurity species (wt %)	
Borax ($Na_2B_4O_7 \bullet 10H_2O$)	0.5, 1, 2, 5
$FeSO_4 \bullet H_2O$	1, 2
K_2SO_4	2, 4
KCl	2, 5
KH_2SO_4	1, 3
$MgCl_2$	1, 2
Na_2SO_4	2, 5
$NaCl$	2, 5
$NiSO_4 \bullet H_2O$	1, 2

4.2. Electrophoretic-mobility measurements

Electrophoretic-mobility measurements were done by the Laser-Doppler electrophoresis technique [102]. The zetasizer 3000 with the AZ4 standard cell was used for measuring electrophoretic-mobility. The zetasizer 3000 is consisted of, two coherent laser beams of red light produced by splitting of a low power He-Ne laser are focused and made to intersect within the quartz capillary cell holding the particle suspension at a point of zero convective flow. As a result, a pattern of interference fringes is formed, and the particles move across the fringes under the influence of the applied electric field scatter light. The of the scattered light varies with a frequency that is related to the velocity of the particles. A fast photomultiplier together with a digital correlator is used to analyse the signals, and the distribution of particle velocity (electrophoretic-mobility) and/or distribution of *zeta potential* is thus determined. The sign of the zeta potential is determined by referencing the observed Doppler frequency of the light scattered by the particles moving through the fringes to the modulation frequency applied to one of the laser beams.

Fig. 4.2. presents a schematic diagram of the AZ4 standard cell used in the present study. This cell consists of a 4 mm diameter quartz capillary. The platinum electrodes are in compartments at each end of the cell. A semipermeable membrane separates the electrodes from the suspension sample to prevent the contamination of the electrodes by the sample. The electrode chambers are filled with an electrolyte which is at least conducting as the sample itself. Polarization of the electrodes is prevented by the application of a periodically reversed field.

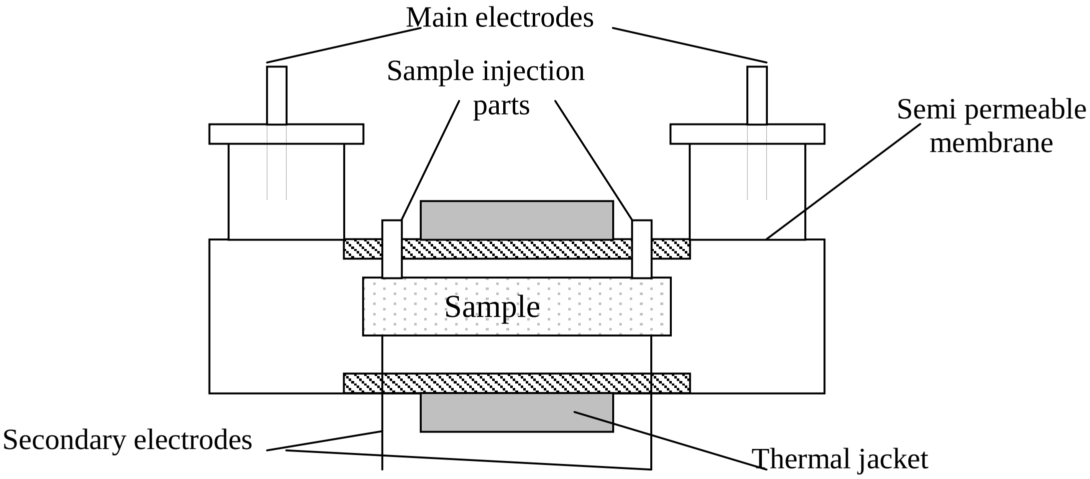

Figure 4.2.: *Schematic diagram of the capillary electrophoresis cell for the zetasizer 3000.*

Of course a zeta potential/electrophoretic-mobility measurement in a saturated solution is impossible because the double layer is collapsed, the high conductivity of saturated solutions causes some measurement problems, and the zeta potential does not exist, even through a surface charge may still be present. In order to describe the electrokinetic behaviour of the soluble-salt particles, the electrophoretic-mobility measurement of the $MgSO_4{\bullet}7H_2O$ *crystals* < 80 *µm were made after diluting the saturated solution by ethanol (45 mole % ethanol in solvent). Importantly, however, these measurements should give a relative indication in the sign of the surface charge of the* $MgSO_4{\bullet}7H_2O$ *crystals in their saturated solution.*

4.2.1. Procedure

The soluble salts were sized and the 80 mesh fraction was used in this study for electrophoretic-mobility measurements. The electrophoretic-mobility of the $MgSO_4{\bullet}7H_2O$ was measured in the following steps:

1. Prepaire a saturated solution of $MgSO_4{\bullet}7H_2O$ in aqueous ethanol solution (45 mole % in solvent).
2. 0.5 g of well defined crystals of a sieve cut, < 80 µm, of $MgSO_4{\bullet}7H_2O$ were added to the saturated solution.
3. The suspension salt crystals was stirred for 1-2 minutes and then quickly injected into the cell of the electrophoretic-mobility measured.
4. Each measurement required approximately 4-10 minutes, depending on the impurities added to the pure solution.

Its should be mentioned that:

1. The salt particles must be suspensioned in the saturated solution, otherwise there is no significant effect to measure the electrophoretic mobility/*zeta potential*.
2. The concentrations of impurities added to the solution were 10-20 wt %, at low impurities concentration there was no change in the values of the electrophoretic-mobility measured for impure solution comparsion with pure solution.
3. Great care is taken to avoid injection of air bubbles into the cell.
4. The experiment was repeated at least 3 times for each impurity under the same conditions to determine the reproducibility of the measurements.

5. Results and discussion

5.1. *NaCl* experiments

Fig. 5.1.1. shows a thermodynamic effect on the growth rate of *NaCl* in the presence of $MgCl_2$. The calculated growth rates as well as the dissolution rates of *NaCl* crystals are plotted over the supersaturation or undersaturation, receptively. The experimental data for the system are presented in ***Table 5.1.1.***. By adding 50, 100, 250 ppm of the impurity $MgCl_2$ the saturation temperature will be shifted to 31, 33, and 36°C, respectively. This means that the solubility of *NaCl* is decreased with increasing amount of $MgCl_2$ in the solution. Therefore the temperature should be raised to dissolve the total amount of *NaCl* added at 30°C. It seems to be obvious from ***Fig. 5.1.1.*** that the impurities are accelerating the growth rate of *NaCl*, but this is a misleading result. There is no kinetic acceleration in the growth rate of *NaCl* but rather a shift in the saturation temperature.

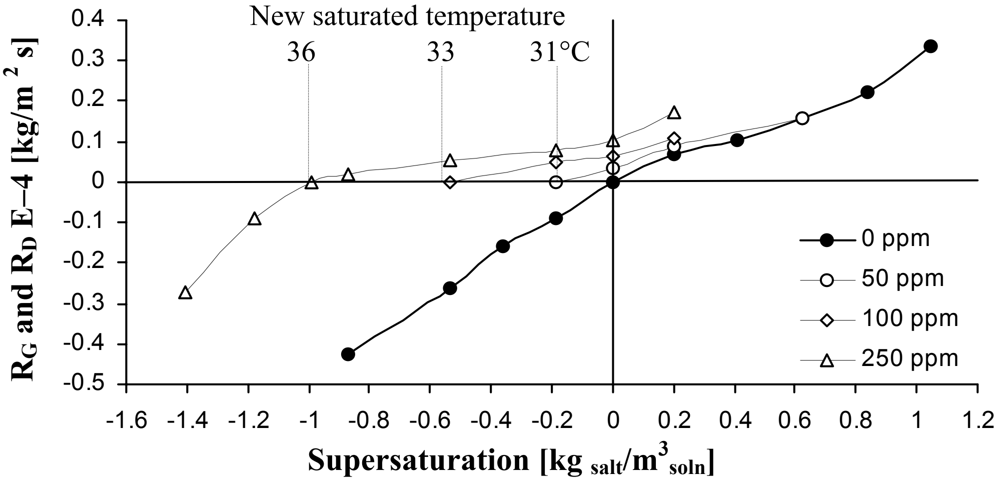

Figure 5.1.1.: *Growth and dissolution rates of NaCl with the additive* $MgCl_2$.

In order to determine the real influence on the growth rate, the saturation temperature must be corrected. This can be done by a correction in temperature (raising the temperature). It is necessary to dissolve the total amount of *NaCl* added at 30°C, which is the basis to compare the different curves with each other. After the correction in temperature, the different corresponding saturation temperatures are 30, 31, 33, and 36°C, for the impurity concentration 0, 50, 100, 250 ppm, respectively. In ***Fig. 5.1.2.*** the data of ***Table 5.1.1.*** are reploted according to the new saturation temperatures. The curves shown in ***Fig. 5.1.2.*** are the actual ones and show the additional kinetic effect on the growth rate. Therefore, it is the final result that the $MgCl_2$ will suppress the growth rate of the *NaCl* crystals and the suppressing in the growth is more pronounced at higher $MgCl_2$ concentration.

Table 5.1.1.: *Experimental data for the mass growth rate of NaCl at different impurity concentration of* $MgCl_2$.

Temp. °C	ΔC (kg $_{salt}$/m$^3_{soln}$)	$R_G \times 10^4$ kg/(m^2 s) *Impurity Conc.*(ppm) *0*	*50*	*100*	*250*
36	-0.993				0.0
35	-0.871				0.019
33	-0.532			0.0	0.052
31	-0.185		0.0	0.050	0.077
30	0	0.0	0.032	0.065	0.105
29	0.202	0.068	0.087	0.108	0.173
28	0.410	0.106			
27	0.627	0.157	0.156		
26	0.840	0.220			
25	1.049	0.333			

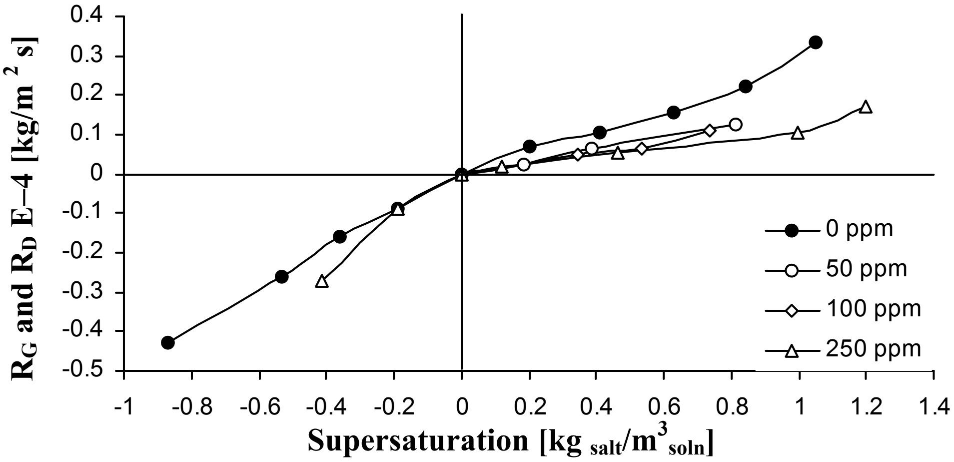

Figure 5.1.2.: *Growth and dissolution rates of NaCl with the additive* $MgCl_2$ *(kinetic effect). Here are the same data used as in* ***Fig. 5.1.1.****, but they are shifted to match the same saturation point.*

Fig. 5.1.3. shows the kinetic effect on the growth rate of *NaCl* due to the presence of $PbCl_2$. It is clear that with increasing impurity concentration the growth rates are suppressed. The experiments with the impurity $K_4Fe(CN)_6•3H_2O$ are similar to those with $PbCl_2$ in the *NaCl* solution (see ***Fig. 5.1.4.***). The presence of $K_4Fe(CN)_6•3H_2O$ results also in a reduction in growth rate and dissolution rate with increasing impurity concentrations for the total range of the investigated supersaturation and undersaturation, receptively.

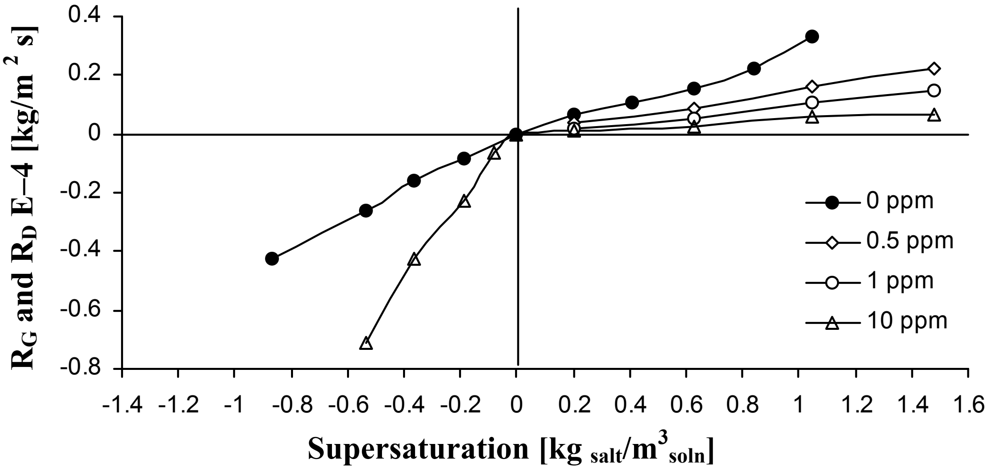

***Figure 5.1.3.**: Growth and dissolution rates of NaCl with the additive* $PbCl_2$.

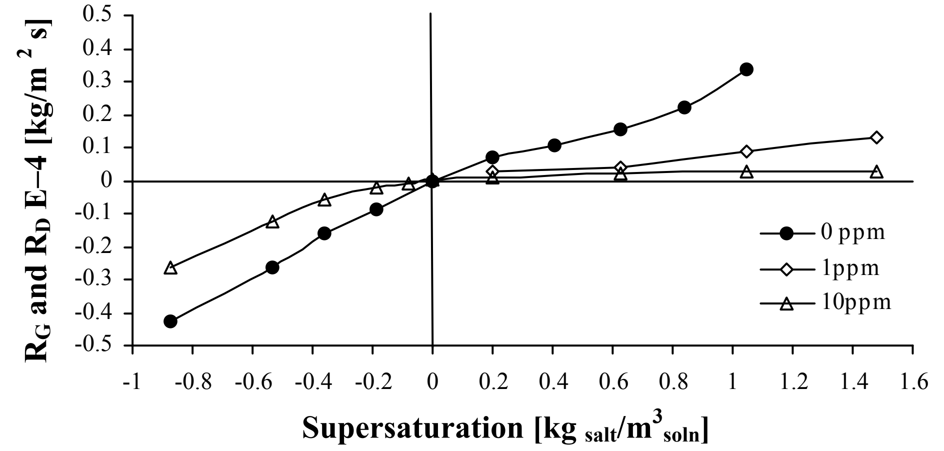

***Figure 5.1.4.**: Growth and dissolution rates of NaCl in the presence of* $K_4Fe(CN)_6$.

While the presence of $CuSO_4•5H_2O$ did not affect the growth rate of *NaCl* at all (see ***Fig. 5.1.5.***). The results shows a good agreement with literature data [105, 106], there was no effect on the single crystal growth rate of *NaCl* in the presence of the additive $CuSO_4•5H_2O$.

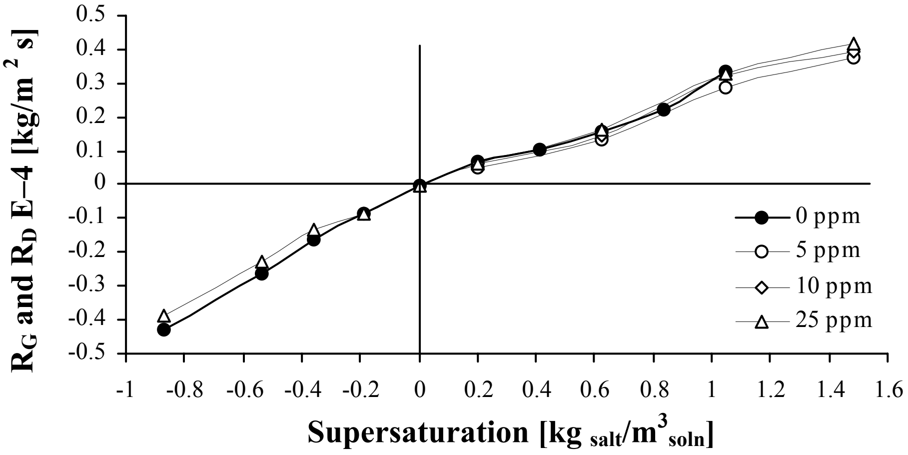

***Figure 5.1.5.**: Growth and dissolution rates of NaCl in the presence of $CuSO_4 \bullet 5H_2O$.*

The overall growth rate constant k_G and the order of growth rate g were estimated from the experimental growth rates by curve fitting according to Eq. 3.3. The values of k_G and g show some difference between this results and results of Langer [62]. The optimal solutions obtained are represented by the following expression:

$$R_G = 2.98 \times 10^{-5} \ \Delta C^{1.21} \quad \text{(this work [85])} \tag{5.1}$$

$$R_G = 6.20 \times 10^{-5} \ \Delta C^{1.25} \quad \text{(Langer [62])} \tag{5.2}$$

The difference in the values of k_G and g are due to the fact that there was a difference in operation conditions (seed size and growth period) for the same supersaturation (see ***Table 5.1.2.***). The growth rate increases as the size of the seeds increase. This is because the seed size increases as the relative fluidization velocity increases in order to keep the crystals fluidized within the same bed height. The increase in fluidization velocity leads to an increase in the mass transfer (see ***Fig. 5.1.6.***).

***Table 5.1.2**: A difference in operation condition between this work and the literature for the same saturation temperature (30°C).*

Author	*Seed size* (µm)	*Growth period* (min)
This work [85]	315–250	15
Langer [62]	500–400	10
Stepanski [103]	500–400	10
Al-Sabbagh [104]	450–400	10

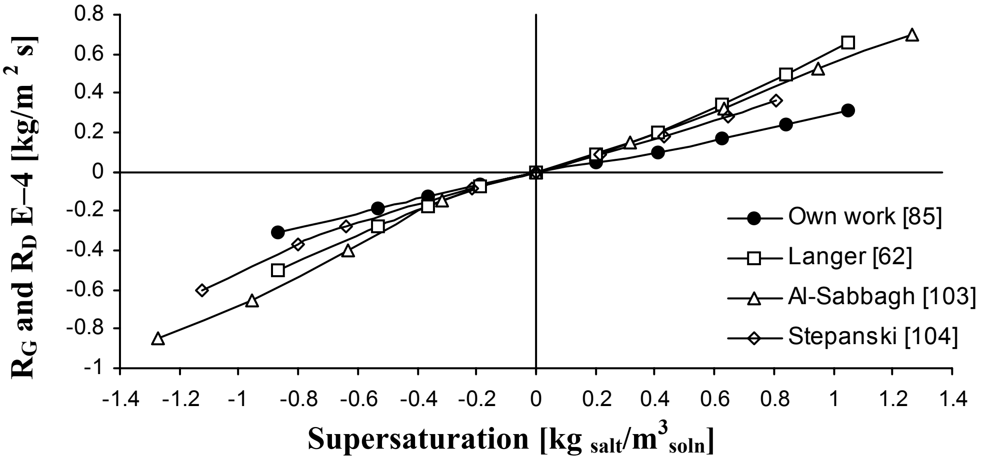

Figure 5.1.6.: *Literature compassion of growth and dissolution rates in a fluidized bed crystallizer.*

5.2. $MgSO_4 \bullet 7H_2O$ experiments

Fig. 5.2.1. shows the growth and dissolution rates of $MgSO_4 \bullet 7H_2O$ crystals in the presence of *borax*. The saturated temperature of pure $MgSO_4 \bullet 7H_2O$ solution is taken to be the reference temperature to calculate the supersaturation at different impurity concentrations. By adding 0.5, 1, 2 and 5 wt % of *borax* impurity the pH-value of the solution will be changed to 7.11, while, the saturation temperature will be shifted to 24.8, 24.4, 24 and 23.1°C, respectively. This means that the solubility of $MgSO_4 \bullet 7H_2O$ is increased with increasing amount of *borax* in the solution (a pure thermodynamic effect). ***Fig. 5.2.2.*** shows the kinetic effect on the growth and dissolution rates of $MgSO_4 \bullet 7H_2O$ crystals after the correction of the saturation temperatures. The presence of *borax* will inhibit the crystal growth/dissolution rate of $MgSO_4 \bullet 7H_2O$ and the inhibition in the crystal growth/dissolution is more pronounced at higher *borax* concentrations [107].

The same result concerning the thermodynamic effect (that the solubility of $MgSO_4 \bullet 7H_2O$ is decreased/increased with increasing amount of impurities) and the corresponding correction in temperature in order to get the kinetic effect can be extended to other impurities investigated in this study as shown in ***Table 5.2.1.***.

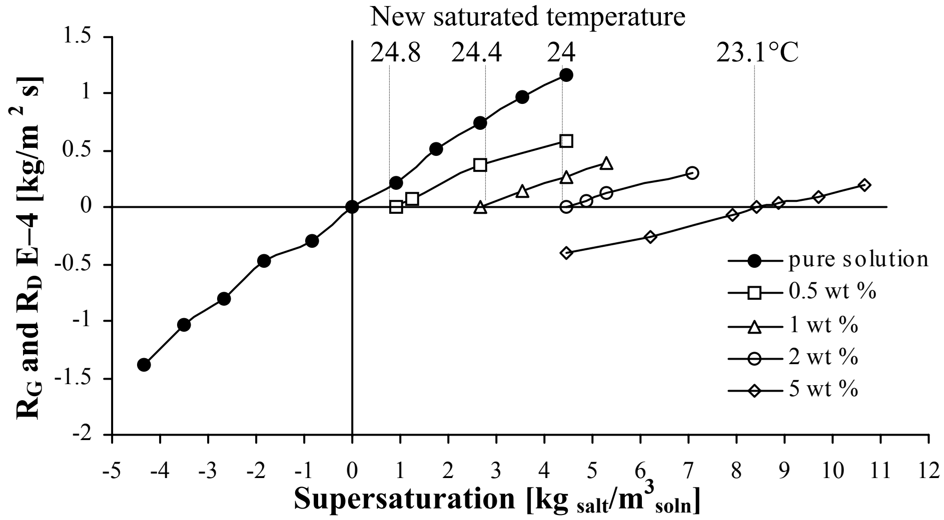

Figure 5.2.1.: *Growth and dissolution rates of $MgSO_4$•$7H_2O$ in the presence of borax (thermodynamic effect).*

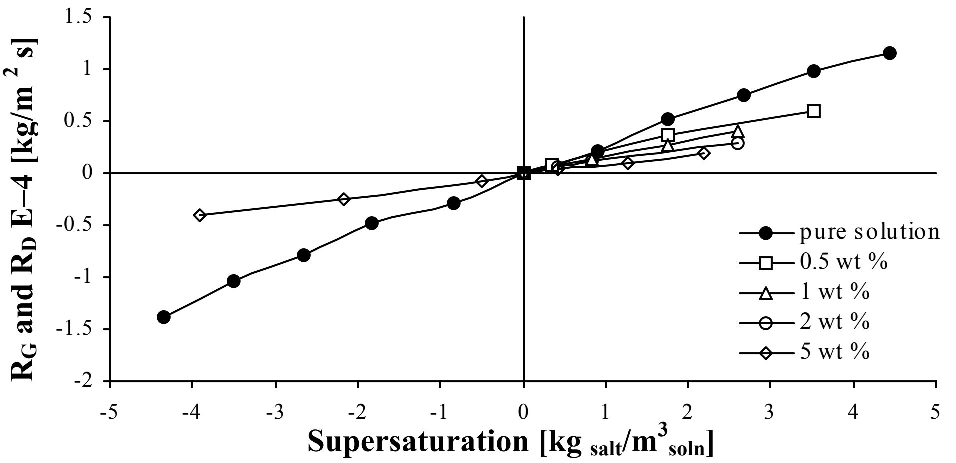

Figure 5.2.2.: *Growth and dissolution rates of $MgSO_4$•$7H_2O$ in the presence of borax after correction of the supersaturation (kinetic effect).*

The effect of pH-value of the solution on the growth and dissolution rates of $MgSO_4$•$7H_2O$ crystals is shown in ***Fig.5.2.3.***. The saturation temperature of the neutral $MgSO_4$•$7H_2O$ solution, having a pH-value of 6.7, is taken to be the reference temperature to calculate the supersaturation at different pH-values. At pH = 2.5, 3.8, 7.7 and 8.6 the saturation temperature will be shifted to 25.4, 25.2, 24.7 and 24.3°C, respectively. This means that the solubility of $MgSO_4$•$7H_2O$ is decreased in acidic media while it is increased in higher alkaline media. In order to find the kinetic effect, all growth and dissolution curves should be shifted to the zero-point. The final result is that the change in pH-value of the solution will suppress crystal growth as well as the dissolution rates of $MgSO_4{\bullet}7H_2O$ (see ***Fig.5.2.4.***).

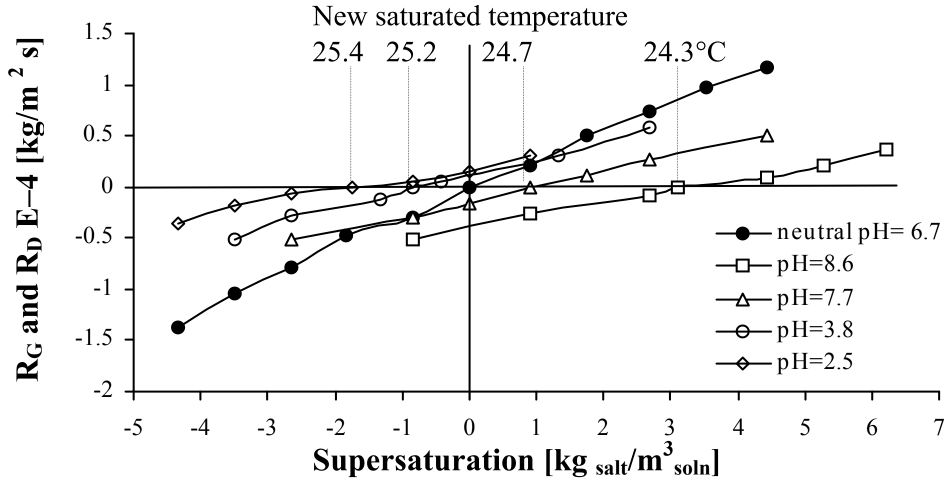

Figure 5.2.3.: *The effect of pH on the crystal growth and dissolution rates of $MgSO_4{\bullet}7H_2O$ (thermodynamic effect).*

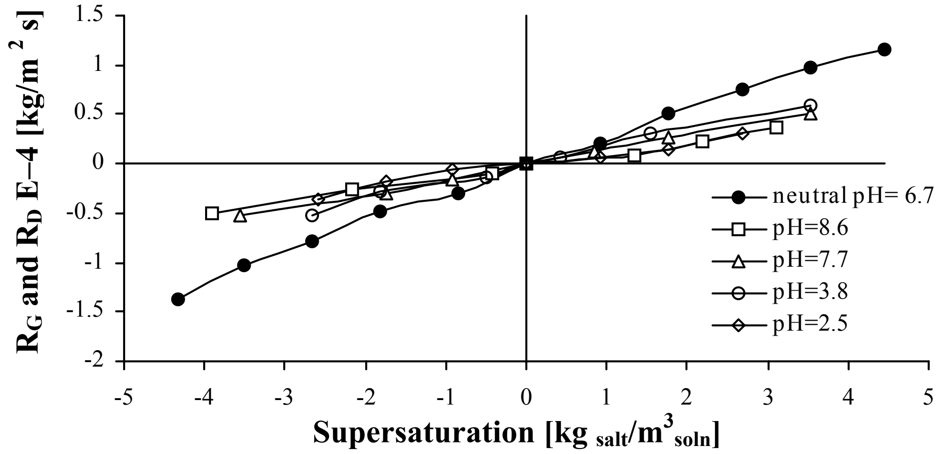

Figure 5.2.4.: *The effect of pH on the growth and dissolution rates of $MgSO_4{\bullet}7H_2O$ with saturation point correction (kinetic effect).*

It may be interested to note that, by adding 1 and 2 wt % of $FeSO_4{\bullet}H_2O$, the pH will be changed to 4.32 and 3.46, respectively, and the solubility is decreased with increasing amount of $FeSO_4{\bullet}H_2O$ in the solution (see ***Table 5.2.1.***). Concerning the increasing in the solubility of $MgSO_4{\bullet}7H_2O$ in the presence of *borax* and the decreasing in the solubility in the presence of $FeSO_4{\bullet}H_2O$, these results show a good agreement with previous results concerning the effect of pH-value (by changing the pH-value of the solution to alkaline/acidic medium) on the solubility of $MgSO_4{\bullet}7H_2O$.

***Table 5.2.1.**: Influence of additives on saturation temperature, kinetics and thermodynamics.*

Additive	*Amount of additive* (wt%)	*New sat. temp.* (°C)	*pH*	*Thermodynamic effects*	*Kinetic effects*
				Solubility	*Growth rate*
Pure	0	25	6.7	=	=
Borax	0.5	24.8	7.11	+	–
Borax	1	24.4	7.11	+	–
Borax	2	24	7.11	+	–
Borax [107]	5	23.1	7.11	+	–
$FeSO_4{\bullet}H_2O$	1	25.4	4.32	–	–
$FeSO_4{\bullet}H_2O$ *[108]*	2	25.8	3.46	–	–
K_2SO_4	2	24.8	6.7	+	–
K_2SO_4 *[109-112]*	4	24.6	6.7	+	–
KCl [109-112]	1, 2 and 5	25	6.7	=	–
KH_2PO_4	1	24.6	3.27	+	–
KH_2PO_4	3	23.8	3	+	–
$MgCl_2$	1	25.9	6.7	–	=
$MgCl_2$ *[109-111]*	2	27.1	6.7	–	=
Na_2SO_4	2	25.4	6.7	–	–
Na_2SO_4 *[112]*	5	25.8	6.7	–	–
$NiSO_4{\bullet}6H_2O$	1	25.6	6.6	–	–
$NiSO_4{\bullet}6H_2O$	2	26.2	6.6	–	–
H_2SO_4		25.4	2.5	–	–
H_2SO_4 *[109-111]*		25.2	3.8	–	–
NaOH		24.7	7.7	+	–
NaOH [109-111]		24.3	8.6	+	–

+ increase, – decrease/suppress, = no effect

6. Interpretation of results

6.1. The magnitude of the two resistances (diffusion and integration steps)

The overall crystal growth phenomenon can be considered as the combination of 3 steps, namely volume diffusion, surface reaction, and heat transfer. The first step is the mass transport of the growth units by diffusion or convection from the bulk of the solution to the crystal surface. The second step is the integration of units into the crystal lattice. The third step are heat related effects from the liberation of the crystallization heat when the crystal grow, and from the heat transfer connected with the mass transfer from and to the phase boundary (liquid/solid) [1–3]. Here the effect of heat transfer can be neglected due to the fact that the value of $\beta_d < 10^{-2}$ [3], and the value of $-\Delta H/(1-w_b)$ is less than 700 J g^{-1}[113]. Therefore, the crystal growth processes from solutions are dominantly either diffusion or reaction controlled. A change in the dominating growth mechanism arises by a change of temperature level or e.g. by traces of certain impurities or additives.

6.1.1. *NaCl* experiments

As mentioned before, see the theory (**Chapter 3.1.**), the dissolution process for pure and impure solutions is running faster than the growth process. Therefore, a possible surface disintegration resistance is here difficult to observe [4, 5]. The diffusion rate constant, k_d, was, therefore, estimated from the experimental dissolution rate by curve fitting of Eq. 3.11. The integration order, r, and the integration rate constant, k_r, were estimated from Eq. 3.10 by curve fitting of the growth rate data. k_r, k_d and r values for pure and impure solution are presented in ***Table 6.1.1.***.

In order to quantify the resistance in growth offered by the volume diffusion or surface reaction the effectiveness factors for surface integration and diffusion was used. When D_a is large, growth is diffusion controlled and the integration effectiveness factor η_r approaches $1/D_a$. Conversely, when D_a is small η_r approaches one, the growth is therefore controlled by the integration step. η_d and η_r values for *NaCl* crystal growth in pure and impure solution are given in ***Table 6.1.1.*** and shown in ***Figs. 6.1.1.*** and ***6.1.2.***. The effectiveness factor indicates that the controlling growth mechanism for *NaCl* crystal growth in the pure *NaCl* solution is split into the diffusion step and the integration step. In the presence of impurities the obtained results indicate that the integration step offers a greater resistance to overall crystal growth rate than the diffusion step (see ***Figs. 6.1.1.*** and ***6.1.2.*** and ***Table 6.1.1.***). The value of integration effectiveness factor, η_r, was approached one, this indicates that the crystal growth rate is controlled mainly by the integration step.

Table 6.1.1.: *The kinetic parameters, η_d and η_r for NaCl crystal growth in the presence of different additives and the contribution in percent of growth resistance for the diffusion step and the integration step.*

Solution	*r*	k_r *E-5*	k_d *E-5*	η_r	η_d	*Integ. %*	*Diffu. %*
NaCl	1.12	7.75	4.84	0.37	0.52	0.42	0.58
NaCl–MgCl₂	1.33	1.56	6.28	0.80	0.16	0.83	0.17
NaCl–PbCl₂	1.04	0.47	12.7	0.96	0.04	0.96	0.04
NaCl–K₂Fe(CN)₆	0.42	0.26	2.67	0.98	0.06	0.94	0.06

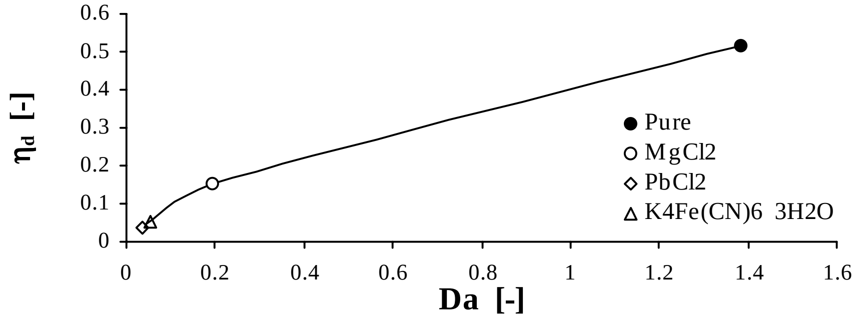

Figure 6.1.1.: *Diffusion effectiveness factor for crystal growth rate of NaCl at different additives.*

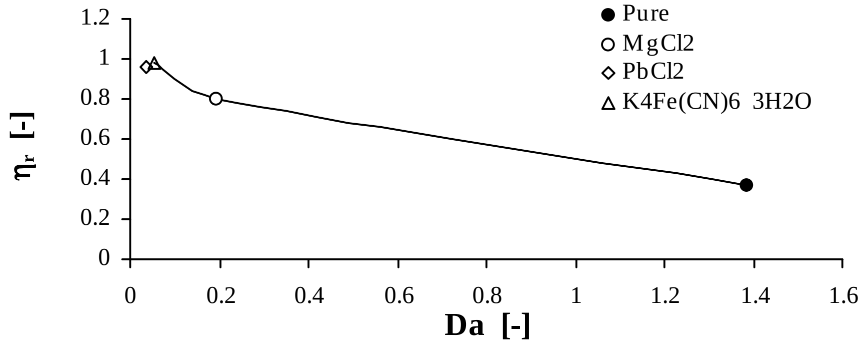

Figure 6.1.2.: *Integration effectiveness factor for crystal growth rate of NaCl at different additives.*

6.1.2. $MgSO_4 \bullet 7H_2O$ experiments

As mentioned previously the concept of the effectiveness factors for the volume diffusion and surface integration are used to qualify the resistance to either growth dominated by the diffusion or integration controlled. The integration order r and the integration rate constant k_r were estimated from Eq. 3.10, by curve fitting of the growth rate data. k_r, k_d and r values for pure and impure solution are presented in ***Table 6.1.2.***.

Table 6.1.2.: *The kinetic parameters, η_d and η_r for $MgSO_4 \bullet 7H_2O$ crystal growth in the presence of different additives and the contribution in percent of growth resistance for the diffusion step and the integration step.*

Solution	*r*	k_r *E-5*	k_d *E-5*	η_r	η_d	*Integ. %*	*Diffu. %*
$MgSO_4 \bullet 7H_2O$	0.96	7.6	3.05	0.30	0.72	0.29	0.71
$MgSO_4 \bullet 7H_2O$–Borax	1.24	2.29	1.09	0.33	0.59	0.36	0.64
$MgSO_4 \bullet 7H_2O$–$FeSO_4$	1.72	1.7	1.98	0.42	0.40	0.51	0.49
$MgSO_4 \bullet 7H_2O$–K_2SO_4	0.98	3.72	1.85	0.41	0.60	0.41	0.59
$MgSO_4 \bullet 7H_2O$–KCl	1.39	1.81	3.26	0.53	0.37	0.59	0.41
$MgSO_4 \bullet 7H_2O$–KH_2PO_4	0.93	3.47	1.94	0.45	0.57	0.44	0.56
$MgSO_4 \bullet 7H_2O$–Na_2SO_4	1.1	2.08	2.12	0.55	0.42	0.57	0.43
$MgSO_4 \bullet 7H_2O$– $NiSO_4$	1.22	2.97	2.09	0.43	0.50	0.46	0.54

Figs. 6.1.3. and ***6.1.4.*** show the diffusion and integration effectiveness factors for $MgSO_4 \bullet 7H_2O$ crystals, respectively. Growth in pure and impure solution were estimated for different supersaturation levels. The effectiveness factor results indicate that the controlling growth mechanism is contributing by means of the diffusion and the integration steps on the crystal growth of $MgSO_4 \bullet 7H_2O$ from pure and impure solution. It is clear from the obtained results that, the diffusion step offers a greater resistance to overall crystal growth rate than the integration step in the case of pure solution. While in the presence of different impurities, the dominating growth

mechanism changes and the integration step offers a greater resistance to overall crystal growth rate than the diffusion step (e.g. $FeSO_4$, KCl and Na_2SO_4, see ***Table 6.1.6***).

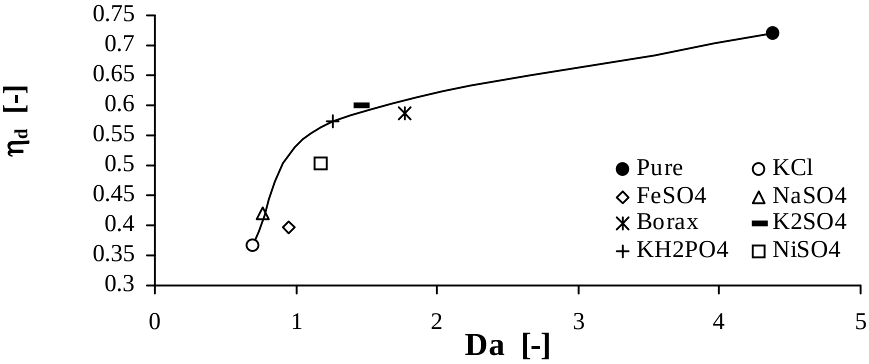

Figure 6.1.3.: *Diffusion effectiveness factor for crystal growth rate of* $MgSO_4 \bullet 7H_2O$ *at different additives.*

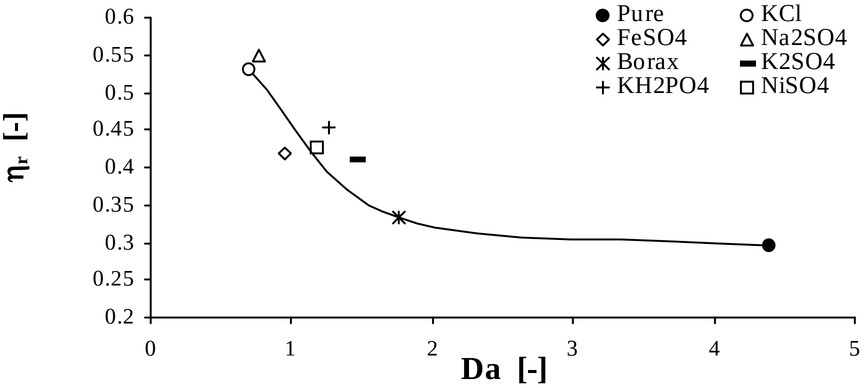

Figure 6.1.4.: *Integration effectiveness factor for crystal growth rate of* $MgSO_4 \bullet 7H_2O$ *at different additives.*

There are some differences between own conclusion [85] in case of *NaCl* crystal growth from pure solution and the conclusions of Zhang et al. [83]. They concluded, that in the case of linear growth and dissolution rates and an equal slope for the crystal growth the growth can be called “diffusion controlled”. With the above assumptions it has been shown that *NaCl* is diffusion controlled growing in the absence of impurities. However, with the used impurities a change in the dominating growth mechanism arises, i.e. the presence of certain impurities lead to a more important role of the reaction step. *In this work it is proven by means of the effectiveness factor concept, that there is almost a match of the integration step and the diffusion step for NaCl crystal growth from pure solution, which is contrary to literature (e.g. [83]).*

6.2. Kinetic effect

Surface adsorbed impurities can reduce the measured growth rate of crystals by reducing or hindering the movement of growth steps on the crystal surfaces. Depending on the amount and strength of adsorption the effect on crystal growth can be very strong or hardly noticeable. Two extremes cases, i.e. adsorption at kinks (mobile impurities) and the surface terrace (immobile impurities), may be distinguished. The models of impurity adsorption considering kinks and the surface terraces deal with the kinetic aspect of adsorption of impurities of F faces, neglecting the thermodynamic effects.

6.2.1. *NaCl* experiments

The Eq. 3.39 enables to calculate K from the experimental $R_G(c_{imp})$ data. The best fits of Eq. 3.39 to the experimental data with a least-squares method are shown in ***Fig. 6.2.1.***. The fitted results are shown in ***Fig. 6.2.1.*** with solid lines for $PbCl_2$ as impurity. It is clear that the relative mass growth rate of *NaCl* is reduced to zero. Therefore, this result may be considered to be examples of the case of $\alpha \cong 1$ (see [49]). Here, the concentration of impurity on the crystal surface is assumed to be in equilibrium with the concentration of the impurity in the solution, i.e. the distance between impurity on the surface is approximately the same as the critical diameter $2\rho_c$ at $\theta = 1$, i.e. a full coverage of the crystal surface leads to growth rates equal to zero.

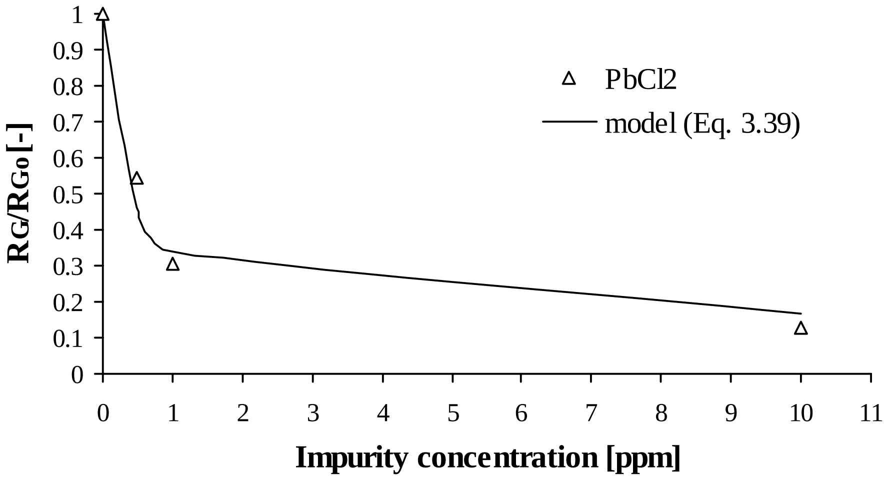

***Figure 6.2.1.**: Effect of $PbCl_2$ impurity on the relative mass growth rate of NaCl. Comparison of own work [114] with the model [Eq. 3.39].*

While in the presence of $MgCl_2$ the relative mass growth rate of *NaCl* is reduced and approaching a non-zero value. The parameter α is determined by fitting of Eq. 3.39 as shown in ***Table 6.2.1.***. According to the Kubota-Mullin model [49] this may be considered to be an example of the case $\alpha < 1$. In the case of $\alpha < 1$, the distance between impurity on the surface is larger than the critical radius of the two-dimensional nucleus $2\rho_c$, even at $\theta = 1$. Hence, the step can easily squeeze out between the impurity, i.e. the impurity is more easy adsorbed on crystal faces, but it has a weaker suppression effect.

Fig. 6.2.2. illustrates the plot of the impurity effect, $\alpha\theta_{eq}$, of adsorption-active sites as a function of Pb^{+2} impurity concentration. Experimental adsorption data are in good agreement with the theoretical Langmuir adsorption isotherm, which was drawn using the value of *K* determined above from crystal growth experiments. This agreement supports the validity of the Kubota-Mullin model [49].

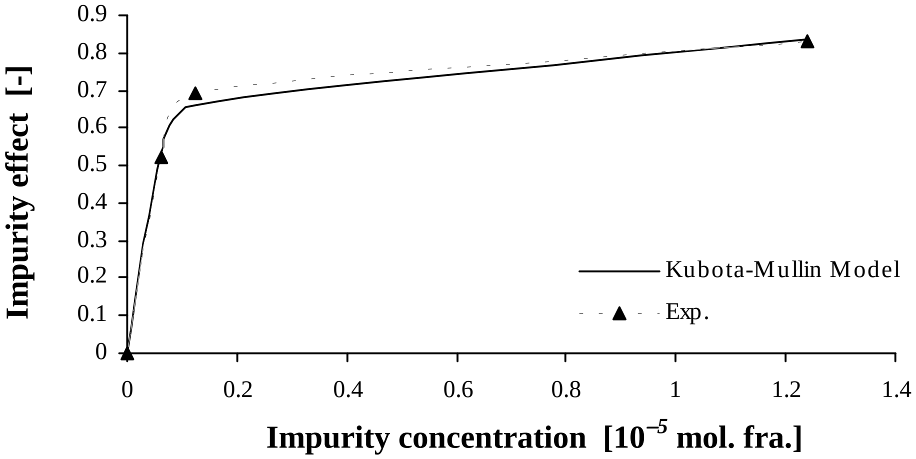

Figure 6.2.2.*: Experimental isotherm of* Pb^{+2} *impurity adsorption onto NaCl crystals Comparison of own work [114] with the model [Eq. 3.39].*

It can be seen from analysis of growth kinetics data that the $R_G(c_{imp})$ data follow a kink and terrace adsorption mechanism with a Langmuir adsorption isotherm. The value of heat adsorption is higher during adsorption at kinks than those involved in adsorption at the surface terraces [14]. Therefore, from the values of the heat adsorption as shown in ***Fig. 6.2.2.***, it may be concluded that adsorption of the impurity Mg^{+2} occurs at kinks.

The relatively low values of the heat of adsorption indicates that adsorption is physical in nature. From ***Fig. 6.2.3.*** it is interesting to note that when the value of supersaturation increases the value of the heat of adsorption Q_{diff} has the tendency to increase while the average distance, λ, between adsorption sites decreases (see ***Table 6.2.1.***). *The former argument is associated with an increasing competition of solute ions in occupying the same sites with the impurity ions. The later reasoning on the other hand is a consequence of a decrease in the average distance between kinks with increasing supersaturation.*

***Table 6.2.1.**: Adsorption parameters for the growth of NaCl crystal at different supersaturations and impurities.*

Solution	σ %	*Adsorption mechanism*	α	K (mol/mol)$^{-1}$	λ (m)	l (m)	Q_{diff} (kJ/mol)
NaCl–MgCl$_2$	0.18	Kink	0.55	2.70E+04	$145a$	$162a$	25.7
		Terrace	0.6	7.40E+03	$132a$	$190a$	22.4
	0.36	Kink	0.57	5.20E+04	$69a$	$73a$	27.4
		Terrace	0.57	2.30E+04	$69a$	$78a$	25.3
NaCl–PbCl$_2$	0.09	Kink	0.92	1.90E+06	$175a$	$183a$	36.4
		Terrace	0.92	8.00E+05	$175a$	$193a$	34.2
	0.27	Kink	0.91	1.90E+06	$57a$	$60a$	36.4
		Terrace	0.91	8.10E+05	$57a$	$63a$	34.3
	0.36	Kink	0.86	2.70E+06	$45a$	$46a$	37.3
		Terrace	0.9	2.30E+05	$43a$	$58a$	31.1

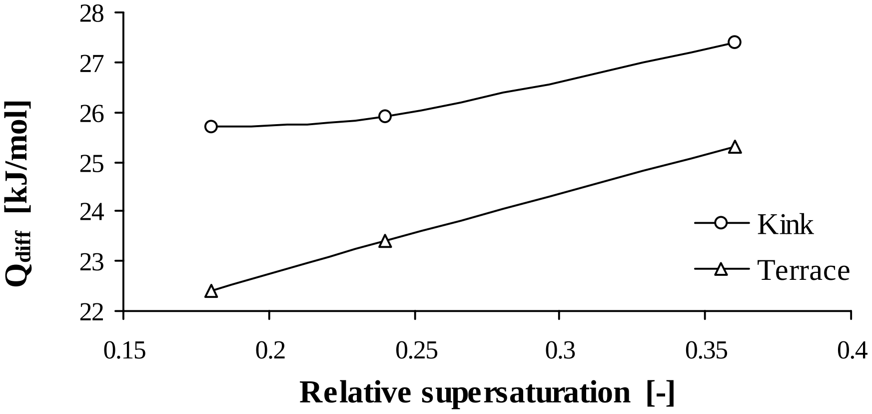

***Figure. 6.2.3.**: The differential heat of adsorption at different supersaturation. Adsorption of Mg^{+2} ions on crystal surface of NaCl.*

Table 6.2.1. shows the impurity effectiveness factor, α, that is determined from the growth experiments as a function of the reciprocal of the relative supersaturation $1/\sigma$. As expected from Eq. 3.33 α increases linearly with a slop equal to $\gamma a/k_BT\lambda$. Therefore, if the value of the edge free energy, γ, is known at a given temperature, T, the average distance, λ, between the adsorption-active sites can be estimated from the Kubota-Mullin model [49] as a function of the growth unit, a. According to Hayashi and Schichiri [115] for *NaCl* crystals growing in aqueous solution the edge free energy, γ, per growth unit is 6.0×10^{-22} J/m. Therefore, $\gamma/k_BT = 0.14$ at $T = 303.15$ (30°C) the temperature of growth rate measurements in this study. However, α is known by fitting of Eq. 6, $\alpha = (\gamma/k_BT)(a/\lambda)$. These two values give the average distance, λ, between the adsorption-active sites as shown in *Table 6.2.1.*. The spacing, l, between the neighbouring active sites occupied by impurities can also be estimated from the relation $\theta_{eq} = \lambda/l$ if the impurity concentration is known. It is clear from *Table 6.2.1.* that these estimated values of λ and l seem to be reasonable, although direct experimental verification is impossible.

6.2.2. $MgSO_4 \bullet 7H_2O$ experiments

For a validation of the experimentally found data a comparison with the Kubota-Mullin model [49] was carried out. As shown in ***Fig. 6.2.4.***, the relative growth rate of $MgSO_4 \bullet 7H_2O$ is reduced asymptotically to zero. Values of the parameter α were determined by fitting Eq. 3.39 to own data. The fitted results are shown in ***Fig. 6.2.4.*** with solid lines for Borax as impurity. The values of α, for different impurities, are given in ***Table 6.2.2.***. Therefore, some of these results may be considered to be examples of the case of $\alpha \cong 1$. Here, the concentration of the impurity on the surface of the crystal is assumed to be in equilibrium with the concentration of the impurity in the solution, i.e. the distance between impurity on the surface approximately the same as the critical diameter $2\rho_c$ at $\theta = 1$, i.e. a full coverage of the crystal surface leads to growth rates equal to zero.

In the presence of K_2SO_4, $\alpha \cong 0.5$, the relative mass growth rate of $MgSO_4 \bullet 7H_2O$ is reduced and approaching a non-zero value. According to the Kubota-Mullin model [49] this is may be considered to be an example of the case $\alpha < 1$. In the case of $\alpha < 1$, as mentioned previously, the step can easily squeeze out between the impurity, i.e. the impurity is more easy adsorbed on crystal faces, but it has a weaker suppression effect.

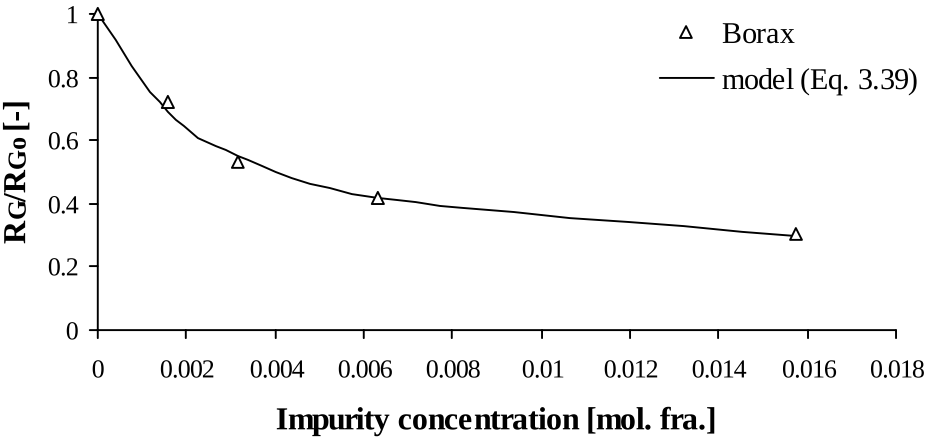

Figure 6.2.4.*: Effect of Borax on the relative growth rate of* $MgSO_4{\bullet}7H_2O$*. Comparison of own work [107] with the model (Eq. 3.39).*

It can also be seen from ***Table 6.2.2.*** that the $R_G(c_{imp})$ data follow kink and terrace adsorption mechanisms according to Langmuir adsorption isotherm. The values of heat adsorption are higher during adsorption at kinks than those involved in adsorption at the surface terraces [14]. Therefore, from the values of the heat adsorption given in ***Table 6.2.2.*** and ***Fig. 6.2.5.***, in this figure the borax is taken as example, it may be concluded that at low supersaturated solution adsorption of impurities occurs at kinks. By increasing the supersaturation, the adsorption of impurities at kinks approximately approaches a constant value.

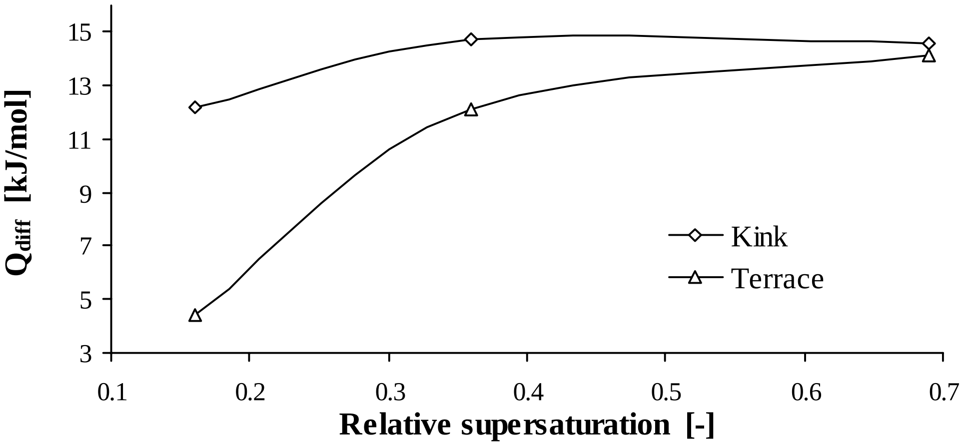

Figure 6.2.5.*: The differential heat of adsorption, (Q_{diff}), at different supersaturaion.*

Table 6.2.2.: *Adsorption parameters for the growth of* $MgSO_4 \bullet 7H_2O$ *crystals in the presence of Borax as impurity at different supersaturations.*

Impurities	σ %	*Adsorption Mechanism*	α	K (mol/mol)$^{-1}$	λ	Q_{diff} (kJ/mol)
Borax [106]	0.16	Kink	0.76	138	801a	12.2
		Terrace	0.8	5.9	338a	4.4
	0.36	Kink	0.67	383	419a	14.7
		Terrace	0.69	131	406a	12.1
	0.69	Kink	0.83	369	175a	14.6
		Terrace	0.73	300	199a	14.1
$FeSO_4$	0.69	Kink	1.3	46	112a	9.5
		Terrace	2.5	3.3	58a	3
	1.04	Kink	1.3	42	74a	9.3
		Terrace	2.2	4.1	44a	3.5
	1.37	Kink	0.91	88	80a	11
		Terrace	1.16	15.7	63a	6.8
K_2SO_4	0.36	Kink	0.58	60.2	483a	10.2
		Terrace	0.9	6.70	312a	4.7
	0.69	Kink	0.5	137	292a	12.2
		Terrace	0.54	40	270a	9.14
	1.04	Kink	0.49	67	196a	10.4
		Terrace	0.66	10.8	145a	5.9
Na_2SO_4	0.69	Kink	0.91	32.3	160a	8.6
		Terrace	2.3	1.27	63a	0.6
	1.04	Kink	1.14	21.3	84a	7.6
		Terrace	2.4	1.19	40a	0.43
	1.72	Kink	0.91	32.3	64a	8.6
		Terrace	2.3	1.27	25a	0.6
$NiSO_4$	0.69	Kink	1.09	53.7	134a	9.9
		Terrace	3.7	1.17	39a	0.4
	1.04	Kink	1.06	45	90a	9.4
		Terrace	3.1	1.40	31a	0.8
	1.37	Kink	0.95	52	77a	9.8
		Terrace	1.7	4.40	43a	3.7

The same argument that the values of the heat of adsorption at kinks are higher than the adsorption at surface terraces can be applied for other impurities investigated in this study (see ***Table 6.2.2.****).*

Several papers dealing with the growth kinetics of crystals in the presence of impurities have been published [116], but there is no paper assessing the adsorption isotherm obtained from experiments through the kinetic model of crystal growth for a suspension growth condition as usual in industrial crystallization. For instance, recently Rauls et al. [117] reported the growth kinetics of ammonium sulfate crystals in the presence of the azo dyes amaranth and fuchsin. Adsorption isotherms were measured for these two impurities but no quantitative discussion was made regarding the growth suppressing caused by these impurities. *Hence, the present work is a successful attempt for assessing the adsorption isotherm from crystal growth experiments for a suspension growth condition.*

6.3. Thermodynamic effect

In the aqueous electrolyte solution two different species can be found, the dissociated ions (cations and anions) and the water molecules, there are different types of forces in the system: water-water, ion-ion, and water-ion interaction [118]. The simplest reaction of the metals, M^{n+}, in aqueous solutions is the loss of a proton to give the hydroxy species, $M(OH)^{(n-1)+}$. The coordination of metal ion to a water molecule will make a proton loss easier. The greater the positive charge on the metal ion, the easier it should be for proton to dissociate from an attached water molecule. Such an equilibrium is given the following equation [119]:

$$M^{n+} + 2H_2O = M(OH)^{(n-1)+} + H_3O^{+} \tag{6.1}$$

6.3.1. The effect of pH *($MgSO_4 \bullet 7H_2O$ experiments)*

The dissociation of a proton from water molecules may effect the structure of the solution. By addition of Mg^{+2} ions to the water, the hydronium ions are generated as a result of the hydration of Mg^{+2} according to the equilibrium in Eq. 6.1 and as shown in the following expression:

$$Mg^{+2} + 2H_2O = Mg(OH)^{+} + H_3O^{+} \tag{6.2}$$

The addition of hydronium ions (H_3O^+) to the solution will affect the position of the equilibrium. According to Le Chatelier principle the position of chemical equilibrium always shifts in a direction that tends to relieve the effect of an applied stress [120]. Thus, an increase H_3O^+ ions in the solution causes to shift the position of the equilibrium to the left side. i.e. the solubility of the salt will decrease. While, the addition of OH^- ions will have the opposite effect. *This may be accepted as an explanation for the change in the solubility of the solution after the change in the pH-value of the solution.*

The change in the structure of the solution by the presence of various ions can be estimated from the entropy data (order or disorder of the system) shown in ***Table 6.3.1.***. If the entropy of an electrolyte has a more negative value, then it is a structure former. If the value is less negative, then it is a structure breaker. For this work the following can be summarised [121]:

- H_3O^+ is a slight structure breaker.
- Cations smaller or more highly charged than H_3O^+ are structure formers.
- OH^- is a structure breaker, while SO_4^{-2} is a structure former.

Table 6.3.1.: *Physical properties of cations and anions at 298 K [122].*

		Physical properties		
Ion	*Ionic Radii* [A°]	H_{hyd} [KJ.mol^{-1}]	S_{hyd} [KJ.mol^{-1}.K^{-1}]	G_{hyd} [KJ.mol^{-1}]
H_3O^+	––	–1129	–131	–1090
Na^+	0.95	–444	–110	–411
K^+	1.33	–360	–74	–338
Fe^{+2}	0.76	–2305	–383	–2191
Mg^{+2}	0.65	–1999	–311	–1906
Ni^{+2}	0.72	–2490	–396	–2372
Pb^{+2}	1.2	–1785	–228	–1717
Cl^-	1.81	–340	–76	–340
OH^-	1.4	–423	–149	–379
SO_4^{-2}	1.5	–1145	–263	––

In supersaturated solution, neutral solution, Mg^{+2} ions will move towards the crystal surface (the crystal growth will be enhanced), while in undersaturated solution Mg^{+2} ions will leave the crystal surface towards the solution (the dissolution rate will be enhanced). In the same way, the addition H_3O^+ ions to the solution (acidic medium) will make the solution unstable (structure breaker). Consequently, in supersaturated solution it is proposed that, the Mg^{+2} ions prefer to remain in the solution (as aqueous ions $Mg(OH)^+$ see Eq. 6.2). Therefore, the number of Mg^{+2} ions arriving to the crystal surface will be reduced, therefore, the growth rate will be suppressed. In undersaturated solution the number of Mg^{+2} ions that must leave the crystal surface towards the solution will be reduced, therefore, the dissolution rate will be suppressed. *This may be accepted as an explanation for a lower growth and dissolution rate of* $MgSO_4\bullet 7H_2O$ *crystals in acidic/alkaline solutions compared with the neutral solutions*.

6.3.2. The effect of K^+ ions *($MgSO_4\bullet 7H_2O$ experiments)*

It can also be seen from the thermodynamic properties of the ions shown in ***Table 6.3.1.***. The smaller the ion is, the stronger the interaction (higher hydration energy) between the ion and water molecules in the coordination sphere, that is to say univalent, divalent and trivalent positive ions (cations) are hydrated. The largest enthalpy of hydration can be expected for the smallest ion (e.g. Mg^{+2} has enthalpy –1999 kJ mol^{-1}). Therefore, the presence of such an ion in the solution has more tendencies for interaction with water molecules than the largest ion, especially, when the latter has such a relatively small enthalpy of hydration (K^+ has enthalpy –360 kJ mol^{-1}). *It is proposed that such an interaction stands behind the increase in the solubility of* $MgSO_4\bullet 7H_2O$ *in the presence of* K^+ *ions in the solution. The later inference has proven the results concerning the increase in the solubility of* $MgSO_4\bullet 7H_2O$ *by adding* K_2SO_4 *and* KH_2PO_4 *as impurities (see **Table 5.2.1.**).*

As mentioned previously the change in the structure of the solution by the presence of various ions can be estimated from the entropy data (order or disorder of the system) shown in ***Table 6.3.1.***. Here the following can be summarised:

- K^+ is a slight structure breaker.
- A cation smaller or more highly charged than K^+ is a structure former.

Here it is proposed, that the presence of K^+ ions in the solution will make the solution unstable (structure breaker). Consequently, K^+ ions prefer to move toward the crystal surface rather than to remain in the solution (as aqueous ions). *Therefore, the number of* K^+ *ions adsorbing on the crystal surface will be increased by increasing the amount of* K^+ *ions adding to the solution, hence the number of* Mg^{+2} *ions arriving at the crystal surface will be reduced (the growth rate will be suppressed). This may be accepted as an explanation for suppressed growth rate compared to the pure solution.*

6.3.3. The effect of hydro-complex ions

6.3.3.1. $MgSO_4 \bullet 7H_2O$ experiments

In the Fe^{+2} ions-free solution the growth rate of $MgSO_4 \bullet 7H_2O$ crystals is affected by pH-value of the solution [109]. However, in the presence of Fe^{+2} ions the growth rate changed significantly with pH (the pH of Fe^{+2} ions contaminated solution decreased to a value of 4.32 and 3.46 corresponding to Fe^{+2} ions concentration of 1 and 2 wt %, respectively [108]). This decreases in pH is due to the hydrolysis reaction of the hydro-complex compound of Fe^{+2} ions [65, 119]. The impurity effect, $\alpha\theta_{eq}$, of Fe^{+2} ions decrease dramatically as the pH was increased (see ***Fig. 6.3.1.***).

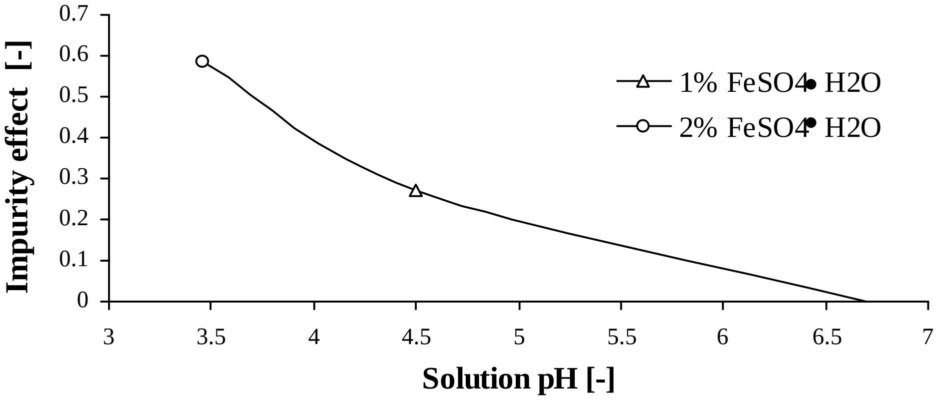

Figure 6.3.1.: *Effect of the pH-value on the impurity effect,* $\alpha\theta_{eq}$, *at* $\sigma = 0.01$.

This result suggests that only part of the adsorbed is growth suppression active. Fe^{+2} ions do not dissolve as bare ions in water but dissolve as hydro-complex ions, producing H_3O^+ ions through hydrolysis reaction like an acid [65, 119]:

$$Fe^{+2} + 2xH_2O = Fe(OH)_x^{(2-x)+} + x\,H_3O^+ \qquad (6.3)$$

Fe^{+2} ions may also dissolve in $MgSO_4 \bullet 7H_2O$ solution in the same way and the hydro-complex ion exchange water molecules with sulfate ions (ligand exchange reaction). The ligand exchange reaction products may also give dimers, which can be also hydrolysis products. The chemistry of Fe^{+2} in $MgSO_4 \bullet 7H_2O$ solution is complicated. For simplicity, only two hydrolysis reaction will be considered here,

$$A = A_1^* + H_3O^+ \qquad (6.4)$$

$$A_1^* = A_2^* + H_3O^+ \tag{6.5}$$

where A is an inactive (both for growth-suppresses and adsorption) hydro-complex compound, A_1^* and A_2^* are hydrolysis products, which could be assumed to be $Fe(OH)^+$ and $Fe(OH)_2$, respectively. Further, it is assumed that these two hydrolysis products both adsorb on the surface of the crystal to be grown (adsorption active) but only A_1^* acts as a growth suppression active species. The concentration of the first hydrolysis product, $[A_1^*]$, (and hence the amount of adsorbed A_1^*) is speculated to decrease in the highr pH range, as discussed below. The concentration, $[A_1^*]$, depends on the relative values of quotients, Q_1 and Q_2, the equilibrium constants defined with actual concentrations, $[A]$, $[A_1^*]$, $[A_2^*]$ and $[H_3O^+]$, by:

$$Q_1 = [A_1^*][H_3O^+]/[A], \tag{6.6}$$

$$Q_2 = [A_2^*][H_3O^+]/[A_1^*]. \tag{6.7}$$

As discussed in detail by Guzman et al. [123] in relation to the impurity effect of Cr^{+3} ions on crystal growth of K_2SO_4 the concentration of A_1^* can be written by Eq. 6.8 as a function of pH with the aid of a simple mass balance ($c_{imp}=[A] + [A_1^*] + [A_2^*]$) and Eqs. 6.6 and 6.7,

$$[A_1^*] = f_1(pH)c_{imp}, \tag{6.8}$$

where f_1(pH) is a fraction of A_1^* present in the solution to the total impurity dissolved, which is a function of the pH:

$$f_1(pH) = \frac{\dfrac{Q_1}{[H_3O^+]}}{1+\dfrac{Q_1}{[H_3O^+]}+\dfrac{Q_1Q_2}{[H_3O^+]^2}} = \frac{Q_1}{10^{-pH}+Q_1+\dfrac{Q_1Q_2}{10^{-pH}}} \tag{6.9}$$

The function, f_1(pH), and hence, $[A_1^*]$ decreased as the pH is increased in the range of $pH \geq -\log (Q_1Q_2)^{1/2}$ (see ***Fig. 6.3.2.***). *This could be a reason why the growth rate decreased contrary to the increasing trend of the adsorbed* Fe^{+2} *ions*. The adsorption isotherm for the growth suppression active species, A_1^*, could be written as,

$$\theta_{eq1} = \frac{K[A_1^*]}{1+K[A_1^*]} = \frac{Kf_1(pH)c_{imp}}{1+Kf_1(pH)c_{imp}} \tag{6.10}$$

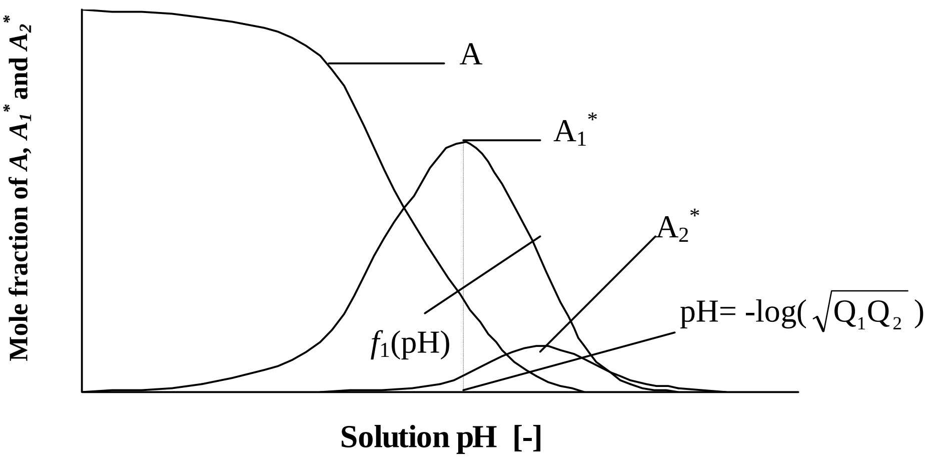

Figure 6.3.2.: *A simple schematic representation of [A], [A_1^*] and [A_2^*] as a function of pH [65].*

Strictly speaking the effect of Fe^{+2} ion concentration on the growth kinetics in terms of surface coverage, θ_{eq} Eq. 3.36, should be considered by using Eq. 6.10. But it is impossible because θ_{eq1} is not determined experimentally. The larger the impurity effectiveness factor, α, is expected with respect to A_1^* (not the total dissolved impurity, c_{imp}), since $K > Kf_1(pH)$ and $\theta_{eq} > \theta_{eq1}$. The increasing trend of impurity effect, $\alpha\theta_{eq}$, with increasing impurity concentration is consistent with the increasing behaviour of θ_{eq} expected from the theory (see Eq. 6.10) under a constant impurity effectiveness factor, α, as shown in ***Fig. 6.3.3.***. The effect of pH on the growth behaviour is shown in ***Fig. 6.3.4.***, the lower the pH, the stronger the impurity effect becomes. This pH effect can be explained as a result of increasing surface coverage, θ_{eq}, ***Fig. 6.3.3.*** and Eq. 6.10.

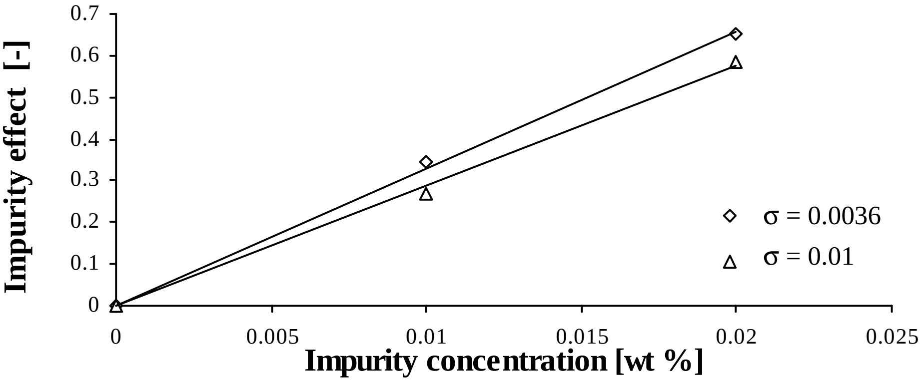

Figure 6.3.3.: *Effect of $FeSO_4 \bullet H_2O$ concentration on the impurity effect, $\alpha\theta_{eq}$.*

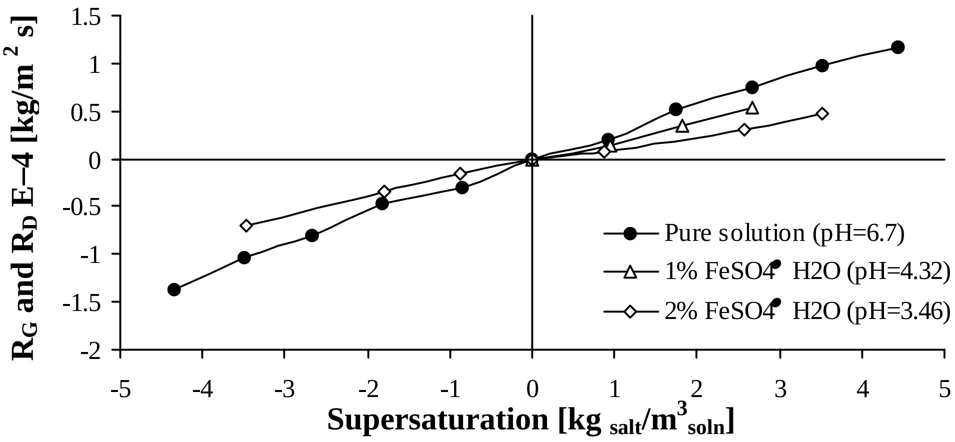

Figure 6.3.4.: *Growth and dissolution rates of* $MgSO_4 \bullet 7H_2O$ *in the presence of* $FeSO_4 \bullet H_2O$ *as impurity.*

The dissolution process is closely related to the growth process, since they are surface-related phenomena [4, 5]. In either process, Fe^{+2} ions have to be adsorbed or desorbed on/off the crystal surface. The dissolution is suppressed with increasing Fe^{+2} ions concentration in the solution as already shown in ***Fig. 6.3.4.***. The adsorption or desorption mechanisms of active Fe^{+2} ion complexes is expected to be the same during both the dissolution and the growth processes, i.e., if these complexes adsorb at growth layer steps and retard growth, it is reasonably to assume that they desorb at dissolution layer steps and retard dissolution. The need for much higher critical concentrations of Fe^{+2} ions for dissolution retardation than for growth retardation have not been satisfactory explained, but the diffusional and kinetic processes involved are fundamentally different in the two cases. Dissolution, a much faster process is an exact reversal of growth. Solute ions are detach from the layer as a direct consequence of hydration and are transported directly, by volume diffusion, to the bulk solution. Impurity adsorption at layer fronts prevent dissolution (or disintegration with hydration), but they are readily removed during the dissolution process. Consequently, larger amounts of impurities are necessary to prevent water molecules reaching and reaction with the solute ions.

The same argument in the presence of Ni^{+2} *ions, as impurity, can be applied for suppressing the growth and dissolution rates of* $MgSO_4 \bullet 7H_2O$ crystals.

6.3.3.2. *NaCl* experiments

By addition of Na^+ ions to the water, the hydronium ions are generated as shown in the following expression:

$$Na^+ + 2H_2O = Na(OH) + H_3O^+ \tag{6.11}$$

The position of the equilibrium will be affected by adding Mg^{+2} ions to the saturated solution as impurity and the later, according to Eq. 6.1, it will cause to generate hydronium ions (H_3O^+). Thus, an increase H_3O^+ ions in the solution causes to shift the position of the equilibrium to the left side, principle of Le Chatelier [120], i.e. the solubility of the salt will decrease. *This may be accepted as an explanation for the change in the solubility of NaCl in the presence of* Mg^{+2} *ions in the solution.*

As mentioned previously, the largest enthalpy of hydration can be expected for the smallest ion (e.g. Mg^{+2} has enthalpy – 1999 kJ mol^{-1}, see ***Table 6.3.1.***). Therefore, the presence of such an ion in the solution has more tendencies for interaction with water molecules than the largest ion, especially, when the latter has such a relatively small enthalpy of hydration (Na^+ has enthalpy –444 kJ mol^{-1}). *It is proposed that such an interaction stands behind the decrease in the solubility of NaCl in the presence of* Mg^{+2} *ions in the solution* (see ***Fig. 5.1.1.***).

The presence of various ions in the solution cause to the change in the structure of the electrolyte solution. This change can be estimated from the entropy data presented in ***Table 6.3.1.***. In this case the following can be summarised:

- Na^+ is a slight structure breaker.
- A cation smaller or more highly charged than Na^+ is a structure former.

In supersaturated solution, pure *NaCl* solution, the crystal growth will be enhanced by adsorption of Na^+ ions on the crystal surface, while in undersaturated solution, Na^+ ions will leave the crystal surface towards the solution (the dissolution rate will be enhanced). In the same way, the presence of Mg^{+2} ions in the solution will give the solution more stability (structure former). Consequently, in supersaturated solution it is proposed that, Mg^{+2} ions will be moved toward the crystal surface and adsorbed on the surface, while Na^+ ions prefer to remain in the solution (as aqueous ions). Therefore, the number of Na^+ ions arriving at the crystal surface will be reduced, hence the growth rate will be suppressed.

This may be accepted as an explanation for suppressed growth rate compared to the pure solution. The same argument in the presence of Pb^{+2} ions, as impurity, can be applied for suppressing the growth rate of NaCl crystal.

In another conclusion, Mg^{+2} ions do not dissociate as bare ions in water but they dissociate as hydro-complex ions, producing H_3O^+ through hydrolysis reaction as shown in Eq. 6.1. Mg^{+2} may also dissociate in $NaCl$ solution in the same way and the hydro-complex ion exchange water molecules with chloride ions (ligand exchange reaction). The ligand exchange reaction products may also give dimers, which can also be hydrolysed. The chemistry of Mg^{+2} in $NaCl$ solution is complicated. For simplicity, only two hydrolysis reactions will be considered (see Eqs. 6.6 and 6.7), where A, is assumed to be Mg^{+2}, is an inactive (both for growth-suppresses and adsorption) hydro-complex compound, A_1^* and A_2^* are hydrolysis products, which could be assumed to be $Mg(OH)^+$ and $Mg(OH)_2$, respectively. Further, it is assumed that these two hydrolysis products both adsorb on the surface of the crystal to be grown (adsorption active), but only A_1^* acts as a growth suppressing active species. The concentration of the first hydrolysis product, $[A_1^*]$, (and hence the amount of adsorbed A_1^*) is speculated to decrease as discussed, previously, in relation to the impurity effect of Fe^{+2} ions on crystal growth of $MgSO_4 \bullet 7H_2O$ [108].

6.4. Electrical double layer

At the interface of a charged solid and a liquid there is always a separation of electrical charge. The surface of the solid has an excess of one charge and the balancing is found in the adjacent surface region of the liquid. The arrangement of the charges at the solid and liquid interface is referred to as the double layer.

The double layer is an electrical cloud near the solid surface composed of both a rigid zone, know as the Stern layer and a diffuse layer. Ions having the opposite charge as the solid are immediately attracted to the surface of the solid and attach, forming the Stern layer. Additional ions of the same charge as the Stern layer are also attracted by the oppositely charged solid's surface but are simultaneously repelled by the a like charges in the Stern layer. This dynamic equilibrium results in the formation of a diffuse layer. The diffuse layer is also composed if ions with the same sign of charge as the solid with the concentration of these ions decreasing with distance from the solid. Together the Stern layer and the diffuse layer form the double layer (***Fig. 3.4.3.***). The thickness of the double layer is a function of the pH and ionic strength of the solution. The boundary between the Stern layer and the diffuse layer is called the shear plane. The electric potential at the shear plane is called the zeta potential. A change in zeta potential reflects a charge in surface charge.

6.4.1. Charged particles

The lattice ion hydration theory describes surface charge development by nonreactive ionic solids when placed in water. This theory applies to ionic solids that do not undergo surface oxidation reactions. Either reaction type would modulate the surface charge that the solid develops in water. The only reaction of consequence then is the hydration of lattice ions, and the differential hydration of these lattice ions at the surface of the solid determines the sign of the surface charge.

The theory as first proposed by de Bruyn and Agar [124] was for simple uni–univalent salts in which the cation and anion are in interchangeable lattice positions, which is to say that their lattice energies are equivalent. In this elementary case, the surface charge can be estimated simply from a comparison of the hydration free energies of the corresponding gaseous ions. The theory was demonstrated for the silver halides [124]. Recently, the lattice ion hydration theory was extended to take into consideration lattice energies effects which were shown to be particularly significant for more complicated nonreactive ionic solids such as calcium fluoride [125]. Thus, a more complete theoretical treatment considers the lattice energy of surface ions which in turn are dependent on the crystal structure and preferential plane of cleavage. The energetic can be represented, for the solid *MX*, as follows:

$$M_g^{+} \rightarrow M_{aq}^{+} \qquad X_g^{-} \rightarrow X_{aq}^{-} \tag{6.12}$$

$$M_s^{+} \rightarrow M_g^{+} \qquad X_s^{-} \rightarrow X_g^{-} \tag{6.13}$$

$$M_s^{+} \rightarrow M_{aq}^{+} \qquad X_s^{-} \rightarrow X_{aq}^{-} \tag{6.14}$$

If the hydration energy of the surface lattice cation is more negative than the hydration energies of the surface lattice anion, as described by reaction 3 (Eq. 6.14), then the surface of MX will carry a negative charge. The converse is also true. The complete analysis requires knowledge of the hydration free energies for gaseous ions (reaction 1 (Eq. 6.12)) and the lattice energy for surface ions (reaction 2 (Eq. 6.13)). The former is available from the literature as determined from the Born and Mayer theory [126], while the latter is determined from electrostatic principles, taking into consideration the geometric arrangement of cations and anions in the lattice as described by the surface Madelung constant [125].

As discussed previously in **Chapter 6.3.** and as shown in ***Table 6.3.1.*** that the largest energy, enthalpy and entropy of hydration can be expected for the smallest ion (e.g. Mg^{+2} ion) compared to SO_4^{-2} ion [121]. *Therefore, here it is proposed that* Mg^{+2} *ions have more energy of hydration than* SO_4^{-2} *ion. Consequently, according to the above theory it may be concluded that the surface of a* $MgSO_4{\bullet}7H_2O$ *crystal is carrying a negative charge.*

6.4.2. Measuring crystal charge (*ζ–potential*)

The charge impacted to crystals dispersed in water is called *ζ–potential*. Instruments designed to measure the value of *ζ–potential* do so by subjecting the sample to an electric field and then observing the movement of crystals toward an electrode of an electrophoresis cell. The sign of the charge of the crystals in the electric field determines direction of movement. A negative charge on the crystals causes it to move toward a positive electrode. A positive charge on the crystal would cause it to move toward the negative electrode. The velocity of the crystal movement is determined by the amount of charge. The velocity of movement of the crystals is measured by evaluating the Doppler shift of scattered light. The velocity of crystal movement is directly related to its charge. The *ζ–potential* is calculated from the velocity. *ζ–potential* is expressed in millivolts (mV). *Here, it is important to note that the surface potential is actually of the opposite sign of the perceived potential, due to the adsorbed ions performing a charge reversal* [100].

In general, $MgSO_4 \bullet 7H_2O$ crystals suspended in a saturated solution have a positive *ζ–potential* at different electric field applied as shown in ***Fig. 6.4.2.***. I.e. the $MgSO_4 \bullet 7H_2O$ crystals are negatively charged. The later inference proves the validate of the above conclusion (**Chapter 6.4.1**), that the surface of $MgSO_4 \bullet 7H_2O$ crystals carry a negative charge from the standpoint of the lattice ion hydration theory.

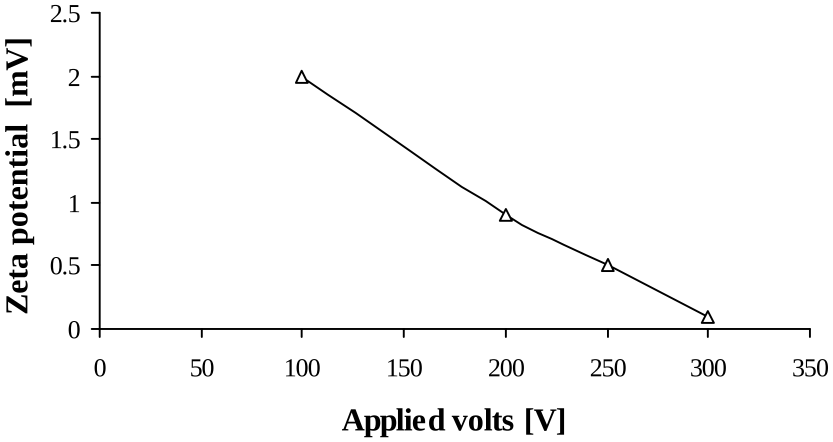

Figure 6.4.2.: *Zeta potential measurements for* $MgSO_4 \bullet 7H_2O$ *crystals at different applied electric field.*

Fig. 6.4.3. shows the mobility and the conductivity of the ions at differently applied electric fields. It is clear from ***Fig. 6.4.3.*** that by increasing the applied of electric field the mobility of the ion will be decreased, while the conductivity of the ions tend to increase. According to Eqs. 3.47 and 3.48, it is true that the mobility of the ions tend to decrease with increasing the electric field and hence the *ζ–potential* of the diffusion layer will be decreased. In another conclusion the conductivity of the

double layer, λ_c, depends linearly on the mobility, u, and the concentration, c, of the ions and may be expressed by the following equation from the theory of electrolytes [127]:

$$\lambda_c = c_{+}\, u_{+}\, ez_{+} + c_{-}\, u_{-}\, ez_{-} \tag{6.15}$$

The mobility of the ions depends on the activation energy of migration, E_{mig}, which irrespective of their charge can be expressed as follows [127]:

$$u = u_0 \exp\left(E_{mig} / k_B T\right) \tag{6.16}$$

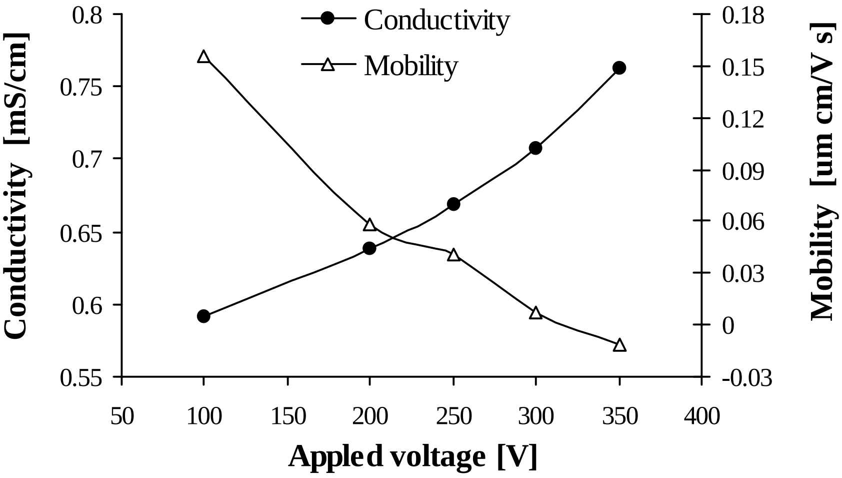

Figure 6.4.3.: *Electrophoretic mobility and conductivity of* Mg^{+2}/ SO_4^{-2} *ions at different electric field.*

The thickness of the diffusion layer will be bigger by the decreasing potential near the crystal surface relative to the bulk of the solution (see Eq. 3.58). This broad of the thickness of the diffusion layer will slow down the diffusion step of the crystallization kinetics, i.e. the movement of Mg^{+2}/ SO_4^{-2} ions inside the diffusion layer will be decreased. The conductivity is increased by increasing the electric field and according to Eq. 6.15 this may be attributed to the increasing of the ionic strength inside the diffusion layer. The present results already indicate that the surface charge of particles are described by measurements of their electrophoretic mobility and the calculation of the corresponding ζ. The potential in the region of shear some distance away from the crystal surface. The measured ζ then provides information regarding the sign (positive/negative) of the prevailing charge at the crystal's surface. Crystals in aqueous electrolyte acquire a charge due to chemical dissociation of the surface groups. This causes the formation of the electrical double layer. Any ion, which will be incorporated in the crystal lattice, should pass through this electrical double layer, which gives extra resistance to crystal growth. If the formation of the electrical double layer is accepted, external effects on this layer and on the crystallization kinetics can be explained more easily.

6.4.3. Effect of pH

Any metal ion in solution is in "equilibrium" with a variety of species e.g., hydrolysis species in aqueous solution that originate from dissolution of the metal ions (see Eq. 6.1). Such hydrolysis species adsorb preferentially and the adsorption of complex hydrolysis ions is responsible for the surface properties of metal hydroxyl. Any ion with a nonelectrostatic adsorption energy contribution can be regarded as preferentially or specifically adsorbed. Within this broad grouping a further division can be made between those ions that adsorb chemically (sharing of electrons) and those do not. For chemical interaction an ion must penetrate the Stern layer. A chemical interaction with the surface is experimentally evidenced by superequivalent adsorption, by reversal of the *ζ–potential*, or by a shift in the *point of zero charge* (*pzc*). In the absence of specific adsorption the *pzc* is identical. The direction of shift is indicative of the sign of the charge on the ion that is specifically adsorbing. The metal hydroxyl surface, which has a positive *ζ–potential*, responds by becoming more positive as the pH is lowered. If the pH is raised it becomes more negative. The surface therefore tends to be more negative the higher the pH and more positive the lower the pH gets. At some intermediate pH these ions, i.e. H_3O^+ and OH^-, which are responsible for generating the surface charge are called the potential determining ions for the system.

As mentioned previously $MgSO_4\bullet 7H_2O$ crystals suspended in a saturated solution have a positive *ζ–potential* charge. By adding more acid to this suspension makes the crystals tend to acquire more positive charges. Adding alkali to the suspension leads to the point where the charge will be neutralized. Further addition of alkali will cause a build up of a negative charge as shown in ***Fig. 6.4.4.***. According to

Eq. 3.45 the potential of the double layer is increased at low pH values and decreased (to a negative charge value) at high pH values.

As a result, according to Eq. 3.58, the highest potential will be at the surface and will be decreased gradually with distance from the surface. The increase of the potential difference as a result of charging the crystal surface will affect the thickness of the diffusion layer. The thickness of the diffusion layer will be smaller by the increasing potential near the crystal surface relative to the bulk of the solution. This reduction of the thickness of the diffusion layer will accelerate the diffusion step of the crystallization kinetics, i.e. the movement of Mg^{+2}/ SO_4^{-2} ions inside the diffusion layer will be accelerated. On the other hand, the adsorption of H_3O^+/OH^- ions on the crystal surface will prevent the adsorption of Mg^{+2}/ SO_4^{-2} ions even though the later have a higher velocity than the ions in the bulk. *This is one reason behind the experimentally observed suppression of the growth rate of* $MgSO_4{\bullet}7H_2O$ *crystals as presented in* ***Fig. 5.2.4.***.

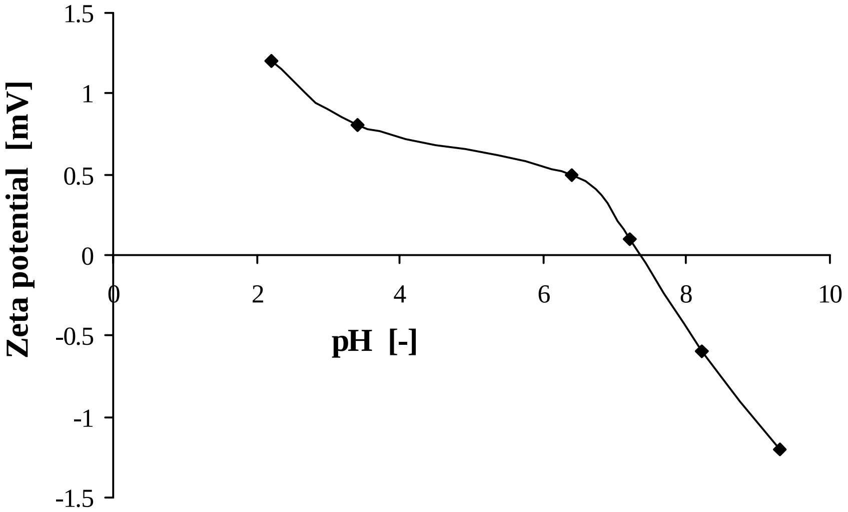

Figure 6.4.4.: *Experimental measurements of zeta potential versus pH values at an applied electric field 250 V.*

On the another side, increasing the potential of the double layer, to more positive charges, by increasing the adsorption of H_3O^+ ions increases the conductivity of the double layer as experimentally observed in ***Fig. 6.4.5.***. This mean that the mobility of the ions will be increased. In another words, according to Eq. 6.16, the activation energy of migration of the ions within the double layer will be reduced by the adsorption of H_3O^+ ions at the crystal surface and hence the growth rate will be decreased. By adsorbing OH^- according to Eq.6.16 the activation energy, E_{mig}, of the ions will be increased. This increases do not effect the conductivity of the double layer, on the contrary the adsorption of H_3O^+ ions. The later inference may be attributed to the reversing the sign of the surface charge to a negative charge. It may be concluded that the conductivity of the ionic strength has a significant effect but not sufficient as an explanation for the crystallization processes. Therefore, taking the adsorption of H_3O^+/ OH^- ions on the crystal surface and their effect on the surface potential and surface charge prove to be important in crystallization phenomena.

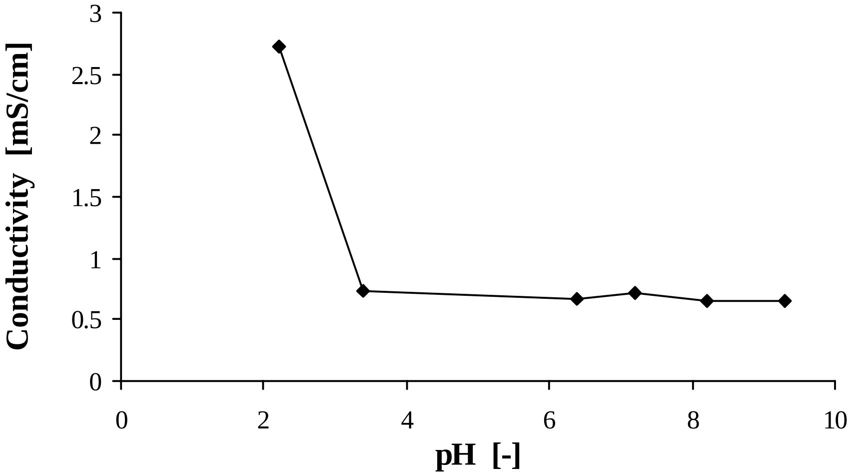

Figure 6.4.5.: *Conductivity of $MgSO_4$•$7H_2O$ crystals versus pH values at an applied electric field 250 V.*

Taking the change in the structure of the solution into account gives a good agreement of found results and understandings of physical phenomena but is still not enough as an explanation for the total crystal growth phenomenon. Especially, in the case of the effect of the adsorption of H_3O^+/ OH^- ions on the potential and charge of the diffuse layer was not be considered so far. It is proven that, the results of ζ measurements indicate that pH plays an exceptional role at the $MgSO_4$•$7H_2O$ crystals surface as shown by the following observation:

- *H_3O^+ ions cause ζ to become more positive than neutral solution.*
- *OH^- ions change the sign of ζ to more negative than neutral solution.*

6.4.4. Effect of adsorption ions

Effect of the increasing ionic strength on the *ζ–potential* of the lattices may shield the charge of the ionic groups on the surface, charge in distribution of the counter-ions and the co-ions in the electric double layer and a decrease in thickness of the electric double layer adjacent to the surface. It is normally accepted in colloidal systems that the charge reversal phenomena occur at higher concentration of inorganic electrolyte when the polarization energy of counter-ions for the interaction with the fixed charge species is sufficiently high. Thus, the total potential across the double layer, commonly referred to as the surface potential, Ψ_0, is determined only by the concentration of potential-determining ions is solution. Indifferent electrolytes do not affect its value unless they have a secondary effects. The *ζ–potential* is more complex and affected by all electrolytes, the effect depending not only on concentration but also on the valence and sign of charge of the ions. Increasing the concentration of indifferent electrolytes in solution reduces the value of *ζ–potential* by compression of the double layer because more ions are forced into Stern layer.

To ascertain the effect of ionic strength on the ζ of $MgSO_4 \bullet 7H_2O$ when the crystal surface is positively or negatively charged, ζ was measured as a function of the concentration of different impurities. As shown in ***Table 5.2.1.*** the growth rate of $MgSO_4 \bullet 7H_2O$ crystal was suppressed by adding impurities and the suppressing of growth rate is more pronounced at higher impurities concentration except in the presence of $MgCl_2$ as impurity, in this case, it was no noticeable effect on the growth kinetic of $MgSO_4 \bullet 7H_2O$ crystals. To confirm this idea, the effect of adding different impurities on the ζ of $MgSO_4 \bullet 7H_2O$ crystals was investigated.

Fig. 6.4.6. shows the effect of impurities concentration of K_2SO_4, KH_2PO_4, KCl, Na_2SO_4 and $MgCl_2$ on the value of ζ of $MgSO_4 \bullet 7H_2O$ crystals. The experiments show that K_2SO_4 and KH_2PO_4 exert an identical influence on ζ of $MgSO_4 \bullet 7H_2O$ crystals over the entire concentration range investigated. The reversal of ζ sign occurs by adding KCl and $Na2SO_4$ to the solution. It is clear that the effect of K^+, Na^+ and $H_2PO_4^-$ ions on ζ indicates that these ions play a special role at the $MgSO_4 \bullet 7H_2O$ crystals surface.

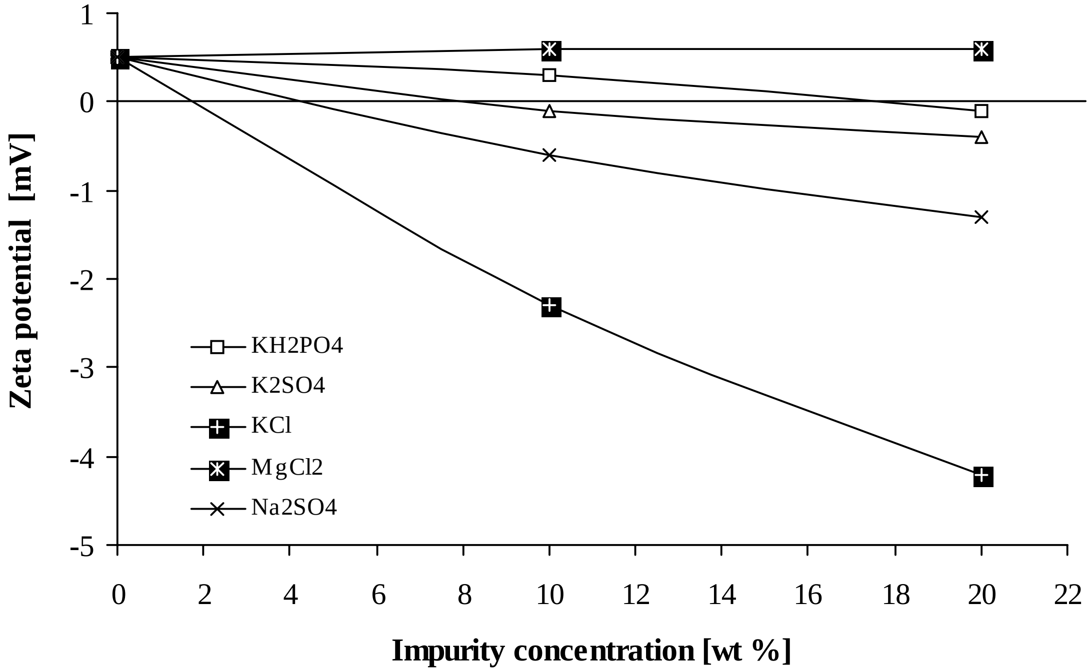

Figure 6.4.6.*: The effect of different impurities concentrations on the ζ–potential of $MgSO_4•7H_2O$ crystals.*

In this study, two main types of ions are considered:

1.. Potential-determining ions

Mg^{+2} and SO_4^{-2} ions are potential-determining ions for $MgSO_4•7H_2O$ surface. Since, adsorption of SO_4^{-2} ions on the surface of $MgSO_4•7H_2O$ will reduce the value of ζ. This is attributed to the negative charge of SO_4^{-2} ions which will cancel some of the positive charges on the $MgSO_4•7H_2O$ crystals. While, in the case of adsorption of Mg^{+2} ions on the surface causes an increase in the value of ζ. Observations in ***Fig. 6.4.6.*** show that the adsorption of Mg^{+2} ions have a relatively weak effect on the value of ζ. *The later inference is accepted as an explanation for the no noticeable kinetic effect on the growth rate of $MgSO_4•7H_2O$ crystals in the presence of $MgCl_2$ impurity (see* ***Table 5.2.1.****).*

2.. Indifferent ions

Which are subdivided into *surface-active* and *surface-inactive* indifferent ions. Each of these types of ions can be characterized by its effect on the *zeta potential*.

1. *surface-inactive indifferent ions*

Surface-inactive electrolytes reduce the value of ζ by compression of the double layer without changing its sign. ζ approaches zero as a limiting value at higher concentration.

2. *surface-active indifferent ions*

If the counter-ions are attracted to the surface not only by simple electrostatic forces, but also by strong chemical or covalent forces, they may reverse the sign of ζ as in the presence of K^+, Na^+ and Ni^{+2} ions (see ***Figs. 6.4.6.*** and ***6.4.7.***). When potential-determining ions, such as OH^- ions change the sign of ζ, the charge at the surface as well as Ψ_0 must change sign; whereas, when a surface active counter-ion changes the sign of ζ, there must be a higher charge in the Stern plane than at the surface. This results in the formation of a *Triple-layer* [128].

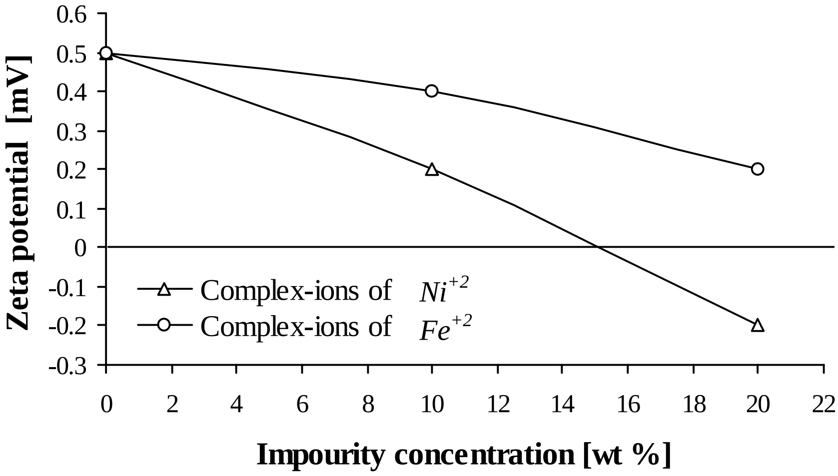

Figure 6.4.7.: *The effect of hydro-complex ions of* Ni^{+2} *and* Fe^{+2} *on the* ζ*–potential of* $MgSO_4 \bullet 7H_2O$ *crystals.*

The Triple-layer model suggested that, the solid-liquid interface visualized in terms of three layers of charge [128]:

1st layer: innermost layer, the surface layer consists of the solid surface itself; locale of *primary potential-determining ions* (e.g. Mg^{+2}, H^+, SO_4^{-2} and OH^-).

2^{nd} layer: the *inner Helmholtz plane* (*IHP*), a *compact-layer* of counter-charge typically consisting of relatively strong bounded (i.e. *specifically adsorbed*) ions (e.g. K^+, Na^+, $Ni^{+2}$and $H_2PO_4^-$).

3^{rd} layer: the *diffuse-layer* the location of ions termed *indifferent ions*. Ions only weakly attracted to the solid surface. The plane of the *diffuse-layer* closest to the solid surface is designated the outer *Helmholtz plane* (*OHP*).

If K^+, Na^+ and Ni^{+2} were *specifically adsorption ions,* ζ would have become more negative on increasing the concentration of impurities, and this has been observed experimentally as shown in ***Figs. 6.4.6.*** and ***6.4.7.***.

The decrease of ζ as a result of charging the crystal surface will affect the thickness of the *diffuse-layer*. The thickness of the *diffuse-layer* is relatively greater than the *compact-layer* by the decreasing potential near the crystal surface relative to the bulk of the solution. This broad of the thickness of the diffuse-layer will slow down the diffusion step of the crystallization kinetics, i.e. the movement of $Mg^{+2}/\ SO_4^{-2}$ ions inside the *diffuse-layer* will be decreased. On the other hand, the thickness of *compact-layer* will be smaller comparison with *diffuse-layer,* this decreasing of the *compact-layer* thickness will accelerate the diffusion step. The *specifically adsorption ions* (e.g. K^+, Na^+ and Ni^{+2}) were presented inside the *compact-laye*r as suggested by the *Triple-layer* model. The presence such as ions causing a relatively strong bound on the crystal surface of $MgSO_4\bullet7H_2O$, thus the adsorption of $Mg^{+2}/\ SO_4^{-2}$ ions is reduced. *This is one reason behind the experimentally observed suppression of the growth rate of $MgSO_4\bullet7H_2O$ crystals as presented in* **Table 5.2.1.**.

Figs. 6.4.8. and ***Fig. 6.4.9.*** show the effect of different impurity concentration on the mobility and conductivity of ions, respectively. It is clear that by reducing the value of ζ by increasing the adsorption of *indifferent ions* increases the conductivity of the *double-layer* as experimentally observed in ***Fig. 6.4.9.***. While, the mobility of the ions is decreased. I.e., according to Eq. 6.16, the activation energy of migration of the ions within the double layer will be increased by the adsorption of *indifferent ions* at the crystal surface of $MgSO_4\bullet7H_2O$ and hence the growth rate will be decreased.

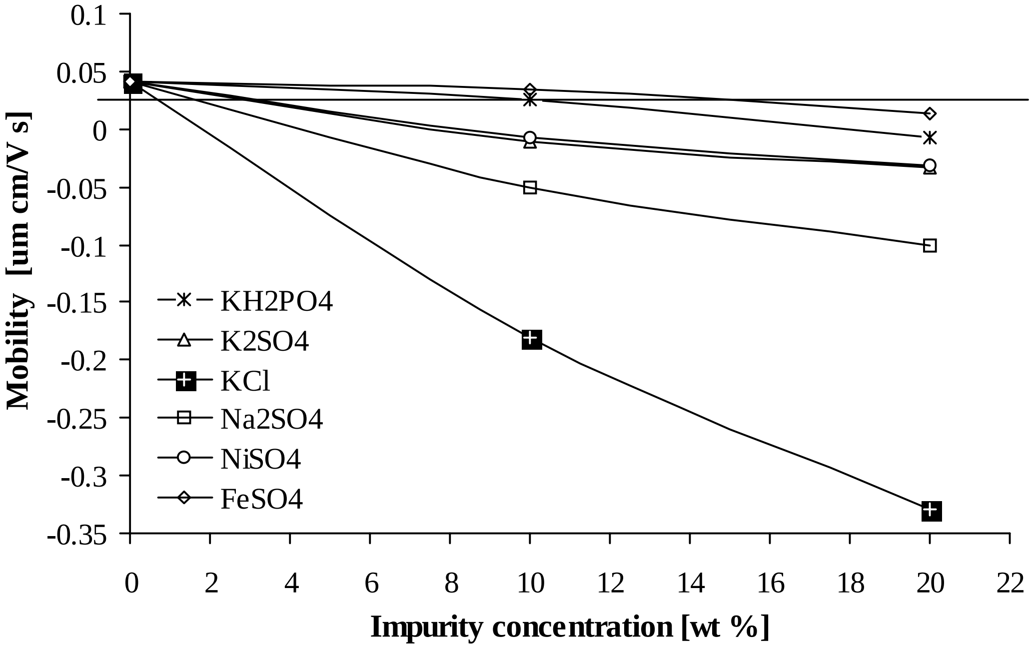

Figure 6.4.8.: *Mobility of the ions as a function of different impurities concentration at an applied electric field 250 V.*

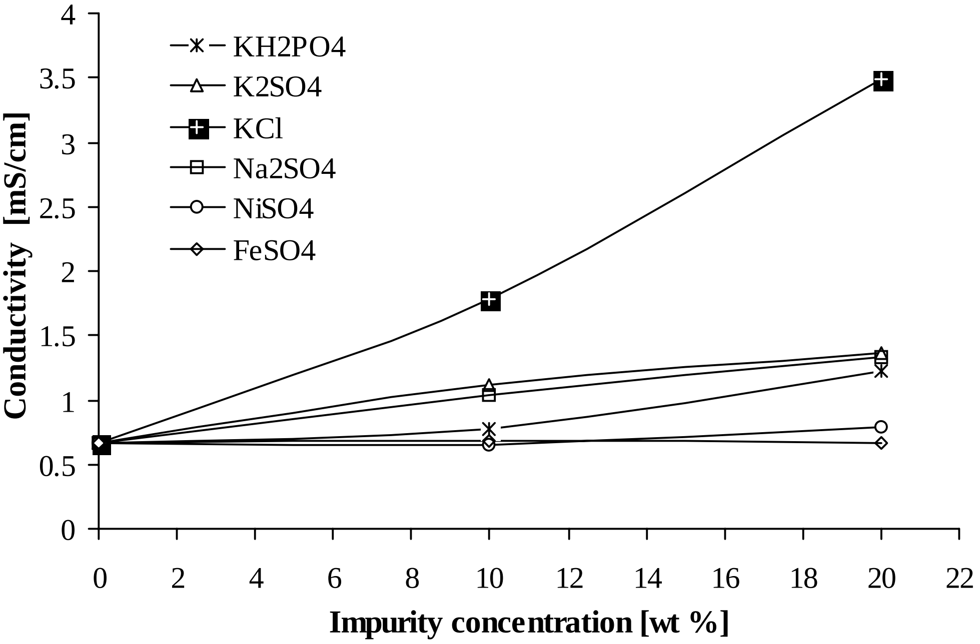

Figure 6.4.9.: *Conductivity of the ions as a function of different impurities concentration at an applied electric field 250 V.*

It is believed that, the Ni^{+2} ions are likely to interact with water molecules to form a complex ions in an aqueous solution (see Eq. 6.1). The *ζ–potential* charge changed from positive to negative when $NiSO_4$ was added. This result suggests that adsorption of the complex ions onto the crystal surface is possible. When a $Ni(OH)^+$ and $Ni(OH)_2$ ion adsorption occurs on the $MgSO_4{\bullet}7H_2O$ surface the Ni^{+2} charge on the surface of the $MgSO_4{\bullet}7H_2O$ is neutralized thus reducing the surface charge. Therefor, the decrease of ζ of $MgSO_4{\bullet}7H_2O$ can result from the adsorption of the complex ions, which replaces the adsorbed $Mg^{+2}/\ SO_4^{-2}$ and reveres the positive value of ζ of the $MgSO_4{\bullet}7H_2O$ crystals. In an aqueous solution containing Ni^{+2} ions, complex ions are adsorbed onto the surface of the $MgSO_4{\bullet}7H_2O$ crystals and changed the polarity of the $MgSO_4{\bullet}7H_2O$ from positive to negative. This phenomenon was found in the suspensions containing $NiSO_4$ as electrolytes.

The same argument can be applied in presence of Fe^{+2} ions in the solution, as mentioned previously by adding Fe^{+2} ions to the saturated solution of $MgSO_4{\bullet}7H_2O$ the pH value of the solution is changed to a lower pH (see ***Table 5.2.1.***) . This decreases in pH is due to hydrolysis reaction of the hydro-complex compound of Fe^{+2} ions [65, 119]. An observation of ***Fig. 6.4.7.*** shows that the value of ζ is reduced by increasing Fe^{+2} ion concentration in the solution. This changes in the value of ζ can be attributed by adsorption of H^+ and hydro-complex of Fe^{+2} ions on the crystal surface of $MgSO_4{\bullet}7H_2O$. If the change is attributed only by adsorption of H^+ ions, which are considered as a *potential-determining ions,* this causes the ζ to become more positive as proven previously (see ***Sec. 6.4.3*** and ***Fig. 6.4.4.***). If the case is attributed only for adsorption of hydro-complex of Fe^{+2} ions this causes to reverse the sign of ζ as in the case of the adsorption of hydro-complex of Ni^{+2} ions. Therefore, the reduction in the value of ζ in the presence of Fe^{+2} ions in the solution is reasonable to the adsorption of hydro-complex of Fe^{+2} and H^+ ions on the crystal surface of $MgSO_4{\bullet}7H_2O$ and hence this is causing a suppressing in crystal growth. Thus, the adsorption of H^+ ions on the crystal surface will cancel some of the negative charge of ζ that reasonable by adsorption of hydro-complex of Fe^{+2} ions.

6.5. Summary of results

From the results presented in this work the following conclusions may be drawn:

1. The influence of the heat transfer on the crystal growth kinetics in solution crystallization was often ignored. By the application of the Three-Step-model it is possible to quantify the importance of heat transfer on the growth kinetics. Especially for substances of high values for the crystallization heat or strong temperature dependencies of the equilibrium concentration this model leads to new predictions of the growth kinetics.

2. By taking the effectiveness factor concept into account good agreements are given for an explanation for the change in the controlling crystal growth mechanism in case of the growth of $NaCl$ and $MgSO_4 \bullet 7H_2O$ crystals in the presence of different impurities.

3. The proposed model (Eq. 3.39) can be used to show that the general relationship of crystallization kinetics in the presence of impurities is valid not only in the case of single crystals but also in industrial crystallizers where many crystals are growing in suspension. Consequently, from the analysis of the growth kinetics of different crystals it may be noted that the data are in general consistent with the proposed model (Eq. 3.39), and hence, the values of heat of adsorption, Q_{diff}, are to be considered sufficiently to determine whether adsorption occurs at kink sites or at the surface terraces. This is a valuable tool of knowledge in predicting growth phenomena.

4. The structure of the solution has been quite often ignored in the studies of crystallization kinetics of soluble salts. Taking the structure of the solution into account proves to be important in order to explain crystallization processes. Here, it is proven from previous conclusion that (see Chapter 6.3.3.) the growth behaviour is reasonably explained by a mechanism in which the hydrolysis product (hydro-complex compound of Fe^{+2} and Ni^{+2} ion) which is in equilibrium with the inactive hydrated complex in the solution, is assumed to be adsorbed on the growth layer steps of $MgSO_4 \bullet 7H_2O$ crystals and retards the growth. These trends in which the first

hydrolysis product of the hydro-complex compound of Mg^{+2} and Pb^{+2} acts as active species for growth inhibition of $NaCl$ crystals were the same as those of the hydro-complex compound of Fe^{+2} and Ni^{+2} ion.

5. The Laser-Doppler electrophoresis (ζ–potential measurements) was used to determine the electrophoretic mobility of $MgSO_4 \bullet 7H_2O$ crystals and thus predict the sign of surface charge in a saturated solution. Such information is of technological importants in the field of crystallization. It is evident from previous experimental results, that surface charge analysis of soluble salt systems is now possible using this Laser-Doppler electrophoresis after reducing the higher conductivity of saturated solution by diluting the solution with Ethanol. Further, by means of ζ–potential techniques it has been proven that $MgSO_4 \bullet 7H_2O$ crystals are positively ζ charged in pure solution. This charge is changed by presenting of potential-determining ions or indifferent-ions. The results of ζ measurements indicates that pH and cations/anions have a very strong effect on the electrical double layer. Consequently, they have a specific effect on crystallization, depending on how the surface charge is affected in way of increasing/decreasing or reversing the sign of the charge. Therefore, knowing the surface potential by measuring the ζ–potential can help to explain the crystallization phenomena which are not clear up to now.

7. Summary

The major objective of the present investigation is to propose a new explanation for the effect of impurities or changing the pH value of the solution on the crystallization kinetics, based on the hypothesis, that the crystal growth rate of salts is dominated by the surface potential distribution.

In this study a fluidized bed crystallizer is employed to investigate the growth and dissolution rate of $MgSO_4 \bullet 7H_2O$ and $NaCl$ crystals. In the experiments the supersaturation, impurity concentration and pH-values in the solution were varied. The growth rate was interpreted in terms of supersaturation levels. The orders and rate constants were reported. The effectiveness factors were estimated from the growth rate data to evaluate the relative magnitude of the two resistances in series, diffusion and integration. The evaluation of the effectiveness factor results indicate that:

1. The crystal growth rate of $NaCl$ is diffusion controlled in the absence of impurities. However, with the used impurities a change in the growth mechanism arises, i.e. the presence of the impurities leads to a more important role of the integration step.

2. The controlling mechanism for $MgSO_4 \bullet 7H_2O$ crystal growth from pure and impure solution is contributing by the integration step and the diffusion step. In the case of pure solution, the diffusion step offers a greater resistance to overall crystal growth than integration step. However, the presence of impurities lead to a more important role of integration step.

Therefore, the effect of different impurities on the growth rate of $MgSO_4 \bullet 7H_2O$ and $NaCl$ crystals can be divided into:

1. Thermodynamic effects: Impurities changing the equilibrium saturation concentration.

2. Kinetic effects: Impurities reducing the crystal growth rate of $MgSO_4 \bullet 7H_2O$ and $NaCl$ crystals.

3. Thermodynamic effects as well as kinetic effects: Impurities affecting the solubility as well as the growth rate of $MgSO_4{\bullet}7H_2O$ and $NaCl$ crystals.

Own found data on crystal growth rates from aqueous solutions as a function of impurity concentration are discussed from the standpoint of Cabrera and Vermileya [14] and Kubota and Mullin [49]. The value of impurity effect, $\alpha\theta_{eq}$, determined from analysis of the data on growth kinetics was found to be in good agreement with the value obtained from direct adsorption experiments. The estimated value of the average spacing between the adjacent adsorption active sites and the average distance between the neighboring impurity-adsorbed sites are also reported.

Finally, the electrophoretic mobility measurements by Laser-Doppler electrophoresis (ζ–potential measurements) are reported for $MgSO_4{\bullet}7H_2O$ crystals. These measurements for inorganic salt have been made for the first time and allow the surface charge to be predicted for $MgSO_4{\bullet}7H_2O$ crystals in their saturated solution. Therefore, knowing the surface potential by measuring ζ–potential can help to explain the crystallization phenomena which are not clear up to now.

In general, the results show that the $MgSO_4{\bullet}7H_2O$ crystals have a positive *ζ–potential* charge. At low pH the surface will acquire more positive charge and at high pH a build up of negative charge will take place, hence, the crystal growth is suppressed. In this study it was proven that the growth rates of $MgSO_4{\bullet}7H_2O$ crystals are suppressed by traces of Fe^{+2}/Ni^{+2} ions. Here, the growth behaviour is reasonably explained by a mechanism in which the adsorbed hydrolysis product (an assumed active species) of hydrated Fe^{+2}/Ni^{+2} ions retards the rate of the processes. The impurity effect is explained by assuming that the first hydrolysis product of the hydro-complex compound of Fe^{+2} and Ni^{+2} ions acts as active species for growth inhibition. The surface charge is changed when Fe^{+2} and Ni^{+2} ion was added. This result suggests, that the adsorption of the complex ions onto the crystal surface is possible. Therefore, this change in the value or the reverse of the sign of ζ is causing a suppressing in crystal growth of $MgSO_4{\bullet}7H_2O$.

8. Zusammenfassung

Die Hauptzielsetzung der Untersuchung ist es, eine neue Erklärung für den Effekt der Verunreinigungen oder des pH-Wertes der Lösung auf die Kinetik der Kristallisation vorzuschlagen. Die Hypothese, basiert darauf, dass die Kristallwachstumrate der hier nur betrachteten anorganischen Salze aus wässeriger Lösungen durch die Oberflächenpotentialverteilung beherrscht wird.

In dieser Arbeit wird ein Wirbelbettkristallisator eingesetzt, um die Wachstums- und Auflösungsgeshwindigkeit von $MgSO_4 \bullet 7H_2O$ und $NaCl$ Kristallen zu vermessen. In den Experimenten wurden die Übersättigung, die Konzentration der Verunreinigungen und die pH-Werte in der Lösung verändert. Die Wachstumsraten wurden in Abhängigkeit des Übersättigungniveaus ermittelt. Die Exponenten und die Konstanten der Wachstumskinetik wurden experimentell ermittelt. Der Wirkungsgrade wurde aus den Wachstumsratedaten erhalten. Die relative Größe der zwei in Reihe, geschalteten Widerstände der Diffusion und der Integration wurde so abgeschätzt. Die Auswertung des Wirkungsgrades zeigt folgendes:

1. In Abwesenheit von Verunreinigungen ist die Kristallwachstumsgeshwindigkeit von NaCl diffusionskontrolliert. Die Verunreinigungen rufen jedoch eine Veränderung des Wachstumsmechanismus hervor, d.h. die Gegenwart der Verunreinigungen führt zu einer wichtigeren Rolle des Integrationsschrittes.

2. Zum Kontrollmechanismus des Kristallwachstums von $MgSO_4 \bullet 7H_2O$ in reiner als auch in unreiner Lösung tragen der Diffusions- und der Intigrationsschritt bei. Im Falle der reinen Lösung liefert der Diffusionsschritt gegenüber dem Gesamtkristallwachstums einen stärkeren Widerstand als der Intgrationsschritt. Die Verunreinigungen lassen dagegen die Rolle des Integrationsschrittes dominieren.

Folglich kann der Effekt der unterschiedlichen Verunreinigungen auf die Wachstumsrate von $MgSO_4 \bullet 7H_2O$ und $NaCl$ Kristallen in drei Gruppe geteilt werden:

1. Thermodynamische Effekte: Verunreinigungen, welche die Gleichgewichtsättigungskonzentration verändern.

2. Kinetische Effekte: Verunreinigungen, welche die Kristallwachstumrate von $MgSO_4 \bullet 7H_2O$ und $NaCl$ Kristallen verringern.

3. Thermodynamische Effekte sowie kinetische Effekte: Verunreinigungen, welche die Löslichkeit sowie die Wachstumsrate von $MgSO_4{\bullet}7H_2O$ und $NaCl$ der Kristalle beeinflussen.

Die von mir ermittelten Daten der Kristallwachstumsraten in wässrigen Lösungen in Abhängigkeit von den Konzentrationen der Verunreinigungen wurden sowohl nach dem Gesichtspunkt von Cabrera und Vermileya [14] als auch nach Kubota und Mullin [49] diskutiert. Der Wert des Verunreinigungseffektes, $\alpha\theta_{eq}$, der aus der Analyse der Daten aus der Wachstumskinetik ermittelt wurde, steht in guter Übereinstimmung mit dem berechneten Wert aus den direkten Adsorptionsexperimenten. Die Werte des mittleren Raumes zwischen benachbarten adsorptionsaktiven Stellen und des mittleren Abstandes zwischen benachbarten mit Verunreinigung adsorpierten Stellen wurden verglichen.

Zuletzt wurde über elektrophoretische Mobilitätsuntersuchungen mittels der Laser-Doppler-Elektrophorese (ζ-Potentialmessungen) für $MgSO_4{\bullet}7H_2O$ Kristalle berichtet. Diese Untersuchungen bei einem anorganischen Salz wurden zum ersten Mal überhaupt durchgeführt und erlauben es, die Oberflächenladung der $MgSO_4{\bullet}7H_2O$ Kristalle in ihren gesättigten Lösungen vorauszusagen. Folglich kann die Kenntnis des Oberflächenpotentials mittels Messung des ζ-Potentials helfen, die Kristallisationsphenomene zu erklären, die bis jetzt unbekannt sind.

Im allgemeinen zeigen die Ergebnisse, dass die $MgSO_4{\bullet}7H_2O$ Kristalle eine positive ζ-Potentials Ladung besitzen. Bei niedrigen pH-Werten erhält die Oberfläche eine positivere Ladung, während bei hohen pH-Werten der Aufbau einer negativen Ladung stattfindet, folglich wird das Kristallwachtum unterdrückt. In dieser Studie wurde nachgewiesen, dass die Kristallwachstumsgeschwindigkeit von $MgSO_4{\bullet}7H_2O$ durch Spuren von Fe^{+2} bzw. Ni^{+2} Ionen unterdrückt werden. Hierbei kam das Wachstumsverhalten angemessen mittels eines Mechanismus erklärt werden, bei dem ein adsorbiertes Hydrolyseprodukt (eine angenommene aktive Spezies) von den hydratisierten Fe^{+2} bzw. Ni^{+2} Ionen die Wachstumsgeschwindigkeit unterdrückt. Die Oberflächenladung wurde bei der Zugabe von Fe^{+2} und Ni^{+2} verändert. Dieses Ergebnis legt den Schluss nahe, dass eine Adsorption von komplexen Ionen an die Kristalloberflache möglich ist. Folglich verursacht die Änderung des Wertes von ζ oder dessen Vorzeichen eine Unterdrückung des Wachstums von $MgSO_4{\bullet}7H_2O$.

9. Notation

A		Hydro-complex compound of divalent ions, inactive both for adsorption and growth suppression.
A_1^*		First hydrolysis product of divalent ions, active both for adsorption and growth suppression.
A_2^*		Second hydrolysis product divalent ions, active only for adsorption.
$[A]$	[mol/dm^3]	Concentration of A.
$[A_1^*]$	[mol/dm^3]	Concentration of A_1^*.
$[A_2^*]$	[mol/dm^3]	Concentration of A_2^*.
a	[m^2]	The length of growth unit.
a_l, a_s	[M]	Activity in the solution and at the crystal surface.
C	[F cm^{-2}]	Capacity of the electrical double layer per area.
C^*	[kg/m^3]	Saturation concentration.
C_b	[kg/m^3]	Bulk concentration.
C_i	[kg/m^3]	Interface concentration.
ΔC	[kg$_{salt}$/m^3$_{soln}$]	Supersaturation.
c	[M]	Ion concentration.
c_{imp}	[ppm or mol. fra.]	Impurity concentration.
cp	[J kg^{-1} K^{-1}]	Specific heat capacity.
D_a	[-]	Damköhler number.
E	[V/m]	Electric field strength.
E_{mig}	[J]	Activation energy of migration.
F_f	[N]	Frictional force.
f	[kg/s]	Friction coefficient.
$f_1(pH)$	[-]	Fraction of A_1^* present in the solution (Eq. 6.9).
G	[m/s]	Overall linear growth rate.
g	[-]	Order of growth rate.
G_{hyd}	[KJ mol^{-1}]	Hydration energy.
h	[J m^{-2} s^{-1} K^{-1}]	Heat transfer coefficient.
H_{hyd}	[KJ mol^{-1}]	Hydration enthalpy.
ΔH	[J/kg]	Heat of crystallization.
K	[(mol/mol)$^{-1}$]	Langmuir constant.
k	[m^{-1}]	Reverse length.
k_B	[J K^{-1}]	Boltzmann constant.

k_d	[m/s]	Dissolution rate constant.
k_G	$[\mathrm{kg/m^2 s(kg/m^3_{sol})^{-g}}]$	Overall growth rate constant.
k_r	$[\mathrm{kg/m^2 s(kg/m^3_{sol})^{-r}}]$	Growth integration rate constant.
L_1, L_2	[m]	Initial and final crystal size, respectively.
l	[m]	The average spacing between the adsorption active sites.
Le	[-]	Lewis number.
M_1, M_2	[g]	Initial and final weight of crystals, respectively.
n^-, n^+	[M]	The local anion and cation concentration, respectively.
n_0	$[\mathrm{m^{-3}}]$	Volume concentration of the salt.
n_i^0	$[\mathrm{m^{-3}}]$	Density of the i^{th} ion.
Pr	[-]	Prandtl number (= $C_p\ \mu/\kappa$).
Q_1, Q_2	$[\mathrm{mol\ dm^{-3}}]$	Quotients defined by Eqs. 6 and 7, respectively.
Q_{diff}	$[\mathrm{kJ\ mol^{-1}}]$	The differential heat of adsorption.
q	[J/V]	Effective charge.
R	$[\mathrm{kJ\ mol^{-1}\ K^{-1}}]$	Gas constant.
r	[-]	Order of integration process.
r_c	[m]	Critical size.
R_G , R_{Go}	$[\mathrm{kg/(m^2\ s)}]$	Mass growth rate for impure and pure solution, respectively.
Sc	[-]	Schmidt number (= $\mu/\rho\ D$).
S_{hyd}	$[\mathrm{kJ\ mol^{-1}\ K^{-1}}]$	Hydration entropy.
t	[s]	Time.
T_b	[K]	Bulk temperature.
T_i	[K]	Interface temperature.
u	$[\mathrm{m^2/V\ s}]$	Mobility.
u_0	$[\mathrm{m^2/V\ s}]$	Frequency constant.
v , v_o	[m/s]	Step velocity for impure and pure solution, respectively.
v_i	[m/s]	Velocity of the ion.
W_i	[J]	Electric work.

Greek symbols

α	[-]	Impurity effectiveness factor.
α_1	[m^3]	Volume shape factor.
β_1	[m^2]	Surface area shape factor.
β_d	[-]	Dimensionless number defined by Matsuoka and Garside [3].
γ	[J/m]	Edge free energy.
λ	[m]	Average distance between adsorption sites.
λ_c	[mS/cm]	Conductivity.
λ_D	[m]	Debye length.
μ	[kg/m s]	Viscosity.
μ^0_l, μ^0_s	[V]	Chemical standard potential in the solution and at the crystal surface.
η'	[-]	Non-isothermal effectiveness factor.
η_d	[-]	Diffusion effectiveness factor for crystal growth.
η_r	[-]	Surface integration effectiveness factor for crystal growth.
σ	[-]	Relative supersaturation $((C-C^*)/C^*)$.
σ_0, σ_d	[μC cm^{-2}]	Surface charge.
ρ_c	[kg/m^3]	Crystal density.
ρ_L	[kg/m^3]	Solution density.
ρ_e	[C/m^2]	Electric charge density.
δ_c	[m]	Concentration boundary layer.
δ_T	[m]	Temperature boundary layer.
θ_{eq}	[-]	Coverage of active sites by impurities adsorbed.
Φ_l, Φ_s	[V]	Galvani potential in the solution and at the crystal surface.
$\Delta\chi^{pzc}$	[V]	Difference of the Galvani potentials.
Ψ_0, Ψ_d	[mV]	Surface potential.
$\varepsilon\varepsilon_0$	[-]	Permittivity of liquid.
ζ	[V]	Zeta potential.

10. References

1. **Kruse, M.:**
   Zur Modellierung der Wachstumskinetik in der Lösungskristallisation, Ph.D. Thesis, University of Bremen, Bremen 1992. VDI-Verlag, Düsseldorf 1993.

2. **Kruse, M. and Ulrich, J.:**
   Kristallwachstum in der Lösungskristallisation als Drei-Stufen-Modell, CIT 65 (1993) 1, 60 – 63.

3. **Matsuoka, M. and Garside, J.:**
   Non-Isothermal Effectiveness Factors and the Role of Heat Transfer in Crystal Growth from Solutions and Melts, Chem. Eng. Sci. 46 (1991) 183-192.

4. **Fabian J.:**
   Untersuchungen Zur Auflösungskinetik in der Lösungskristallisation. Ph.D. Thesis, University of Bremen, Bremen 1996.

5. **Fabian, J. and Ulrich, J.:**
   Dissolution Like Crystal Growth-a Two Step Process-Presentation of Experimental Evidence", in proceedings 12th Symposium on Industrial Crystallization, Ed. Z. H. Rojkowski, Warsaw, Poland, 1993, 4-041-4-046.

6. **Nývlt, J. and Ulrich, J.:**
   Admixtures in Crystallization, VCH, Weinheim; 1995, ISBN 3-527-28739-6.

7. **Davey, R. J. :**
   The Control of Crystal Habit, in : Industrial Crystallization 78, Eds. de Jong E. J. and Jancic S. J., North-Holland, Amsterdam, 1979, 169-183.

8. **Simon, B. and Boistelle, R.:**
   Crystal Growth from Low Temperature Solutions, J. Crystal Growth 52 (1981) 779-788.

9. **van Rosmalen G. M., Witkamp, G. J. and de Vreugd, C. H.:**
   Additive and Impurity Effects in Crystallization Processes, in: Industrial Crystallization 87, Eds. Nyvlt J. and Jacek S., Akademia, Prague, 1989, 15-20.

10. **Rosmalen van, G. M. and Bennema, P.:**
Characterization of Additive Performance on Crystallization: Habit Modification, J. Crystal Growth 99 (1990) 1053-1060.

11. **Sangwal, K.:**
Effect of Impurities on the Processes of Crystal Growth, J. Crystal Growth 128 (1993) 1236-1244.

12. **Buckley, H. E.:**
Crystal Growth, Wiley, New York 1951.

13. **Frank, F. C.:**
On the Kinematic Theory of Crystal Growth and Dissolution Processes, in: Growth and Perfection of Crystals, Eds. Doremus R. H., Roperts B. W. and Turnbull, Wiley, New York, 1958, 411-419.

14. **Cabrera, N. and Vermilyea, D. A.:**
The Growth of Crystals from Solution, in: Growth and Perfection of Crystals, Eds. Doremus R. H., Roperts B. W. and Turnbull, Wiley, New York, 1958, 393-410.

15. **Bliznakov, G. M.:**
Über die Wachstumsformen der Kristalle und den Einfluß der Adsorption auf die lineare Kristallisationsgeschwindigkeit, Bull. Acad. Sci. Bulg. Ser. Phy. 4 (1954) 135-152.

16. **Kirkova, E. K. and Bliznakov, G. M:**
Der Einfluß der Adsorption auf das Kristallwachstum, Z. Physik. Chem. 206 (1957) 271-280.

17. **Bliznakov, G. M., Kirkova, E. K. and Nikolaeva, R. D.:**
Über die Wachstumsgeschwindigkeit von KBr-Kristallen in Anwesenheit von Phenol, Z. Physik. Chem. 228 (1965) 23-32.

18. **Julg, A. and Deprick, B.:**
The Influence of Glycine, According to pH, upon the Growth Habit of NaCl and KI,in Aqueous Solution, J. Crystal Growth 62 (1983) 587-594.

19. **Davey, R. J.:**
The Role of the Solvent in Crystal Growth from Solution, J. Crystal Growth 76 (1986) 637-644.

20. **Sano, C., Nagashima, N., Kawakita, T. and Iitaka, Y.:**
The Effects of Additives on the Crystal habit of Monosodium L-Glutamate Monohydrate, J. Crystal Growth 99 (1990) 1070-1075.

21. **Li, L., Tsukamoto, K. and Sunagawa, I.:**
Impurity Adsorption and Habit Changes in Aqueous Solution Grown KCl Crystals, J. Crystal Growth 99 (1990) 150-155.

22. **Bliznakov, G. M. and Kirkova, E. K.:**
A Study of the Effect of Sulfate Ions on the Growth of Sodium Chlorate Crystals, Kristall Tech. 4 (1969) 331-336.

23. **Kirkova, E. K. and Nikolaeva, R. D.:**
Influence of Phenol on the Habit of Sodium Chloride Crystals, Kristall Tech. 6 (1971) 741-746.

24. **Kirkova, E. K. and Nikolaeva, R. D.:**
Investigation of the Crystallization of the System KAl(Cr)(SO4)2*12H2O under Various Conditions, Kristall Tech. 8 (1973) 463-470.

25. **Simon, B., Grassi, A. and Boistelle, R.:**
Cinetique De Croissance de la Face (110) de la Paraffine C36H74 en Solution II. Croissance en presence d'un inhibiteur, la dioctadecylamine, J. Crystal Growth 26 (1974) 90-96.

26. **Dugua, J. and Simon, B.:**
Crystallization of Sodium Perborate from Aqueous Solutions. I. Nucleation Rates in Pure Solution and in Presence of a Surfactant, J. Crystal Growth 44 (1978) 265-279.

27. **Simon, B. and Dugua, J.:**
Crystallization of Sodium Perborate from Aqueous Solutions. II. Growth Kinetics of Different Faces in Pure Solution and in the presence of a Surfactant, J. Crystal Growth 44 (1978) 280-286.

28. **Chu, Y. D., Shiau, L. D. and Berglund, K. A.:**
Effects of Impurities on Crystal Growth in Fructose Crystallization, J. Crystal Growth 97 (1989) 689-696.

29. **Kimura, H.:**
Impurity Effect on Growth Rates of $CaCl_2 \bullet 6H_2O$ crystals, J. Crystal Growth 73 (1985) 53-62.

30. **Sasaki, T. and Yokotani, Y.:**
Growth of Large KDP Crystals for Laser Fusion Experiments, J. Crystal Growth 99 (1990) 820-826.

31. **Owczarek, I. and Sangwal, K.:**
Effect of Impurities on the Growth of KDP Crystals: on the Mechanism of Adsorption on (100) Faces from Tapering Data, J. Crystal Growth 99 (1990) 827-831.

32. **Owczarek, I. and Sangwal, K.:**
Effect of Impurities on the Growth of KDP Crystals: Mechanism of Adsorption on (101) Faces, J. Crystal Growth 102 (1990) 574-580.

33. **Davey, R. J. and Mullin, J. W.:**
Growth of the (101) Faces of Ammonium Dihydrogen Phosphate Crystals in the Presence of Ionic Species, J. Crystal Growth 23 (1974) 89-94.

34. **Dunning, W. J. and Albon, N.:**
The Kinetics of Crystal Growth of Sucrose from Aqueous Solution, in: Growth and Perfection of Crystals, Eds. Doremus R. H., Roperts B. W. and Turnbull, Wiley, New York, 1958, 446-457.

35. **Davey, R. J. and Mullin, J. W.:**
Growth of the (100) Faces of Ammonium Dihydrogen Phosphate Crystals in the Presence of Ionic Species, J. Crystal Growth 26 (1974) 45-51.

36. **Hottenhuis, M.H.J. and Oudenampsen, A.:**
Fe^{3+} and Ce^{3+} Acting as Competitive Impurities in the Crystallization Process of Potassium Hydrogen Phtalate from Solutions, J. Crystal Growth 92 (1988) 513-529.

37. **Hottenhuis, M. H. J. and Lucasius, C. B.:**
The Influence of Impurities on Crystal Growth; in Situ Observation of the (010)-Face of Potassium Hydrogen Phthalate, J. Crystal Growth 78 (1986) 379-388.

38. **Yokotani, A., Fujioka, K., Nishida, Y., Sasaki, T., Yamanaka, T. and Yamanaka, Y.:**
Formation of Macroscopic Hillocks on the Prismatic Faces of KDP Crystals Due to Microbes in the Solution, J. Crystal Growth 85 (1987) 549-552.

39. **Chernov, A. A. and Malkin, A. I.:**
Regular and Irregular Growth and Dissolution of (101) ADP Faces under low Supersaturations, J. Crystal Growth 92 (1988) 432-444.

40. **Dam, B. and Enckevort van, W. J. P.:**
In Situ Observation of Surface Phenomena on (100) and (101) Potassium Dihydrogen Phosphate Crystals, J. Crystal Growth 69 (1984) 306-316.

41. **Hamza, S. M., Abdul-Rahman, A. and Nancollas, G. H.:**
The Influence of Magnesium Ion on the Kinetics of Crystal Growth and Dissolution of Strontium Fluoride, J. Crystal Growth 73 (1985) 246-250.

42. **Boistelle, R. and Astier, J. P.:**
Crystallization Mechanisms in Solution, J. Crystal Growth 90 (1988) 14-30.

43. **Herden, A., Lacmann, R., Mayer, C. and Schröder, W.:**
Nucleation of KCl, NH_4Cl and $BaCl_2$: the Influence of Additives on Supercoolings, J. Crystal Growth 130 (1993) 245-252.

44. **Nielsen A. E.:**
Electrolyte Crystal Growth Mechanisms, J. Crystal Growth 67 (1984) 289-310.

45. **Veintemillas-Verdaguer S. and R. Rodriguez-Clemente:**
Crystal Growth of KDP from Boiling Solutions in the Presence of Impurities, J. Crystal Growth 79 (1986) 198-204.

46. **Sangwal, K.:**
Etching of Crystals: Theory, Experiment and Application, North-Holland, Amsterdam, 1987.

47. **Sears, G. W.:**
Effect of Poisons on Crystal Growth, J. Chem. Phys. 29 (1958) 1045-1048.

48. **Davey, R. J.:**
The Effect of Impurity Adsorption on the Kinetics of Crystal Growth from Solution, J. Crystal Growth 34 (1976) 109-119.

49. **Kubota, N. and Mullin, J.W.:**
A Kinetic Model for Crystal Growth from Aqeous Solution in the Presence of Impurity, J. Crystal Growth 152 (1995) 203-208.

50. **Pitzer, K. S.:**
Thermodynamics of Electrolytes. I. Theoritcal Basis and General Equations. J. Phys. Chem. 77 (1973) 268-277.

51. **Pitzer, K. S., Peiper, J. C. and Busey, R. H.:**
Thermodynamics Properties of Aqueous Sodium Chloride Solutions. J. Phys. Chem. Ref. Data 13 (1984) 1-102.

52. **Pitzer, K. S.:**
Theoretical Consideration of Solubility with Emphasis on Mixed Aqueous Electrolytes. Pure Appl. Chem. 58 (1986) 1599-1610.

53. **Mohameed, H. A.:**
Wachstumskinetik in der Lösungskristallisation mit Fremdstoffen, Ph.D. thesis, University of Bremen, Bremen 1996.

54. **Mohameed, H. A. and Ulrich, J.:**
Influence of the pH-Value on the Growth and Dissolution Rate of Potassium Chloride, Crystal Research and Technology 31 (1996) 27-31.

55. **Nalbandyan, A. G. and Nalbandyan, H. G.:**
The Effect of Additives on Nucleation in Aqueous Solution, in: Industrial Crystallization 87, Eds. Nyvlt J. and S. Zacek, Elsevier, New York 1989, 245-248.

56. **Mullin J. W. and Amatavivadhana, A.:**
Growth Kinetics of Ammonium- and Potassium-Dihydrogen Phosphate Crystals, J. Appl. Chem. 17 (1967) 151-156.

57. **Mullin J. W., Amatavivadhana, A. and Chakkraborty, M.:**
Crystal Habit Modification Studies with Ammonium and Potassium Dihydrogen Phosphate, J. Appl. Chem. 20 (1970) 153-158.

58. **Alexandru, H. V.:**
The Kinetics of Growth and Dissolution of Ammonium Dihydrogen Phosphate Crystals in Solution. J. Crystal Growth 10 (1971) 151-157.

59. **Tai, C. Y. and Chen, P. C.:**
Nucleation, Agglomeration and Crystal Morphpology of Calcium Carbonate, AIChE J. 41 (1), (1995) 68-77.

60. **Takasaki, S., Parsiegla, K. and Katz, J.:**
Calcite Growth and the Inhibiting Effect of Iron (III), J. Crystal Growth 143 (1994) 261-268.

61. **Seifert, D.:**
Untersuchung der Kristallisation von Kaliumchlorid aus wäßriger Lösung. VDI-Forschungsheft 591, VDI-Verlag, Düsseldorf 1979.

62. **Langer, H.:**
Zum Stofftransport beim Kristallwachstum aus Lösungen, Ph.D. Thesis, RWTH Aachen, Aachen 1985.

63. **Kuznetsov, D. A. and Hodorowicz, S.:**
On the Effect of pH of Solution on the Kinetics of Crystallization, Kristall und Technik 13 (1978) 1413-1416.

64. **Kubota, N., Fukazawa, J., Yashiro, H. and Mullin, J.W.:**
Pseudo-Solubilities of Potassium Sulphate Caused by Races of Chromium (III) Salts under Controlled pHs, J. Crystal Growth 143 (1994) 287-293.

65. **Baes, C. F. Jr. and Mesmer, R. E.:**
The Thermodynamic of Cations Hydrolysis, Amer. J. Sci. 281 (1981) 935-962.

66. **Karpinski, P. H.:**
Crystallization as a Mass Transfer Phenomenon. Chem. Eng. Sci., 35 (1980) 2321-2324.

67. **Mullin, J. W.:**
Crystallization. 3rd edition. Butterworth Heinemann, London. 1993.

68. **Myerson, A. S.:**
Handbook of Industrial Crystallization. Butterworth Heinemann, Boston 2002, Ch. 2.

69. **Ohara, M. and Reid, R. C.:**
Modelling Crystal Growth Rates from Solution, Prentice-Hall, Englewood Cliffs, NJ. 1973.

70. **Nyvlt, J., Sohnel, O., Matuchova, M. and Broul, M.:**
The Kinetics of Industrail Crystallization. 1st edition. Elsevier Science Publishing Company, Inc., New York, 1985.

71. **Garside J., Mersmann, A. and Nyvlt, J.:**
Measurments of Crystal Growth Rates, 1st ed., European Federation of Chemical Engineering, 1990.

72. **Mullin, J. W. and Gaska, C.:**
The Growth and Dissolution of Potassium Sulphate Crystals in a Fluidized Bed Crystallizer, Can. J. Chem. Eng. 47 (1969) 483-489.

73. **Rosner, D. E.:**
The Apparent Chemical Kinetics of Surface Reactions in External Flow System: Diffusional Falsification of Activation Energy and Reaction Order, AIChE J. 9 (1963) 321-330.

74. **Carberry, J. J. and Kulkarni, A. A.:**
The Non-Isothermal Catalytic Effectiveness Factor for Monolith Supported Catalysts, J. of catalysis 31 (1973) 41-50.

75. **Bird, R. B., Stewart, W. E. and Lightfoot, E. N.:**
Transport Phenomena, John Wiley, New York, 1960.

76. **Garside, J.:**
The Concept of Effectiveness Factors in Crystal Growth. Chem. Eng. Sci. 26 (1971) 1425-1431.

77. **Kubota, N., Yokota, M. and Mullin, J. W.:**
Kinetic Models for the Crystal Growth from Aqueous Solution in the Presence of Impurities–Steady and Unsteady State Impurity Actions, in: Proceeding of the 13th Symposium on Industrial Crystallization, B. Biscans and N. Gabas, Eds., Toulouse, France 1996, 111-116.

78. **Burton, W. K., Cabrera, N. and Frank, F. C.:**
The Growth of Crystals and the Equilibrium Structure of their Surfaces, Phil. Trans. A 243 (1951) 299-358.

79. **Boer, J. H. de.:**
The Dynamical Character of Adsorption, Oxford University Press, Oxford, 1953.

80. **Oscik, J.:**
Adsorption, PWN, Warsaw, 1982.

81. **Sangwal, K.:**
Growth Kinetics and Surface Morphology of Crystals Grown from Solutions: Rezent Observation and Their Interpretation", Prog. Cryst. Growth Charact. **36** (1998) 163-248.

82. **Sangwal, K.:**
Kinetic Effect of Impurities on the Growth of Single Crystals from Solutions", J. Crystal Growth 203 (1999) 197-212.

83. **Zhang, S.-B., Stepanski, M., Yuan, J.-J, and Ulrich, J.:**
Investigations of Crystal Growth Rates in the Presence of Different Additives. Proceedings of the 11th Symposium on Industrial Crystallization, Ed. A. Mersmann, Garmisch 1990, 695-700.

84. **Al-Jibbouri, S. and Ulrich, J.:**
The Influence of Impurities on Crystallization Kinetics of Sodium Chloride, Cryst. Res. Technol. 36 (2001) 1365-1375.

85. **Al-Jibbouri, S. and Ulrich, J.:**
The Growth and Dissolution of Sodium Chloride in a Fluidized Bed Crystallizer", J. Crystal Growth 234 (2002) 237-246.

86. **Ulrich, J., Kruse, M. and Stepanski, M.:**
On the Growth Behaviour of NaCl Crystals With and Without Additives. Seventh Symposium on Salt, Vol. II, Eds. H. Kakihana, H. R. Herdy, T. Hoshi, K. Toyokura, Elsevier, Amsterdam 1993, 209-212.

87. **Al-Sabbagh, A., Mignon, D. and Offermann, H.:**
Kinetics and Impurity Uptake in Various Multicomponent Systems, in: Proceeding of the 13th Symposium on Industrial Crystallization, B. Biscans and N. Gabas, Eds., Toulouse, France 1996,165-170.

88. **Hunter, R. J.:**
Zeta Potential in Colloid Science, Acadamic Press, London, 1981.

89. **Lyklema, J.:**
Fundamentals of Interface and Colloid Science,Vols. I and II, Academic, London, 1991.

90. **Smith, A. L.:**
In: Dispersion of Powder in Liquids, 2nd edn., G. D. Parfitt, Ed., Applied Science Publishers, London 1973, p. 86.

91. **Hunter, R. J. and Wright, H. J. L.:**
The Dependence of Electrokinetic Potential on Concentration of Electrolyte, J. of Colloid and Interface Science 37 (1971) 564-580.

92. **Wright, H. J. L. and Hunter, R. J.:**
Adsorption at Solid–Liquid Interfaces: I. Thermodynamic and the Adsorption Potential, Aust. J. Chem. **26** (1973) 1183-1189.

93. **Wright, H. J. L. and Hunter, R. J.:**
Adsorption at Solid–Liquid Interfaces: II. Models of the Electrical Double Layer at the Oxide–Solution Interface, Aust. J. Chem. **26** (1973) 1191-1206.

94. **Levine, S., Bell, G. M. and Smith, A. L.:**
A Theory of the Electrical Capacity of the Inner Region in the Absence of Ionic Adsorption at the Mercury-Water Interface. J. Phy. Chem. 73 (1969) 3534-3545.

95. **Lyklema, J. and Overbeek, J. Th. G.:**
On the Interpretation of Electrokinetic Potentials, J. of Colloid and Interface Science 16 (1961) 501-512.

96. **Lyklema, J.:**
Water at Interfaces: A Colloid–Chemical Approach, J. of Colloid and Interface Science 58 (1977) 242-250.

97. **Smith, A. L.:**
Electrokinetics of the Oxide–Solution Interface, J. of Colloid and Interface Science 55 (1976) 525-530.

98. **Hosse, M. and Wilkinson, K. J.:**
Determination of Electrophoretic Mobility and Hydrodynamic Radii of Three Humic Substances as a Function of pH and Ionic Strength, Environ. Sci. Technol. 35 (2001) 4301-4306.

99. **Velegol, D., Feick, J. D. and Collins, L. R.:**
Electrophoresis of Spherical Particales with a Random Distribution of Zeta Potential and Surface Charge, J. of Colloid and Interface Science 230 (2000) 114-121.

100. **Malvern Instruments Zetasizer 3000:**
PCS Theory, Manual No. MAN0152, Issue 1.1, 1996.

101. **Al-Jibbouri, S.:**
Measurment of Growth Rate and Dissolution Rate of Potassium Dihydrogen Phosphate (KH_2PO_4) Crystals, M.Sc. thesis, University of Jordan, Jordan 1999.

102. **Malvern Instruments Zetasizer 3000:**
Zeta Potential Measurements, Manual No. MAN0150, Issue 2, 2000.

103. **Al-Sabbagh, A.:**
Zur KCl- und NaCl- Kristallisation in Anwesenheit von Fremdstoffen, Ph.D. Thesis, RWTH Aachen, Aachen 1996. Shaker Verlag, Aachen 1996.

104. **Stepanski, M.:**
Zur Wachstumskinetik in der Lösungskristallisation, Ph.D. Thesis, University of Bremen, Bremen 1990.

105. **Ulrich, J., Mohameed, H., Zhang, S.-B. and Yuan, J.-J.:**
Effect of Additives on the Crystal Growth Rate: Case Study NaCl, Bull. Soc. Sea Water Sci. Jpn. 51 (1997) 2, 73-77.

106. **Zhang, S.-B., Yuan, J.-J. Mohameed, H. A. and Ulrich, J.:**
The Effect of Different Inorganic Salts on the Growth Rate of NaCl Crystallized from Sea Water, Cryst. Res. Technol. 31 (1996) 19-25.

107. **Al-Jibbouri, S. and Ulrich, J.:**
Growth Kinetics in the Presence of Adsorption of Impurity: A Comparison of Models and Experimental Data, Can. J. Chem. Eng., “submitted”.

108. **Al-Jibbouri, S. and Ulrich, J.:**
Impurity Effect of Iron (II) on the Growth and Dissolution of $MgSO_4{\bullet}7H_2O$ crystal in Aqueous Solution, Crystal Growth and Design, “submitted”.

109. **Al-Jibbouri, S., Strege, C. and Ulrich, J.:**
Crystallization Kinetics of Epsomite Influenced by pH-Value and Impurities, J. Crystal Growth 236 (2002) 400-406.

110. **Al-Jibbouri, S., Strege, C. and Ulrich, J.:**
Effects of Additives and pH-Value on Crystal Growth Rate, Proceeding of 13th International Conference on Crystal Growth in Conjunction with 11th International on Vapor Growth and Epitaxy. Doshisha University, Kyoto, Japan 2001.

111. **Al-Jibbouri, S., Strege, C. and Ulrich, J.:**
The Influence of Additives and pH-Value on Growth Rate and Metastable Zone Width of $MgSO_4{\bullet}7H_2O$, in: Proceeding of BIWIC 2001-8th International Workshop on Industrial Crystallization, Eds. Jansens, P., Kramer, H. and Roelands, M., DocVision Delft, the Netherlands 2001, 150-155.

112. **Al-Jibbouri, S. and Ulrich, J.:**
The Effect of Different Additives on the Crystal Growth Mechansim of $MgSO_4{\bullet}7H_2O$, in: Proceeding of 15th International Symposium on Industrail Crystallization, Ed. Chianese, A., Sorrento, Italy 2002, Vol. 1, 262-268.

113. **Hayakawa, T. and Matsuoka, M.:**
Effect of Heat Transfer on Crystal Growth Rate for Inorganic Salt-Water Systems. Heat Transfer Jpn. Res. 2 (1973) 104-115.

114. **Al-Jibbouri, S. and Ulrich, J.:**
Impurity Adsorption Mechanism for a Suspension Growth Condition: A Comparison of Models and Experimental Data. in: Proceeding of BIWIC 2002-9th International Workshop on Industrial Crystallization, Ed. Ulrich, J., Universitatsdruckerei, Halle, Germany 2002, 162-169.

115. **Hayashi, M. and Schichiri, T.:**
Theoretical and Experimental Study of the Growth Perfect Crystal, J. Crystal Growth 21 (1974) 254-260.

116. **Meenan, P. A., Anderson, S. R. and Klug, D. L.:**
The Influence of Impurities and Solvents on Crystallization, in: Handbook of Industrial Crystallization, 2nd edn., Ed. A. S. Myerson, Butterworth-Heinemann, Boston 2002, 67-100.

117. **Rauls, M., Bartosch, K., Kind, M., Kuch, St., Lacmann, R. and Mersmann, A.:**
The Influence of Impurities on Crystallization Kinetics – a Case Study on Ammonium Sulfate, J. Crystal Growth 213 (2000) 116-128.

118. **Murrel, J. N., and Jenkins, A. D.:**
Properties of Liquids and Solution, John Wiley and Sons ltd., Chichester 1994, Ch. 9.

119. **Burgess, J.:**
Ions in Solution, Basic Principles of Chemical Interactions, Ellis Horwood ltd., Chichester 1987, Ch. 5.

120. **Skoog, D. A., West, D. M., Holler, F. J., and Crouch, S. R.:**
Analytical Chemistry: An Introduction, Harcourt Inc., Florida 2000, Ch. 4.

121. **Horvath, A. L.:**
Handbook of Aqueous Electrolyte solutions: Physical Properties, Estimation and Correlation Methods, Ellis Horwood ltd., Chichester 1985, part 1.

122. **Friedman, H. L., and Krishnan, C. V.:**
Water, a Comprehensive Treatise, Ed. F. Franks, Plenium Press, London 1973 Vol. 3, Ch. 1.

123. **Guzman, L. A., Maeda, K., Hirota, S., Yokota, M. and Kubota, N.**
Unsteady-State Impurity Effect of Chromium (III) on the Growth Rate of Potassium Sulfate Crystal in Aqueous Solution, J. Crystal Growth 181 (1997) 272-280.

124. **De Bruyn, P. L. and Agar, G. E.:**
Surface Chemistry of Flotation, Ch. 5 in Froth flotation, 50th Anniversary Volume, Ed. Fuerstenau, D. W., American Institute of Mining, Metallurgical and Petroleum Engineers, New York 1962.

125. **Calara, J. V. and Miller, J. D.:**
Determination of Madelung Constant for Infinite and Semi-Infinite Lattices by Direct Summation, J. Chem. Phys. 65 (1976) 843-844.

126. **Hunt, J. P.:**
Metal Ions in Aqueous Solution, W. A. Benjamin, Inc., New York 1963.

127. **Karpinski, P. H., Buds, J. and Larson, M. A.:**
Influence of Cationic Admixtures on Kinetics of Crystal Growth, in: Industrial Crystallization, Eds. Jancic, S. J. and de Jong, E. J., Elsevier Science Publishers B.V., Amsterdam, The Netherlands 1984, 85-90.

128. **Kruyt, H. R.:**
Colloid Science, Vol. 1, Elsever Publishing Co., New York 1952, Chs. 4, 5 and 8.

CURRICULUM VITAE

Name: Sattar Al-Jibbouri

Date of Birth: 29.12.1972 Kadisia–Iraq

Nationality: Iraqi

Marital Status: Married

E-Mail saljibbouri@hotmail.com

Education: (***Dr. in Chemical Engineering***) at the Martin-Luther-Universität Halle-Wittenberg, Department of Process Chemical Engineering in 19.12.2002.
Ph.D. thesis entitle: *Effects of Additives in Solution Crystallization.*

(***M.Sc. in Chemical Engineering***) at the University of Jordan, College of Engineering/ Department of Chemical Engineering in 20.06.1999.
GPA (**3.5** from **4**).
M.Sc. thesis entitle: *Measurement of Growth Rate and Dissolution Rate of Potassium Dihydrogen Phosphate (KH_2PO_4) Crystals.*

(***B.Sc. in Chemical Engineering***) at the University of Baghdad, College of Engineering, Department of Chemical Engineering in 01.07.1995.
GPA (82.077 %). Rank (**1** from **121**).

Experience:

March, 1997-July, 1999	Worked as a research assistant at the University of Jordan, College of Engineering, Chemical Engineering Laboratory with main focus on industrial crystallization process.
March, 1997-June, 1999	Worked as a lectures assistant teaching courses in Thermodynamic, Mass transfer, and Reaction engineering; at the University of Jordan College of Engineering/ Department of Chemical Engineering.
Oct., 1998-June, 1999	Worked as a computer Lab. technician with knowledge of (AutoCAD, HTML Design for Web Pages, Win95, Win98, and Win3.11. and application. Such as *"WinWord, Excel, PowerPoint"*, and MATLAB); at the University of Jordan, College of Engineering, Computer Laboratory.
July, 1999-Oct., 1999	Worked as a research assistant in design and simulation of chemical engineering at the University of Jordan, College of Engineering, Department of Chemical Engineering.